

quatrième série - tome 50 fascicule 4 juillet-août 2017

*ANNALES
SCIENTIFIQUES
de
L'ÉCOLE
NORMALE
SUPÉRIEURE*

Laura DEMARCO & Kevin PILGRIM

The classification of polynomial basins of infinity

SOCIÉTÉ MATHÉMATIQUE DE FRANCE

Annales Scientifiques de l'École Normale Supérieure

Publiées avec le concours du Centre National de la Recherche Scientifique

Responsable du comité de rédaction / *Editor-in-chief*

Emmanuel KOWALSKI

Publication fondée en 1864 par Louis Pasteur

Continuée de 1872 à 1882 par H. SAINTE-CLAIRE DEVILLE
de 1883 à 1888 par H. DEBRAY
de 1889 à 1900 par C. HERMITE
de 1901 à 1917 par G. DARBOUX
de 1918 à 1941 par É. PICARD
de 1942 à 1967 par P. MONTEL

Comité de rédaction au 1^{er} janvier 2017

P. BERNARD A. NEVES
S. BOUCKSOM J. SZEFTEL
E. BREUILLARD S. VŨ NGỌC
R. CERF A. WIENHARD
G. CHENEVIER G. WILLIAMSON
E. KOWALSKI

Rédaction / *Editor*

Annales Scientifiques de l'École Normale Supérieure,
45, rue d'Ulm, 75230 Paris Cedex 05, France.
Tél. : (33) 1 44 32 20 88. Fax : (33) 1 44 32 20 80.
annales@ens.fr

Édition / *Publication*

Société Mathématique de France
Institut Henri Poincaré
11, rue Pierre et Marie Curie
75231 Paris Cedex 05
Tél. : (33) 01 44 27 67 99
Fax : (33) 01 40 46 90 96

Abonnements / *Subscriptions*

Maison de la SMF
Case 916 - Luminy
13288 Marseille Cedex 09
Fax : (33) 04 91 41 17 51
email : smf@smf.univ-mrs.fr

Tarifs

Europe : 519 €. Hors Europe : 548 €. Vente au numéro : 77 €.

© 2017 Société Mathématique de France, Paris

En application de la loi du 1^{er} juillet 1992, il est interdit de reproduire, même partiellement, la présente publication sans l'autorisation de l'éditeur ou du Centre français d'exploitation du droit de copie (20, rue des Grands-Augustins, 75006 Paris).

All rights reserved. No part of this publication may be translated, reproduced, stored in a retrieval system or transmitted in any form or by any other means, electronic, mechanical, photocopying, recording or otherwise, without prior permission of the publisher.

ISSN 0012-9593

Directeur de la publication : Stéphane Seuret
Périodicité : 6 n^{os} / an

THE CLASSIFICATION OF POLYNOMIAL BASINS OF INFINITY

BY LAURA DEMARCO AND KEVIN PILGRIM

ABSTRACT. – We consider the problem of classifying the dynamics of complex polynomials $f : \mathbb{C} \rightarrow \mathbb{C}$ restricted to the basins of infinity $X(f)$. We synthesize existing combinatorial tools—tableaux, trees, and laminations—into a new invariant of basin dynamics we call the pictograph. For polynomials with all critical points escaping to infinity, we obtain a complete description of the set of topological conjugacy classes with given pictograph. For arbitrary polynomials, we compute the total number of topological conjugacy classes of basins $(f, X(f))$ with a given pictograph. We also define abstract pictographs and prove that every abstract pictograph is realized by a polynomial. Extra details are given in degree 3, and we provide examples that show the pictograph is a finer invariant than both the tableau of [5] and the tree of [10].

RÉSUMÉ. – Nous étudions la question de la classification de la dynamique des polynômes complexes $f : \mathbb{C} \rightarrow \mathbb{C}$ restreints à leur bassin de l’infini. Nous faisons la synthèse d’outils de combinatoire — tableaux, arbres, laminations — en un nouvel invariant du bassin dynamique que nous appelons *pictogramme*. Pour les polynômes dont tous les points critiques s’échappent vers l’infini, nous obtenons une description complète de l’ensemble des classes de conjugaison topologiques ayant un pictogramme donné. Plus généralement, pour tout polynôme, nous calculons le nombre de classes de conjugaison topologiques du bassin $(f, X(f))$ à pictogramme donné. Nous définissons les pictogrammes de façon abstraite et prouvons que chacun d’eux est réalisable par un polynôme. Nous donnons plus de détails en degré 3 et donnons des exemples montrant que le pictogramme est un invariant plus fin que les tableaux de [5] et que les arbres de [10].

1. Introduction

This article continues a study of the moduli space of complex polynomials $f : \mathbb{C} \rightarrow \mathbb{C}$, in each degree $d \geq 2$, in terms of the dynamics of polynomials on their basins of infinity [4, 5, 10, 8, 7]. Our main goal is to classify the topological conjugacy classes of a polynomial f restricted to its basin

$$X(f) = \{z \in \mathbb{C} : f^n(z) \rightarrow \infty\}.$$

The basin $X(f)$ is an open, connected subset of \mathbb{C} . In degree $d = 2$, there are only two topological conjugacy classes of basins $(f, X(f))$, distinguished by the Julia set being connected or disconnected; see, for example, [19, Theorem 10.1]. In every degree $d > 2$, there are infinitely many topological conjugacy classes of basins, even among the structurally stable polynomials in the shift locus. The main objective of this article is the development of combinatorial methods that allow us to distinguish and enumerate these conjugacy classes in all degrees.

By definition, a polynomial f of degree d is in the shift locus if all of its $d - 1$ critical points are in $X(f)$. In this case, the basin $X(f)$ is a rigid Riemann surface, admitting up to Möbius transformations a unique embedding into the Riemann sphere ([18, §2.8], [1, §IV.4]). In this case, the restriction $f : X(f) \rightarrow X(f)$ uniquely determines the conformal conjugacy class of $f : \mathbb{C} \rightarrow \mathbb{C}$. Thus, our results on basin dynamical systems $(f, X(f))$ —given as Theorems 1.1, 1.2, 1.3, and 1.4 below—also provide a combinatorial classification of topological conjugacy classes of polynomials in the shift locus.

In the theory of dynamical systems, the study of a system like $(f, X(f))$ is somewhat nonstandard. On the one hand, since all points tend to ∞ under iteration, the system is transient. On the other hand, the structure of $(f, X(f))$, with an induced dynamical system on its Cantor set of ends as a topological space, carries enough information to recover the full entropy of the polynomial (f, \mathbb{C}) ; see [10, Theorem 1.1]. Our methods and perspective are inspired by the two foundational articles of Branner and Hubbard on polynomial dynamics which lay the groundwork and treat the case of cubic polynomials in detail [4, 5].

1.1. The pictograph, informally described

We begin with a rough description of the pictograph $\mathcal{D}(f)$ associated to a polynomial basin dynamics $(f, X(f))$. A formal presentation is given in §2.2 (for cubic polynomials) and Section 10 (in arbitrary degree).

Global setup. – The basin dynamics $f : X(f) \rightarrow X(f)$ fits naturally into a sequence of dynamical systems related by semiconjugacies. These are organized in the diagram below, and are explained in the following paragraphs.

$$(1.1) \quad \begin{array}{ccccccc} \begin{array}{c} \mathcal{F} \\ \curvearrowright \\ \mathcal{X}(f) \end{array} & \xrightarrow{g_f} & \begin{array}{c} f \\ \curvearrowright \\ X(f) \end{array} & \xrightarrow{\pi_f} & \begin{array}{c} F \\ \curvearrowright \\ T(f) \end{array} & \xrightarrow{h_f} & \begin{array}{c} \cdot d \\ \curvearrowright \\ (0, \infty) \end{array} \\ & & & \searrow & \swarrow & & \\ & & & & G_f & & \end{array}$$

The map G_f is the harmonic *Green's function*; its values we call *heights* or sometimes *escape rates*. The grand orbits (under multiplication by d) of heights of critical points are called *nongeneric heights*. We endow $(0, \infty)$ with a simplicial structure in which the nongeneric heights are vertices. The map π_f collapses connected components of level sets of G_f to points; its image is the *DeMarco-McMullen tree* $T(f)$, and f induces a self-map $F : T(f) \rightarrow T(f)$. By construction, the factor $h_f : T(f) \rightarrow (0, \infty)$ is simplicial.

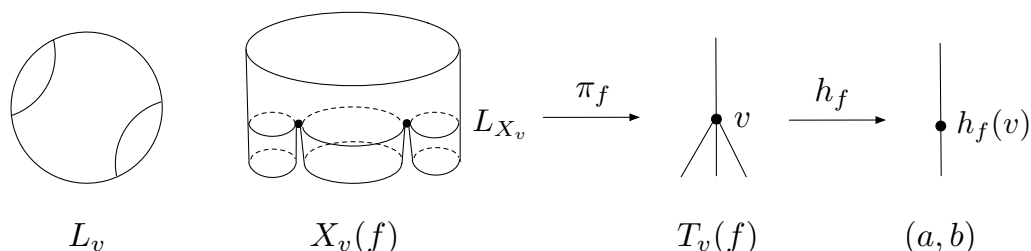


FIGURE 1.1. The local features of the quotient maps in (1.1) at a vertex v of $T(f)$ and the associated lamination L_v .

Local features. – See Figure 1.1. Every vertex v of $T(f)$ has a nongeneric height $h_f(v)$; and for each vertex, there is a maximal interval $(a, b) \subset (0, \infty)$ containing $h_f(v)$ for which all heights $t \in (a, b) - \{h_f(v)\}$ are generic. The connected component $X_v(f)$ of $G_f^{-1}(a, b)$ containing $\pi_f^{-1}(v)$ is a planar Riemann surface that we call a *local model surface*. The intersection $L_{X_v} := X_v(f) \cap \pi_f^{-1}(v)$ is called the *central leaf* of $X_v(f)$. The central leaf L_{X_v} is a connected component of a fiber of G_f , is homeomorphic to the underlying space of a finite planar graph, and is the boundary of the unbounded component of its complement. This implies it is naturally the quotient of the unit circle by a certain kind of equivalence relation, a *finite lamination*, denoted L_v . The lamination L_v is encoded by a simple picture in a disk, a *lamination diagram*. The lamination diagram is not endowed with coordinates—rotating the picture does not change it—but the circle is equipped with a metric induced by the 1-form $|\partial G_f|$. For example: if two critical points c_1, c_2 belong to the same central leaf L_{X_v} , their relative angles in L_v are determined by the metric.

The pictograph. – The pictograph $\mathcal{D}(f)$ is a diagram consisting of a collection of laminations L_v , associated to vertices in the convex hull of the critical points of $(F, T(f))$, together with labels that mark the orbits of the critical points. For illustration, Figure 1.2 shows a pictograph associated to a polynomial of degree 4 in the shift locus. The markings on each lamination indicate which iterate of a critical point lands on a central leaf or is seen through the “pant leg” of the local model surface. We emphasize two things.

1. The pictograph contains both combinatorial and metric information. For example, if the iterates of two critical points, say $f^i(c_1)$ and $f^j(c_2)$, both lie on a central leaf L_{X_v} , then the lamination L_v is labeled by symbols i_1 and j_2 , placed on the unit circle at a distance recording the metric information of how these points are deployed in L_{X_v} .
2. The pictograph is a static object. It does not, by definition, include a self-map of an object. However, it allows for reconstruction of dynamics, as described in the main results presented below.

The next paragraph describes what the pictograph captures.

The tree of local models. – The *tree of local models* is the disjoint union $\mathcal{X}(f) := \bigsqcup_v X_v(f)$, indexed by the vertices v of the tree $T(f)$. It is equipped with a holomorphic self-map \mathcal{F} induced by f . The collection of inclusions $\{X_v(f) \hookrightarrow X(f)\}_{v \in T(f)}$ induces a (generically two-to-one) *gluing quotient map* $g_f : \mathcal{X}(f) \rightarrow X(f)$, which is not part of the data of the tree of local models.

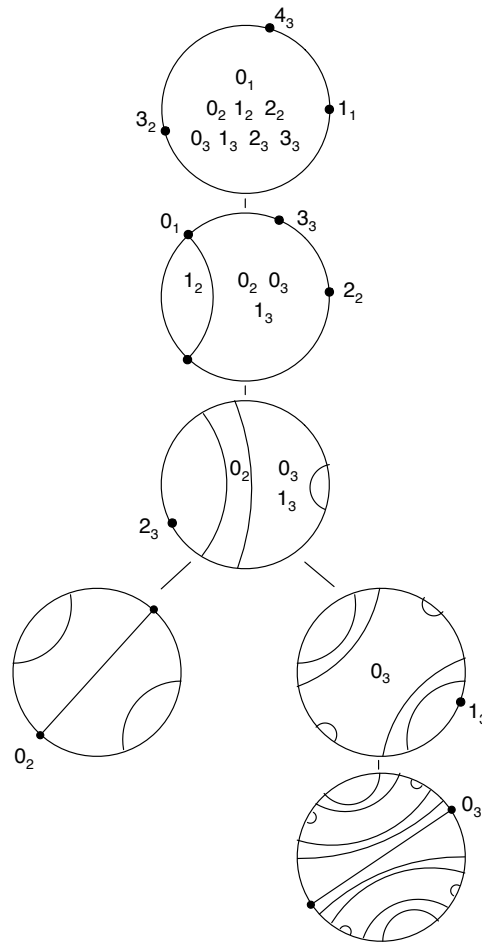


FIGURE 1.2. A degree 4 pictograph, with critical escape rates $(M, M/4^2, M/4^3)$ for some $M > 0$.

As we shall see, if we are given the heights of the critical points, then the pictograph $\mathcal{D}(f)$ determines $\mathcal{F} : \mathcal{X}(f) \rightarrow \mathcal{X}(f)$ up to holomorphic conjugacy. But a gluing map is required to determine the conformal conjugacy class of a basin $(f, X(f))$, and there can be many polynomials with the same pictograph.

1.2. Relation with other invariants: a quick summary

The pictograph synthesizes the pattern and tableau of Branner and Hubbard, the metric tree equipped with dynamics of DeMarco and McMullen, and the laminations of Thurston. For cubic polynomials, we will give a more detailed account of the relationships between the pictograph and other invariants in Section 3. Here, we confine ourselves to some brief remarks for experts.

Suppose f is a cubic polynomial. The *Branner-Hubbard tableau* $\tau(f)$ records the first-return map along the “critical nest”. The critical nest is a nested sequence $P_1 \supset P_2 \supset$

$P_3 \supset \dots$ where for each n , the *puzzle piece* P_n contains a critical point and is a bounded component of the complement of some $L_{X_{v_n}}$. The tableau data has an equivalent form, the *Yoccoz τ -sequence*. The DeMarco-McMullen tree $F : T(f) \rightarrow T(f)$ records a first-return map along a “decorated critical nest”, and so is a finer invariant than the tableau $\tau(f)$. The pictograph $\mathcal{D}(f)$ records the first return to a “decorated critical nest together with an embedding into the plane,” and so is finer than both the DeMarco-McMullen tree and the tableau. Our methods are inspired also by techniques in [2], [16], [22], [23], and [25].

1.3. Main results: realization and counting

If all critical points of f have bounded orbits, then $(f, X(f))$ is conformally conjugate to $(z^d, \{|z| > 1\})$. We therefore restrict our attention to the case where at least one critical point of f lies in $X(f)$.

Branner-Hubbard and DeMarco-McMullen formulated axioms for classes of abstract tableaux and abstract trees, respectively, and they used these axioms to characterize those tableaux and trees arising from polynomials. Similarly, we introduce an abstract notion of the pictograph, and we prove:

THEOREM 1.1. – *Every abstract pictograph arises for some polynomial.*

Next, we study the problem of determining when two polynomials have the same pictograph.

THEOREM 1.2. – *The pictograph is a topological-conjugacy invariant. For any given pictograph \mathcal{D} , the number of topological conjugacy classes $\text{Top}(\mathcal{D})$ of basins $(f, X(f))$ with pictograph \mathcal{D} is algorithmically computable from the data of \mathcal{D} .*

There is a unique topological conjugacy class of quadratic polynomials with disconnected Julia set; accordingly, there is a unique quadratic pictograph \mathcal{D} , and $\text{Top}(\mathcal{D}) = 1$. For degrees $d \geq 3$, the computation of $\text{Top}(\mathcal{D})$ is achieved by an analysis of the quasiconformal twist deformations on the basin of infinity, as introduced in [4] and [19], and of the symmetries of the pictograph \mathcal{D} that we carry out in Section 8. The algorithmic computation of $\text{Top}(\mathcal{D})$ has the simplest formulation in degree 3, where the symmetries are easy to analyze; the count is given explicitly in Theorems 4.1 and 4.2.

As mentioned in §1.2, the pictograph is a strictly finer invariant than both the tableau of [5] defined for cubic polynomials and the tree of [10] defined for polynomials of all degrees. Nevertheless, there exist examples with $\text{Top}(\mathcal{D}) > 1$ in every degree $d > 2$; see Figure 3.3 and §12.9. Though the pictograph is not a complete invariant of topological conjugacy of basins $(f, X(f))$, Theorem 1.2 implies that it “knows” its failure. Furthermore, the algorithms for counting $\text{Top}(\mathcal{D})$ for a given pictograph \mathcal{D} can be augmented to also count all possible pictographs, subject to given combinatorial constraints. Indeed, this algorithm is completed and implemented in degree $d = 3$ in [9] and [6]. As an application, the algorithm is used in [6] to compute the Euler characteristic of the algebraic curves

$S_p = \{(a, v) \in \mathbb{C}^2 \mid f(z) = z^3 - 3a^2z + (2a^3 + v) \text{ has a periodic critical point of period } p\}$, introduced in [22].

1.4. Main results: the structure of moduli space

In [8] we studied the moduli space \mathcal{B}_d of basin dynamical systems $(f, X(f))$ for polynomials f of degree $d \geq 2$. Here we prove that, once the pictograph and critical escape rates are fixed, the locus in \mathcal{B}_d with this data admits the following description. See §2.1 for a more thorough discussion of the notion of critical heights mentioned in the statement.

THEOREM 1.3. – *Fix a pictograph \mathcal{D} with $N = N(\mathcal{D})$ grand orbits of nongeneric heights and a corresponding list of N compatible critical heights. Then the locus in the space \mathcal{B}_d of basin dynamical systems with this data is a compact locally trivial fiber bundle $\mathcal{B}_d(\mathcal{D}) \rightarrow (S^1)^N$ over a torus with totally disconnected fibers. The total space is foliated by N -manifolds, and the leaves are in bijective correspondence with topological conjugacy classes of basins with the given pictograph.*

The *twisting deformation* of [19] induces the local holonomy of the fiber bundle. The counting of these topological conjugacy classes in Theorem 1.2 is done via an analysis of the monodromy of this bundle.

The main result of [8] is that the projection $\pi : \mathcal{M}_d \rightarrow \mathcal{B}_d$, from conformal conjugacy classes of polynomials (f, \mathbb{C}) to conformal conjugacy classes of basins $(f, X(f))$, has compact and connected fibers. Moreover, $\pi : \mathcal{M}_d \rightarrow \mathcal{B}_d$ is a homeomorphism on the shift locus. Thus, the description in Theorem 1.3 pulls back to \mathcal{M}_d , at least where the fibers of π are points. In fact, the conformal class of $(f, X(f))$ uniquely determines the conformal class of (f, \mathbb{C}) unless there is a critical point in a periodic end of $X(f)$; see [26], [5]. The fibers of $\pi : \mathcal{M}_d \rightarrow \mathcal{B}_d$ over basins with periodic critical ends contain continua. For example, in the case of cubics, these fibers contain small copies of the Mandelbrot set coming from renormalizations around periodic components of the filled-in Julia set. Combining these facts, we have the following result about \mathcal{M}_d , similar to Theorem 1.3:

THEOREM 1.4. – *Fix a pictograph \mathcal{D} with $N = N(\mathcal{D})$ grand orbits of nongeneric heights and a corresponding list of N compatible critical heights. Then the locus in the moduli space \mathcal{M}_d of polynomials with this data is a compact locally trivial fiber bundle $\mathcal{M}_d(\mathcal{D}) \rightarrow (S^1)^N$ over a torus. The fibers are totally disconnected if and only if \mathcal{D} has no periodic critical ends. In this case, the total space is foliated by N -manifolds, and the leaves are in bijective correspondence with topological conjugacy classes of polynomials with the given pictograph.*

The structure of the bundle when \mathcal{D} has periodic critical ends is delicate. A pictograph \mathcal{D} has a periodic critical end if and only if any polynomial f with this pictograph has a periodic component of its Julia set containing a critical point. A result of [24, 17] (and [5] in degree 3) states that this occurs if and only if the Julia set of f has connected components that are not points. As observed in [8], one might expect that each non-singleton fiber of $\pi : \mathcal{M}_d \rightarrow \mathcal{B}_d$ is a homeomorphic copy of a product of connectedness loci $\prod_i \mathcal{C}_{d_i} \subset \prod_i \mathcal{M}_{d_i}$ for some integers $d_i \geq 2$ with $\sum_i (d_i - 1) \leq d - 1$. Indeed, the straightening theorem of Douady and Hubbard gives a map from any non-singleton fiber $\pi^{-1}(x)$ to such a product, where d_i is the degree of a polynomial-like restriction [11]. But the discontinuity of straightening suggests that this expectation may fail; see [14]. In degree $d = 3$, it is known each fiber $\pi^{-1}(x)$ is either a point or a homeomorphic copy of the Mandelbrot set [5, Theorem 9.1]; while in degree 2, each fiber of π is either a point or the Mandelbrot set itself.

1.5. Structure of the article

The article is divided into five parts:

Part I. Cubic pictographs. – (Sections 2, 3, 4) We begin in Section 2 with a description of our main object, the pictograph, in the simplest yet nontrivial setting of cubic polynomials. (The simplest case is that of degree $d = 2$, where all polynomials with disconnected Julia set are topologically conjugate.) In fact, we do not give the full definition of the pictograph in these sections, but a simplified though equivalent version. In Section 3, we provide a comparison of our simplified pictograph and the known invariants for cubic polynomials, the tableau of [5] (or, equivalently, the τ -sequence) and the tree of [10]. We give explicit examples illustrating that the pictograph is a strictly finer invariant than the tree, which is itself a strictly finer invariant than the tableau and τ -sequence. Section 4 contains a precise version of Theorem 1.2, appearing as Theorems 4.1 and 4.2. Proofs will be given in Part V.

Part II. Local structure and laminations. – (Section 5) In this part, we begin the formal analysis needed to define and study pictographs in all degrees. Our focus is on *local model maps*: restrictions $f : X_v(f) \rightarrow X_{F(v)}(f)$, where f is a polynomial, and $X_v(f)$ is a local model surface as described in §1.1. In [8], we introduced local model surfaces and local model maps. Here, we prove that the conformal structure of a local model surface is recorded by a *finite lamination*. We also prove that the local model map, up to symmetries and variation of heights, can be recovered from the static data consisting of the domain lamination and its degree. This is the central ingredient allowing for the recovery of local model maps up to symmetries from purely static data. The main result is stated as Theorem 5.1.

Part III. The tree of local models. – (Sections 6, 7, 8) Throughout Part III, we fix a polynomial $f : \mathbb{C} \rightarrow \mathbb{C}$ of degree $d \geq 2$, such that at least one critical point of f lies in $X(f)$. In Section 6 we provide a review of the polynomial tree $(F, T(f))$, defined in [10]. There we also introduce a key concept—the *spine of the tree* $(F, T(f))$. This is defined as the convex hull of the critical vertices, and it plays a crucial role for us. In Section 7 we define formally the *tree of local models* $(\mathcal{F}, \mathcal{X}(f))$ associated to f that was introduced in §1.1. The *spine of the tree of local models* is the analogous collection of local models over the convex hull of the critical vertices. We show (Proposition 7.2) that the dynamical system $(\mathcal{F}, \mathcal{X}(f))$ is determined by the first-return map $(\mathcal{R}, \mathcal{S})$ on its spine. We study the symmetries of a tree of local models in Section 8. There are local symmetries, for a local model at a vertex, and global symmetries in the underlying tree. The analysis of this symmetry is a crucial ingredient in the algorithmic count of $\text{Top}(\mathcal{D})$ in Theorem 1.2.

Both trees and trees of local models can be defined abstractly, from a list of axioms. Following the proof of the realization theorem for trees [10, Theorem 1.2], we prove the analogous realization theorem (Theorem 7.1): every abstract tree of local models comes from a polynomial.

Part IV. The moduli space and topological conjugacy. – In Part IV (Section 9), we study our dynamical systems in families. We begin by recalling facts about the quasiconformal deformation theory of polynomials from [19], specifically the *wringing, twisting, and stretching deformations* on the basin of infinity. These quasiconformal conjugacies parametrize the

topological conjugacy classes of basins. We show (Theorem 9.1) that the tree of local models is a twist-conjugacy invariant.

Fixing a tree of local models $(\mathcal{F}, \mathcal{X})$, we examine the structure of the subset $\mathcal{B}_d(\mathcal{F}, \mathcal{X})$ in the moduli space \mathcal{B}_d of basins $(f, X(f))$ with a given tree of local models $(\mathcal{F}, \mathcal{X})$. This is the core of the proof of Theorem 1.3.

Part V. Combinatorics and counting. – (Sections 10, 11, 12) In Part V, we formally define the pictograph for polynomials of arbitrary degree. We prove that the pictograph is a topological-conjugacy invariant of polynomials (Theorem 10.1). We also prove that a tree of local models can be reconstructed from its pictograph and the list of critical escape rates (Proposition 10.2), thus completing the proof of Theorem 1.3 when combined with the work of Part IV. We define an abstract pictograph as the pictograph associated to an abstract tree of local models and give the proof of Theorem 1.1.

We complete the proof of Theorem 1.2 in Section 12, providing the arguments for counting topological conjugacy classes associated to each pictograph. We treat the case of cubic polynomials first and in greatest detail, giving the proofs of Theorems 4.1 and 4.2 in Section 11.

1.6. Acknowledgements

We thank Jan Kiwi, Curt McMullen, and Tan Lei for helpful discussions. We also thank the anonymous referees for numerous thoughtful suggestions. Our research was supported by the National Science Foundation and the Simons Foundation.

2. Basic definitions and the cubic pictograph

In this section, we give some key definitions needed throughout the article. We introduce the pictograph in the simplest, yet nontrivial, setting of cubic polynomials. In fact, we introduce a simpler version that exists only for cubic polynomials, the *simplified pictograph* (also called a truncated spine in [9, 6]) which is equivalent to the pictograph in this setting. Because we go to great length to give formal definitions later, we err on the side of informality here, in order to provide a working definition as quickly as possible.

2.1. Basic definitions

We recall some basic facts from [21]. Fix a polynomial f of any degree $d \geq 2$. The *basin of infinity* of f is

$$X(f) = \{z \in \mathbb{C} : f^n(z) \rightarrow \infty \text{ as } n \rightarrow \infty\}.$$

The *escape-rate* (or *Green's*) *function* of f is

$$G_f(z) = \lim_{n \rightarrow \infty} \frac{1}{d^n} \log^+ |f^n(z)|.$$

It is continuous on \mathbb{C} and harmonic on $X(f)$, with $G_f(z) > 0$ if and only if $z \in X(f)$. Since $G_f(f(z)) = dG_f(z)$, we see that G_f induces a semiconjugacy between $f : X(f) \rightarrow X(f)$ and multiplication by d in the real interval $(0, \infty)$.

The *critical escape rates* of f are the elements of $\{G_f(c) : f'(c) = 0\}$. We define $N = N(f)$ to be the maximal number of positive, independent critical escape rates, where

two rates x and y are *dependent* if $x = d^n y$ for some $n \in \mathbb{Z}$. In other words, it is the number of grand orbits of positive critical escape rates $\{G_f(c) : f'(c) = 0 \text{ and } c \in X(f)\}$ under multiplication by d on $(0, \infty)$.

The *maximal critical escape rate* is the value

$$M(f) = \max\{G_f(c) : f'(c) = 0\}.$$

It is zero if and only if f has connected Julia set, and if and only if $(f, X(f))$ is conformally conjugate to $(z^d, \{|z| > 1\})$.

The basin $X(f)$ is naturally equipped with a holomorphic 1-form

$$\omega_f = 2i \partial G_f.$$

It follows that $|\omega_f|$ gives a locally Euclidean metric on $X(f)$ away from its zeros, which are the critical points in $X(f)$ and their iterated preimages. The functional equation $G_f(f(z)) = d G_f(z)$ implies that

$$\frac{1}{d} f^* \omega = \omega$$

and hence away from zeros of ω , with respect to the metric $|\omega|$, the map f is locally a homothety with constant expansion factor d . Since $G_f(z) \sim \log |z| + O(1)$ (see [21, §9]) as $z \rightarrow \infty$, each level curve $\{z \in X(f) : G_f(z) = c\}$ has length 2π in the metric $|\omega|$.

2.2. The cubic pictograph, simplified form

Now assume that f is a polynomial of degree 3 with maximal critical escape rate $M(f) > 0$. Label the critical points of f as c_1 and c_2 so that $G_f(c_1) \geq G_f(c_2)$. The *length* $L(f)$ of the polynomial f is the least integer l so that

$$G_f(f^l(c_2)) \geq G_f(c_1).$$

If no such integer exists, then we set $L(f) = \infty$; this occurs if and only if the orbit of c_2 is bounded.

The *simplified pictograph* of f is a column of $\max\{L(f), 1\}$ diagrams, each consisting of the unit circle and a finite collection of hyperbolic geodesics in the unit disk, together with a collection of non-negative integers; see Figures 2.1–2.3. These integers, or *labels*, either label regions in the disk bounded by geodesics, or label particular points on the unit circle. We emphasize that rotating a diagram leaves it unchanged: our unit circles do not have coordinates. The diagrams are constructed as follows.

Let L_0 be the level set

$$L_0 = \{z : G_f(z) = G_f(c_1)\}.$$

For length $L(f) > 1$ and each $0 < i < L(f)$, let L_i be the connected component of the level set

$$\{z : G_f(z) = G_f(c_1)/d^i\}$$

that separates the critical point c_2 from ∞ . Each L_i inherits a metric from $|\omega_f|$ (or equivalently from external angles) that we normalize by scaling to have total length 2π . Its orientation in the plane induces an oriented parameterization by arc length of a circle. It is important to note that we *forget the marking by external angles and fix any choice of parametrization by arc length* from $S^1 = \mathbb{R}/2\pi\mathbb{Z}$ to L_i , respecting the orientation.

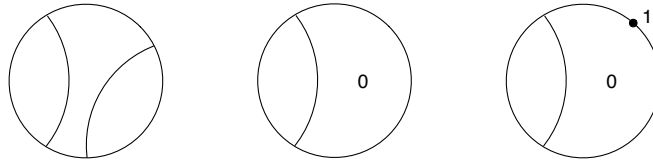


FIGURE 2.1. The simplified pictographs for three cubic polynomials of lengths 0 and 1. Left: an example with length 0; i.e., with $G_f(c_2) = G_f(c_1)$. Center: the simplified pictograph of every cubic polynomial of length 1 and $G_f(c_1) > G_f(c_2) > G_f(c_1)/3$. Right: an example of a length 1 cubic polynomial with $G_f(c_2) = G_f(c_1)/3$; as we shall see, the location of the dot on the circle, relative to the hyperbolic geodesic, distinguishes the topological conjugacy class of f in this setting.

We represent each L_i independently as a unit circle in the plane. With respect to the chosen parametrization, we draw hyperbolic geodesics between pairs of points that are identified in L_i . For example, for every cubic polynomial f with length $L(f) > 0$, the curve L_0 is represented by a disk with a single hyperbolic geodesic partitioning the unit circle into arcs of length $4\pi/3$ and $2\pi/3$, as in the two right-hand diagrams of Figure 2.1. Because the parametrization was arbitrary, any rotation of the disk with its drawn-in geodesics is considered an equivalent presentation of L_i .

We refer to this circular diagram of L_i , determined uniquely up to rotation, as the *finite lamination* of f at level i . The hyperbolic geodesics partition the unit disk into finitely many connected components. Each open component with boundary of positive length in the circle is called a *gap* of the lamination. The gaps correspond to the bounded, connected components of $\mathbb{C} \setminus L_i$ in the plane.

It remains to define the labeling of the finite laminations. The symbols introduced will represent the locations of the points $f^k(c_2)$ for each $k \leq L(f)$. If $L(f) = 0$, no labellings are necessary.

Now assume $L(f) > 0$ and fix $0 \leq i < L(f)$. With respect to the chosen parametrization $S^1 \rightarrow L_i$, mark a point on the circle S^1 with a dot, and label this point by the integer $k \geq 0$ if $f^k(c_2)$ is equal to that point in L_i . Label a gap with the integer k if $f^k(c_2)$ lies in that connected component of $\mathbb{C} \setminus L_i$.

We have now constructed $\max\{L(f), 1\}$ labeled lamination diagrams. We organize these labeled lamination diagrams into a column, with L_0 at the top and $L_{L(f)-1}$ at the bottom (if $L(f) < \infty$). This column of diagrams is called the *simplified pictograph* of the cubic polynomial f .

2.3. Examples of simplified pictographs

In Figures 2.1, 2.2, and 2.3, we provide examples of simplified pictographs for cubic polynomials of lengths $L(f) = 0, 1, 2, 3$. The pictograph is defined in Section 10; the reader should then compare Figure 2.3 to the (unsimplified) pictograph of the same polynomial in Figure 10.2.

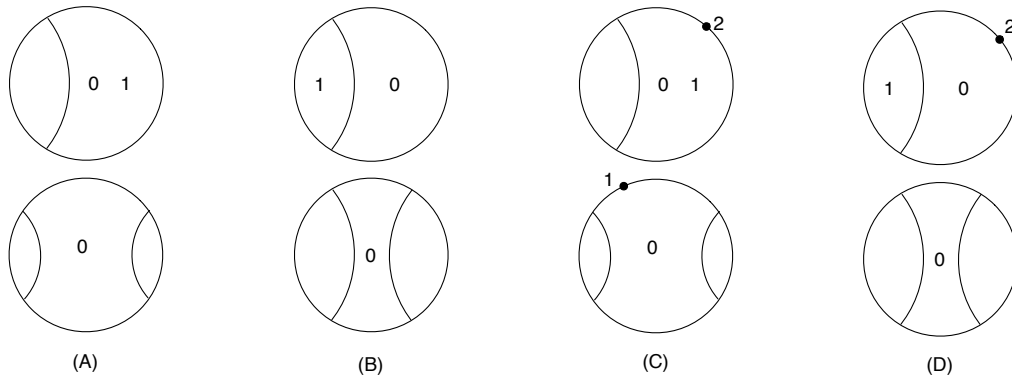


FIGURE 2.2. The simplified pictographs for four cubic polynomials of length 2. (A, B): Every cubic polynomial with $G_f(c_1)/3 > G_f(c_2) > G_f(c_1)/9$ will have one of these two simplified pictographs. (C, D): Examples for length 2 polynomials with $G_f(c_2) = G_f(c_1)/9$.

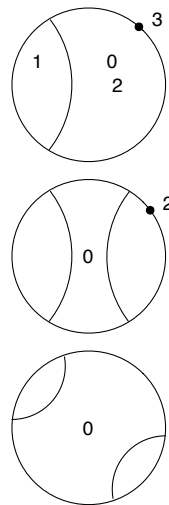


FIGURE 2.3. The simplified pictograph for a cubic polynomial of length 3, with $G_f(c_2) = G_f(c_1)/27$. (Its full pictograph is shown in Figure 10.2.)

3. More examples in degree 3: A comparison of invariants

In this section, we compare the simplified pictographs of §2.2 to the tableaux of [5] (equivalently, the Yoccoz τ -sequences) and the trees of [10]. We show how to compute the τ -sequence and the tree code from the simplified pictograph. (In [10], it was shown that the τ -sequence can be computed from the tree code of a cubic polynomial, and a tree code uniquely characterizes a cubic tree up to the choice of critical escape rates, which amounts to fixing a metric on the tree.)

To illustrate the distinction between the invariants—trees being strictly finer than tableaux, pictographs being strictly finer than trees—we include examples showing the existence of cubic polynomials with

1. the same tableau (or τ -sequence) but different trees (F, T) ,
2. the same tree (F, T) but different pictographs, and
3. the same pictographs but different topological conjugacy classes.

The examples we provide are structurally stable in the shift locus and have minimal length in the sense of §2.2, and so these provide the simplest possible examples.

In the remainder of this section, we show how the τ -function of [5] and tree code of [10] may be computed from the data of the simplified pictograph. The reader not familiar with these invariants may take our results as their definition. Later on in §11.5, however, we do give the definition of the τ -sequence of a cubic polynomial as part of our discussion of counting topological conjugacy classes of cubics. Further results on trees will appear in Section 6.

3.1. From simplified pictographs to trees and tableaux

Fix a cubic polynomial with length $L(f)$. The τ -sequence is a certain sequence of non-negative integers of length $L(f)$; see §11.5 (or [5]) for its definition. Here, we give an equivalent version, using the language of simplified pictographs. For $L(f) = 0$, the τ -sequence is an empty sequence. We have $\tau(1) = 0$ for every polynomial with length $L(f) > 0$. For $L(f) > 1$ and each $0 < n < L(f)$, it is immediate from the definitions that

$$\tau(n) = \max\{j : \text{lamination at level } j \text{ is labeled by } (n - j)\}.$$

To compute $\tau(L(f))$, we consider the set

$$\mathcal{L} = \{j : \text{the central gap in lamination at level } j \text{ is labeled by } (L(f) - j - 1)\},$$

where the central gap of the lamination is the gap containing the symbol 0. We then have

$$\tau(L(f)) = \begin{cases} 1 + \max\{j : j \in \mathcal{L}\} & \text{if } \mathcal{L} \neq \emptyset, \\ 0 & \text{if } \mathcal{L} = \emptyset. \end{cases}$$

As an example, the τ -sequence for the simplified pictograph of Figure 2.3 is 0, 0, 1.

The *tree code* for a cubic polynomial of length $L(f)$ is a certain sequence of pairs $(k(i), t(i))$, where i ranges from 1 to $L(f)$, defined in [10, §11]. A *minimal symbol* in a gap of a lamination in the simplified pictograph of f is the smallest integer in a labeled gap. The *lifetime* $k(i)$ is equal to the number of times the symbol j appears as a minimal symbol in a gap at level $i - j - 1$, as j ranges from 0 to $i - 1$. In particular, $k(1) = 1$. The *terminus* $t(i)$ is computed as follows:

1. let $j(i)$ be the smallest j which appears at level $i - j - 1$ but is *not* a minimal symbol. If such a j does not exist, then let $j(i) = i$;
2. let $m(i)$ be the minimal symbol at level $i - j(i) - 1$ in the gap containing $j(i)$. When $j(i) = i$, set $m(i) = 0$;
3. let $t(i) = i - j(i) + m(i)$.

As an example, the tree code for the simplified pictograph of Figure 2.3 is (1, 0), (2, 0), (1, 1).

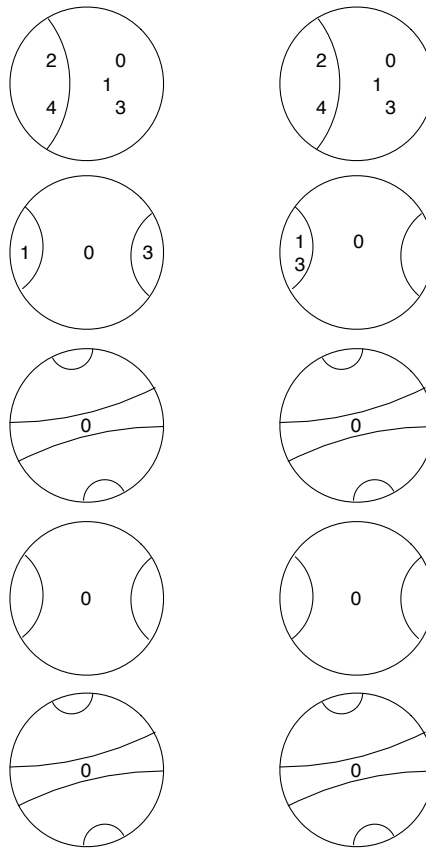


FIGURE 3.1. Simplified pictographs associated to two different trees with the same τ -sequence 0, 1, 0, 1, 0.

3.2. Examples from Figures 3.1, 3.2, and 3.3

Figure 3.1 shows two simplified pictographs. Using the computation of §3.1, we find their tree codes are

$$(1, 0), (1, 1), (3, 0), (1, 1), (2, 3)$$

for the pictograph on the left, and

$$(1, 0), (1, 1), (3, 0), (1, 1), (1, 3)$$

for the pictograph on the right. These examples are also presented in [10, §11]. Since tree codes characterize cubic trees [10, Theorem 11.3], this shows their trees are different. However, the τ -sequence for each simplified pictograph is 0, 1, 0, 1, 0.

Figure 3.2 shows two inequivalent simplified pictographs associated to the same tree. The tree code for these pictographs is

$$(1, 0), (1, 1), (1, 2), (4, 0), (1, 1), (1, 2), (3, 4).$$

The difference in the pictographs is in the relative locations of the first and fourth iterates of critical point c_2 in the lamination at level 2.

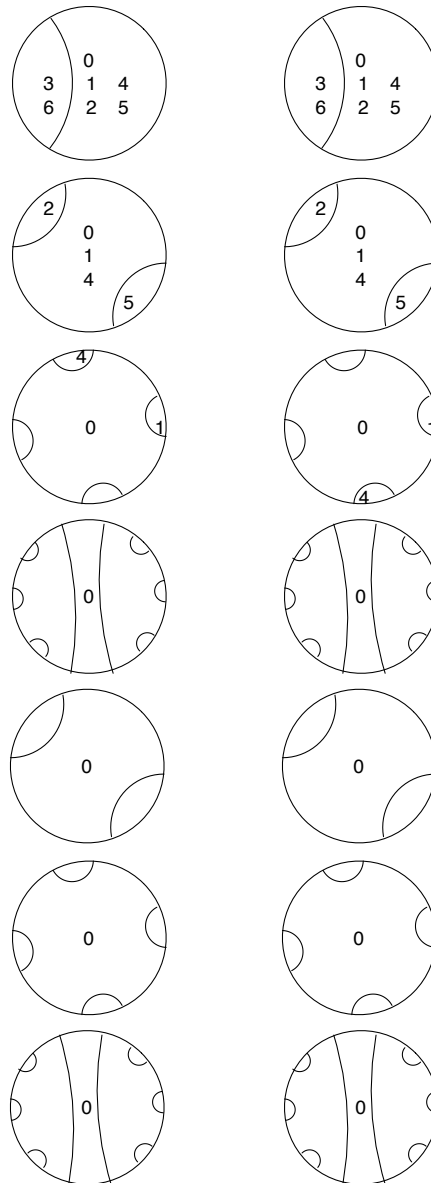


FIGURE 3.2. Inequivalent simplified pictographs associated to the same tree. The two pictographs differ in the cyclic ordering of the 1 and 4 at level 2 (the third lamination).

Figure 3.3 gives an example of a single simplified pictograph determining exactly two distinct conjugacy classes. The τ -sequence for this example is $0, 0, 1, 2, 0$. Following the algorithm presented in Theorem 4.1, we first enumerate the marked levels $l_0 = 0, l_1 = 2$; then compute the sums of relative moduli $m_0 = 0, m_1 = 1$; then compute $t_0 = 1, t_1 = 1$.

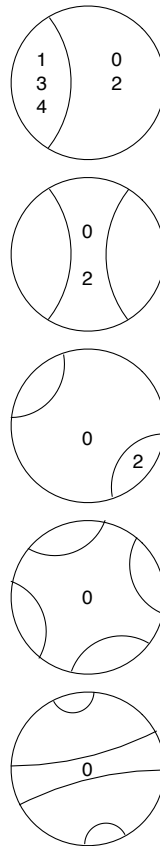


FIGURE 3.3. Simplified pictograph of length 5 determining exactly two topological conjugacy classes.

The number of conjugacy classes is the maximum of $2^0/1$ and $2^1/1$; therefore there are two conjugacy classes determined by this pictograph.

It is not hard to show that these examples are the shortest of their type; that is, any τ -sequence giving rise to more than one tree must have length ≥ 5 ; any two pictographs giving rise to the same tree must have length ≥ 7 ; any pictograph giving rise to more than one conjugacy class must have length ≥ 5 . Indeed, one can easily compute by hand all combinatorial possibilities to length 6. An enumeration of all admissible τ -sequences, simplified pictographs, and (structurally stable) topological conjugacy classes to length 21 is given in [9], implementing an algorithm derived from Theorem 4.1, while an enumeration of all cubic trees to length 17 was presented in [10].

4. The counting theorems in degree 3

In this section, we give a more precise statement of Theorem 1.2 in the case of cubic polynomials. It provides the computation of $\text{Top}(\mathcal{D})$, the number of topological conjugacy classes of basins $(f, X(f))$ with a given simplified pictograph \mathcal{D} in degree 3. The proofs are

given later, in Section 11, after describing the construction of the pictograph in all degrees. The formulas build upon the expansive treatment of cubic polynomials in [4], [5] and the encoding of the cubic trees in [10]. (The proofs of the theorems also use arguments of Branner in [3, Theorem 9.1] and Harris in [12].)

Figure 3.3 shows an example of a simplified pictograph that corresponds to exactly two topological conjugacy classes. We conclude this section with an example of a pictograph corresponding to infinitely-many topological conjugacies that organize themselves into exactly two *solenoids* in the moduli space \mathcal{M}_3 of cubic polynomials.

4.1. Computing the number of topological conjugacy classes in degree 3

To state the two theorems, we need a few more definitions. As in §2.2, we assume that f is a cubic polynomial with a disconnected Julia set, so at least one critical point lies in the basin $X(f)$. We label the two critical points of f by c_1 and c_2 so that $G_f(c_1) \geq G_f(c_2)$. Let $L(f)$ be the length of f , defined as the least integer so that $G_f(c_2) \geq G_f(c_1)/3^{L(f)}$. For each integer $0 < l \leq L(f)$, there is a unique connected component P_l of $\{z \in X(f) : G_f(z) < G_f(c_1)/3^{l-1}\}$ containing c_2 . Let $B_l \subset P_l$ be the closed subset where $G_f(z) \leq G_f(c_1)/3^l$. A *marked level* is an integer $0 < l < L(f)$ where the orbit of c_2 intersects $B_l \setminus P_{l+1}$. We remark that this concept appears elsewhere under different names: marked levels are called *semi-critical* in [20], and are called *off-center* in [3, Theorem 9.1] when the polynomials f have infinite length. Marked levels can be read from the pictograph, and in fact, from the underlying τ -sequence; see Lemma 11.4.

Let

$$A_0 = \{z : G_f(c_1) < |z| < 3G_f(c_1)\}$$

denote the *fundamental annulus*. For each $0 < n < L(f)$, denote by A_n the annular component of $\{G_f(c_1)/3^n < |z| < G_f(c_1)/3^{n-1}\}$ separating the two critical points (these are not the fundamental subannuli of §9.1). For each $0 \leq n < L(f)$, the *relative modulus* at level n is the ratio

$$m(n) = \text{mod}(A_n) / \text{mod}(A_0).$$

The value $m(n)$ is also completely determined by the τ -sequence of f ; in fact, $m(n) = 2^{-k(n)}$, where $k(n)$ is the number of times the orbit of A_n surrounds the critical point before landing on A_0 .

THEOREM 4.1. – *Suppose \mathcal{D} is a degree 3 simplified pictograph with finitely many marked levels. The number of topological conjugacy classes of basins $(f, X(f))$ with pictograph \mathcal{D} is*

$$\text{Top}(\mathcal{D}) = \max_j \frac{2^j}{\max\{t_i : i \leq j\}},$$

where

1. the marked levels are indexed as $\{l_j\}_{j \geq 1}$, in increasing order;
2. for each j , we let m_j be the sum of the relative moduli $\sum_{l=1}^{l_j} m(l)$; and
3. t_j is the smallest positive integer for which $t_j m_j$ is integral.

If there are no marked levels, then $\text{Top}(\mathcal{D}) = 1$. The computation of $\text{Top}(\mathcal{D})$ depends only on the τ -sequence of \mathcal{D} .

The hypothesis of Theorem 4.1 is clearly satisfied for all polynomials in the shift locus, because their pictographs have finite length. Recall that in that case, by rigidity of $X(f)$, the holomorphic conjugacy class of a basin $(f, X(f))$ determines the holomorphic conjugacy class of the polynomial itself.

In [9], an explicit algorithm is developed and implemented using Theorem 4.1 to enumerate all topological conjugacy classes of a given length in the shift locus of cubic polynomials. In particular, the algorithm includes an enumeration of all τ -sequences of a given finite length, followed by the enumeration of all possible pictographs (for structurally stable polynomials) associated to a given τ -sequence.

4.2. Solenoids

Branner and Hubbard showed there exist examples where the set of polynomials with a given tableau and maximal escape rate forms solenoids in the moduli space of cubic polynomials containing infinitely many distinct topological conjugacy classes. They construct the “Fibonacci solenoid” in [5], based on the combinatorics of the Fibonacci numbers. In [3], Branner proved that there is exactly one (connected) Fibonacci solenoid in the moduli space \mathcal{M}_3 of cubic polynomials. Here, we explain how to compute the number of solenoids associated to a given pictograph (from which can be computed the number of solenoids associated to a given tableau, when combined with [9, Theorem 3.1]). We use the notation of Theorem 4.1.

THEOREM 4.2. – *Suppose \mathcal{D} is a degree 3 pictograph with infinitely many marked levels. Then there are infinitely many topological conjugacy classes of cubic polynomials with pictograph \mathcal{D} . Fixing the maximal critical escape rate $M > 0$, either*

- (a) $\sup_j t_j = \infty$ and the conjugacy classes form

$$\text{Sol}(\mathcal{D}) = \sup_j \frac{2^j}{\max\{t_i : i \leq j\}}$$

solenoids in the moduli space \mathcal{M}_3 ; or

- (b) $\sup_j t_j < \infty$ and each conjugacy class is homeomorphic to a circle.

The computation of $\sup_j t_j$ and $\text{Sol}(\mathcal{D})$ depends only on the τ -sequence of \mathcal{D} .

4.3. Two-solenoid example

This example is similar to the Fibonacci solenoid of [5], but here we provide a τ -sequence that determines a unique pictograph and exactly two solenoids in \mathcal{M}_3 . Let $l_0 = 0, l_1 = 2, l_2 = 4$, and $l_j = 2l_{j-1} + 1$ for all $j > 2$. Consider the τ -sequence given by

$$0, 0, 1, 2, 0, 1, 2, 3, 4, 0, 1, 2, \dots, 9, 0, 1, 2, \dots, 19, 0, 1, \dots, l_5, 0, 1, \dots, l_6, 0, 1, \dots$$

More precisely, we have

$$\tau(1) = 0$$

and

$$\tau(n) = n - 2 - j - (l_1 + l_2 + \dots + l_j)$$

for $j + 1 + l_1 + l_2 + \dots + l_j < n \leq j + 2 + l_1 + l_2 + \dots + l_{j+1}$. It can be proved inductively that this sequence determines a unique pictograph; see [9, Theorem 3.1]. The first five laminations of

the simplified pictograph (for the truncated τ -sequence $0, 0, 1, 2, 0$) are shown in Figure 3.3. The marked levels are given by the sequence $\{l_j : j > 0\}$. Computing inductively, the relative moduli sums are $m_1 = 1, m_2 = 3/2$, and $m_j = m_{j-1} + 1/2 + m_{j-1}/2$ for all $j > 2$. Therefore $t_1 = 1, t_2 = 2$, and $t_j = 2^{j-1}$ for all j . The numbers $\max\{t_i : i \leq j\} = 2^{j-1}$ are unbounded, and Theorem 4.2 implies that this τ -sequence determines

$$\lim_{j \rightarrow \infty} 2^j / 2^{j-1} = 2$$

solenoids in the moduli space \mathcal{M}_3 .

5. Local models and finite laminations

In this section, we first recall and then further develop some notions from [8, §4].

A *local model surface* (X, ω) is a pair consisting of a planar Riemann surface X and a holomorphic 1-form ω on X that satisfies certain properties. A *local model map* is a holomorphic branched cover

$$(Y, \eta) \rightarrow (X, \omega)$$

between local model surfaces. Local model maps arise as particular restrictions of a polynomial branched cover $f : \mathbb{C} \rightarrow \mathbb{C}$. Here, we introduce *finite laminations* and *branched covers of finite laminations* as combinatorial representations of local model maps. The main result of this section is

- THEOREM 5.1.** – 1. *A local model surface (X, ω) is uniquely determined, up to isomorphism, by its associated lamination and the heights of its inner and outer annuli.*
 2. *A local model map $(Y, \eta) \rightarrow (X, \omega)$ is uniquely determined, up to post-composition by an isomorphism of (X, ω) , by the data consisting of the lamination associated to (Y, η) , the heights of its inner and outer annuli of (Y, η) , and its degree.*

5.1. Local models

A *local model surface* is a pair (X, ω) consisting of a planar Riemann surface X and holomorphic 1-form ω on X obtained in the following manner. Begin with a slit rectangle in the plane

$$R = \{x + iy : 0 < x < 2\pi, h_{\min} < y < h_{\max}\} \setminus \Sigma,$$

where Σ is a (possibly empty) finite union of vertical slits of the form

$$\Sigma_j = \{x + iy : x = x_j, h_{\min} < y \leq c_0\}$$

for a distinguished value of $c_0 \in (h_{\min}, h_{\max})$. We think of R as the interior of a polygon. Each slit defines a pair of sides of this polygon. On the left-hand vertical side of R , the vertical segment joining the two points $h_{\min}i$ and c_0i on the imaginary axis is a side, as is the vertical segment joining c_0i and $h_{\max}i$. Similarly, on the right-hand vertical side of R , the vertical segment joining $2\pi + h_{\min}i$ and $2\pi + c_0i$ is a side, as is the vertical segment joining $2\pi + c_0i$ and $2\pi + h_{\max}i$. Given a collection of horizontal translations that identify sides in pairs, the corresponding quotient space obtained by gluing sides via these translations is a local model surface. The 1-form ω is then defined by dz in the coordinates on R . The y -coordinate in the rectangular representation induces a *height function* $h : X \rightarrow \mathbb{R}$. The *central leaf* L_X of the

local model surface is the level set $\{z : h(z) = c_0\}$ containing all (if any) zeros of ω ; these are the images of the topmost points of the slits. The complement $X \setminus L_X$ is a disjoint union of the *outer annulus* given by the quotient of $\{c_0 < y < h_{\max}\}$ and finitely many *inner annuli* given by the quotient of $\{h_{\min} < y < c_0\}$. For convenience, we often suppress mention of the 1-form and write simply X for (X, ω) .

Note that the rectangular coordinates can be recovered up to a translation from the pair (X, ω) via integration $\varphi(z) = \int_{z_0}^z \omega$, and the height function is given by $h(z) = \text{Im } \varphi(z)$, up to the addition of a real constant.

A *local model map* (or simply a *local model*) is a branched cover between local model surfaces

$$f : (Y, \eta) \rightarrow (X, \omega)$$

such that

$$\eta = \frac{1}{\deg f} f^* \omega$$

and f sends the central leaf of Y to the central leaf of X . In [8, Lemma 4.2], we observed that every local model arises as the restriction of a polynomial branched cover $f : (\mathbb{C}, \eta) \rightarrow (\mathbb{C}, \omega)$ for a meromorphic 1-form ω having purely imaginary residue at each of its poles.

An *isomorphism* of local model surfaces is a degree 1 local model map.

5.2. Finite laminations

Let C be an oriented Riemannian 1-manifold, isometric to $\mathbb{R}/2\pi\mathbb{Z}$ with the standard metric and affine structure. A *finite lamination* is an equivalence relation L on C such that

1. each equivalence class is finite,
2. all but finitely many classes are trivial (consist only of one element), and
3. classes are *unlinked*.

The third condition means that if two pairs of equivalent points $\{a, b\}$ and $\{c, d\}$ lie in distinct equivalence classes, then a and b are in the same connected component of $C \setminus \{c, d\}$. We will deal exclusively with finite laminations, so we henceforth drop the adjective “finite”. More general types of laminations play a crucial role in the classification of the dynamics of polynomials; cf. [25], [15].

A lamination is conveniently represented by a planar *lamination diagram*, defined as follows. Given a lamination on the circle C , choose an orientation-preserving, isometric identification of C with $S^1 = \{z \in \mathbb{C} : |z| = 1\} = \partial\mathbb{D}$. For each nontrivial equivalence class, join pairs of points in this class that are consecutive in the cyclic order on C by the hyperbolic geodesic ending at those points, as in Figure 5.1. Condition (3) that classes are unlinked guarantees that the hyperbolic geodesics do not intersect.

Two laminations are *equivalent* if there exists an orientation-preserving isometry (i.e., rotation) of their underlying circles taking one to the other. Thus, there is no distinguished marking by angles on the circle C .

Clearly, laminations are determined by their lamination diagrams.

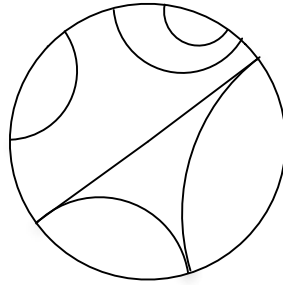


FIGURE 5.1. A finite lamination with four non-trivial equivalence classes.

5.3. Laminations and local model surfaces

Let (X, ω) be a local model surface, and let L_X be its central leaf. The 1-form ω induces an orientation and length-function on L_X , giving it the structure of the quotient of a circle by a finite lamination. Therefore, there is a uniquely determined finite lamination associated to the local model surface (X, ω) .

LEMMA 5.2. – *A finite lamination L determines a local model surface (X, ω) , up to the heights of its inner and outer annuli.*

Proof. – As we defined in §5.1, a local model surface is determined by its rectangular representation. For any values $-\infty \leq h_{\min} < c_0 < h_{\max} \leq \infty$, we can construct a surface (X, ω) from the rectangle $\{0 < x < 2\pi, h_{\min} < y < h_{\max}\}$ with central leaf determining the lamination L . Indeed, choose any point on the circle C to represent the edges $\{x = 0 = 2\pi\}$. For each point on C in a non-trivial equivalence class, place a vertical slit from the bottom to height $y = c_0$. Vertical edges leading to points in an equivalence class are paired by horizontal translation if they are joined by a hyperbolic geodesic in the diagram for L . The unlinked condition in the definition of the finite lamination guarantees that X is a planar Riemann surface. The 1-form dz on the rectangle glues up to define the form ω . It is immediate to see that the local model surface (X, ω) is determined up to isomorphism, once the values of h_{\min} , c_0 , and h_{\max} have been chosen. \square

5.4. Branched covers of laminations

See Figure 5.2. If L_1 and L_2 are finite laminations, a *branched covering* $\delta : L_1 \rightarrow L_2$ is an orientation-preserving covering map $\delta : C_1 \rightarrow C_2$ on their underlying circles such that

1. δ is affine; i.e., $\delta(t) = ((\deg \delta) t + c) \bmod 2\pi$ where each $C_i \simeq \mathbb{R}/2\pi\mathbb{Z}$;
2. for each equivalence class A of L_1 , the image $\delta(A)$ is equal to an (entire) equivalence class of L_2 ; and
3. δ is *consecutive-preserving*.

Consecutive-preserving means that for each equivalence class A of L_1 , either the image class $\delta(A)$ is trivial, or consecutive points $x, y \in A$ (with respect to the cyclic ordering on A) are sent to consecutive points $\delta(x), \delta(y)$ in $\delta(A)$.

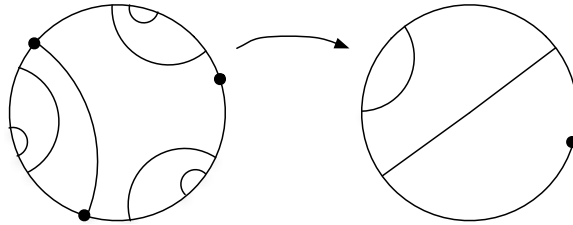


FIGURE 5.2. A degree 3 branched cover of laminations. The three marked points on the left are sent to the marked point on the right.

LEMMA 5.3. – *A branched cover of laminations is determined by its domain and degree, up to symmetries. More precisely, given branched covers $\delta : L_1 \rightarrow L_2$ and $\rho : M_1 \rightarrow M_2$ of the same degree, and given an isometry $s_1 : L_1 \rightarrow M_1$, there exists a unique isometry $s_2 : L_2 \rightarrow M_2$ such that the diagram*

$$\begin{array}{ccc}
 L_1 & \xrightarrow{s_1} & M_1 \\
 \delta \downarrow & & \downarrow \rho \\
 L_2 & \xrightarrow{s_2} & M_2
 \end{array}$$

commutes.

Proof. – The lamination diagram of L_2 is determined by L_1 and the degree; indeed, the rules for a branched covering determine the equivalence classes of L_2 , as the images of those of L_1 . By hypothesis, there exists an isometry $s_1 : L_1 \rightarrow M_1$ taking equivalence classes to equivalence classes, and δ and ρ have the same degree. Therefore, there exists an isometry $r_2 : L_2 \rightarrow M_2$.

Note that any branched cover $L_1 \rightarrow L_2$ of degree d is determined by the image of a single point; this is because, in suitable coordinates, the covering is given by $t \mapsto d t$. Now, suppose there exists an equivalence class x in L_1 such that $r_2 \circ \delta(x) \neq \rho \circ s_1(x)$ in M_2 . Combining the above facts, there is a uniquely determined symmetry $s : M_2 \rightarrow M_2$ sending $r_2 \circ \delta(x)$ to $\rho \circ s_1(x)$. We conclude that $s \circ r_2 \circ \delta = \rho \circ s_1$. Set $s_2 = s \circ r_2$. \square

In the proof of Theorem 1.2, we will need to compute orders of rotation symmetry of certain lamination diagrams and record how these symmetry orders transform under branched covers.

LEMMA 5.4. – *Let $\delta : L_1 \rightarrow L_2$ be a branched cover of laminations of degree d . If L_1 has a rotational symmetry of order k , then L_2 has a rotational symmetry of order $k / \gcd(k, d)$.*

Proof. – Suppose $s_1 : L_1 \rightarrow L_1$ is a symmetry of order k , so it rotates the circle underlying L_1 by $2\pi/k$. By Lemma 5.3, there exists a unique rotational symmetry $s_2 : L_2 \rightarrow L_2$ so the diagram

$$\begin{array}{ccc}
 L_1 & \xrightarrow{s_1} & L_1 \\
 \delta \downarrow & & \downarrow \delta \\
 L_2 & \xrightarrow{s_2} & L_2
 \end{array}$$

commutes. Fix coordinates on L_1 and L_2 so $\delta(t) = dt \bmod 2\pi$. As s_1 is a translation by $2\pi/k$, it follows that s_2 is a translation by $2\pi d/k \bmod 2\pi$. Therefore, s_2 is a symmetry of order $k/\gcd(k, d)$. \square

5.5. Gaps and local degrees

Suppose L is a finite lamination. For each equivalence class of L , its hyperbolic convex hull is either empty (if the class consists of a single point), a hyperbolic geodesic (if the class consists of two points), or an ideal polygon in the disk. Let \hat{L} denote the union of these hyperbolic convex hulls. A *gap* of L is a connected component $G \subset \mathbb{D}$ of the complement of \hat{L} . We remark that our terminology conflicts with that of [25]; when an equivalence class consists of three or more points, we do not consider the ideal polygon it bounds in the disk as a gap. The *ideal boundary* ∂G of a gap G is the interior of $\overline{G} \cap S^1$ in S^1 . Thus, the ideal boundary ∂G is a maximal open subset of the circle such that any pair of points in it is unlinked with any pair of points that are equivalent under the relation defined by L . Given L , it is clear that a gap G is determined by its ideal boundary ∂G , and conversely.

The following lemmas are immediate from the definitions.

LEMMA 5.5. – *Suppose $\delta : L_1 \rightarrow L_2$ is a branched cover of laminations and G_1 is a gap of L_1 . Then there is a unique gap G_2 of L_2 with $\overline{\partial G_2} = \delta(\overline{\partial G_1})$. In other words, δ takes the closure of the ideal boundary of a gap surjectively to the closure of the ideal boundary of a gap.*

Note that δ need not take the ideal boundary of a gap onto the ideal boundary of a gap. An example is shown in Figure 5.2.

Lemma 5.5 shows that a branched cover $\delta : L_1 \rightarrow L_2$ induces a function from ideal boundaries of gaps of L_1 to ideal boundaries of gaps of L_2 . Since gaps are determined by their boundaries, δ induces a function from gaps of L_1 to gaps of L_2 . If G is a gap of L_1 , we denote the gap of L_2 to which it corresponds under δ by δG . We call δG the *image* of G under δ —even though we have not extended δ over \mathbb{D} . Below, by topological degree of a map, we mean the maximum cardinality of a fiber.

LEMMA 5.6 (and definition). – *Suppose $\delta : L_1 \rightarrow L_2$ is a branched cover of laminations, and G is a gap of L_1 . The local degree of δ at G is defined as*

$$\deg(\delta, G) = \frac{\deg(\delta)|G|}{|\delta G|},$$

where $|G|$ is the length of ∂G . The quantity $\deg(\delta, G)$ is a positive integer which coincides with the topological degree of the restriction $\delta|_{\partial G}$.

LEMMA 5.7 (and definition). – *Suppose $\delta : L_1 \rightarrow L_2$ is a branched cover of laminations, and A is an equivalence class of L_1 . The local degree of δ at A is defined as*

$$\deg(\delta, A) = \frac{\#A}{\#\delta(A)}.$$

The quantity $\deg(\delta, A)$ is a positive integer and coincides with the topological degree of the restriction $\delta|_A$.

5.6. Critical points of a lamination branched cover

Suppose $\delta : L_1 \rightarrow L_2$ is a branched cover of laminations. A gap G of L_1 we call *critical* if $\deg(\delta, G) > 1$. Similarly, an equivalence class A of L_1 we call *critical* if $\deg(\delta, A) > 1$. Abusing terminology, we refer to critical gaps and critical equivalence classes as *critical points* of δ .

LEMMA 5.8. – *The total number of critical points of a branched cover δ , computed by*

$$\sum_{\text{classes } A} (\deg(\delta, A) - 1) + \sum_{\text{gaps } G} (\deg(\delta, G) - 1),$$

is equal to $\deg \delta - 1$.

Proof. – By collapsing equivalence classes to points, a lamination determines, and is determined by, a planar, tree-like 1-complex with a length metric of total length 2π . Tree-like means that it is the boundary of the unique unbounded component of its complement. A branched covering determines, and is determined up to equivalence by, a locally isometric branched covering map between such complexes which extends to a planar branched covering in a neighborhood. This lemma therefore follows from the usual Riemann-Hurwitz formula. \square

5.7. Branched covers of laminations and local models

Let $f : (Y, \eta) \rightarrow (X, \omega)$ be a local model map. Let L_Y and L_X denote the finite laminations associated to the central leaves of Y and X . It is immediate to see that f induces a branched cover of laminations $L_Y \rightarrow L_X$.

Conversely, we have:

LEMMA 5.9. – *A branched cover of finite laminations $\delta : L_1 \rightarrow L_2$ determines a local model map, up to the heights of the inner and outer annuli of the local model surfaces.*

Proof. – Let $\delta : L_1 \rightarrow L_2$ be a branched cover of laminations of degree k . By Lemma 5.2, we may construct, for each $i = 1, 2$, a local model surface (X_i, ω_i) so that its central leaf is identified with the lamination L_i ; we may choose the heights of the inner and outer annuli to be $h_{\min} = -\infty$ and $h_{\max} = +\infty$ for $i = 1, 2$. Because the height function is fixed, up to an additive constant, the surface (X_i, ω_i) is uniquely determined. By choosing both h_{\min} and h_{\max} to be infinite, each inner annulus (X_i, ω_i) is isomorphic to the punctured disk $\{0 < |z| < 1\}$ equipped with the 1-form $ri dz/z$, where $r > 0$ is the length of the corresponding gap in L_i , while the outer annulus of (X_i, ω_i) is isomorphic to the punctured disk $\{1 < |z| < \infty\}$ equipped with the 1-form $i dz/z$.

In these punctured-disk local coordinates, we extend δ by z^k , sending the outer annulus of X_1 to that of X_2 . For each gap G of L_1 , we extend δ by $z^{\deg(\delta, G)}$ in its punctured-disk coordinates. The local degree $\deg(\delta, G)$ is well-defined by Lemma 5.6, and the extension is well-defined by Lemma 5.5. By construction, we obtain a branched cover $f : (X_1, \omega_1) \rightarrow (X_2, \omega_2)$ of degree k such that $f^*\omega_2 = k\omega_1$ and f induces the lamination branched cover $\delta : L_1 \rightarrow L_2$.

Note that finite choices of heights h_{\min} and h_{\max} give rise to local model maps that are restrictions of the constructed f . In this case, there is a compatibility condition on

the heights: if an annulus has finite modulus m , then any degree k cover is an annulus of modulus m/k . If the domain surface (X_1, ω_1) has central leaf at height $h_0 \in \mathbb{R}$, and $h_{\min} = h_{-1}$ and $h_{\max} = h_1$, then the image surface (X_2, ω_2) will have outer annulus of height $k(h_1 - h_0)$ and inner annuli of height $k(h_0 - h_{-1})$. \square

Proof of Theorem 5.1. – The first conclusion is the content of Lemma 5.3. More functorially, an isometry between local model surfaces is determined by its restriction to the corresponding central leaves, so in particular the group of isometric symmetries of a local model surface is faithfully represented by the group of symmetries of its lamination. More generally, since a branched cover $(Y, \eta) \rightarrow (X, \omega)$ in local Euclidean coordinates has differential a multiple of the identity, it is also determined by its restriction to the associated central leaves. The second conclusion then follows from Lemma 5.9. \square

6. Polynomial trees

Suppose f is a polynomial and $X(f)$ its basin of infinity. By collapsing components of level sets of the Green's function $G_f : X(f) \rightarrow (0, \infty)$ to points, we obtain a quotient map $X(f) \rightarrow T(f)$ from $X(f)$ onto $T(f)$ that yields a semiconjugacy from the holomorphic map $f : X(f) \rightarrow X(f)$ to a map $F : T(f) \rightarrow T(f)$. The tree $T(f)$ inherits both a length metric structure and a simplicial structure. Metrically, F expands each edge of $T(f)$ by the constant factor d . Combinatorially, F is simplicial, i.e., maps edges homeomorphically to edges.

Abstract simplicial tree-maps (F, T) were defined in [10], and those arising from polynomials were characterized. In this section, we first recall these results in more detail, and then develop them further. We introduce the *spine* $S(T)$ of (F, T) , which is a certain subtree of T . The portion of the spine of (F, T) below the maximal escape-rate is a finite subtree if and only if the corresponding polynomial lies in the shift locus.

The main result, Proposition 6.2, asserts that a polynomial tree (F, T) is determined by a much simpler piece of data that we call *spine star return data*. Roughly (but not exactly), this data takes the form of the first-return map of a unit neighborhood of the spine to itself. The precise statement is given in §6.6. The concepts of spines and related return maps will be used twice more: in the discussion of trees of local models in §7.4, and in the definition of the pictograph in §10.1.

6.1. The metrized polynomial tree

Fix a polynomial $f : \mathbb{C} \rightarrow \mathbb{C}$ of degree $d \geq 2$. Assume that at least one critical point of f lies in the basin of infinity $X(f)$, so that its filled Julia set $K(f) = \mathbb{C} \setminus X(f)$ is not connected. Recall that the escape-rate function is defined by

$$(6.1) \quad G_f(z) = \lim_{n \rightarrow \infty} \frac{1}{d^n} \log^+ |f^n(z)|;$$

it is positive and harmonic on the basin $X(f)$. The *tree* $T(f)$ is the quotient of $X(f)$ obtained by collapsing each connected component of a level set of G_f to a point.

There is a unique locally-finite simplicial structure on $T(f)$ such that the set of vertices of $T(f)$ coincides under the projection $\pi_f : X(f) \rightarrow T(f)$ with the set of grand orbits of the critical points of f in $X(f)$. The polynomial f then induces a simplicial branched covering

$$F : T(f) \rightarrow T(f)$$

of degree d .

The function G_f descends to the *height function*

$$h_f : T(f) \rightarrow \mathbb{R}_+.$$

The height function induces a *height metric* on $T(f)$. This is a length metric, and it is determined by the following property: given adjacent vertices v and w , the length of the unique edge joining them is $|h_f(v) - h_f(w)|$.

Let $E(f)$ be the set of edges in $T(f)$ and $V(f)$ the set of vertices in $T(f)$. Under the projection $\pi_f : X(f) \rightarrow T(f)$, the preimage of each open edge e is an open annulus A_e , and the preimage of each vertex v , denoted L_v , is homeomorphic to the underlying space of a finite graph. The topological degree (defined here as the maximum cardinality of a point in a fiber) of the restriction of f to A_e and to L_v defines the *degree function*

$$\deg_f : E(f) \cup V(f) \rightarrow \mathbb{N}$$

of the tree $(F, T(f))$. The degree of any vertex v is then the degree of the unique edge incident to and above v , and is also equal to the sum of the degrees of the edges incident to and below v .

6.2. Fundamental edges and vertices

In this paragraph, we introduce some terminology and notation that will be employed throughout the paper. Let v_0 denote the highest vertex of valence > 2 , and let $v_1, v_2, \dots, v_N := F(v_0)$ be the consecutive vertices above v_0 in increasing height; we refer to v_0, \dots, v_{N-1} as the *fundamental vertices* and the edges e_i joining v_{i-1} and v_i , $i = 1, \dots, N$, as *fundamental edges*. Note that the union of the fundamental edges and fundamental vertices is a fundamental domain for the action of F on $T(f)$.

The number N of fundamental edges coincides with the number $N(f)$ of independent critical escape rates of a polynomial f , appearing in the statement of Theorems 1.3 and 1.4. The definition of $N(f)$ was given in §2.1.

6.3. The Julia set and weights

Being a non-compact topological space, $T(f)$ has ends, and is compactified by its end-point compactification which adds a point for each end. One end, determined by the loci $\{h_f > t\}$ for $t \rightarrow \infty$, is isolated and corresponds to the point at infinity in the dynamical plane of f . The other ends correspond to connected components of the filled-in Julia set $K(f)$ of f . The *Julia set* $J(F)$ of the tree $(F, T(f))$ is the set of ends at height 0; equivalently, it is the metric boundary of the incomplete length metric space determined by h_f as in the previous subsection. We let $\overline{T}(f) = T(f) \cup J(F)$. The quotient map $X(f) \rightarrow T(f)$ extends continuously to $\mathbb{C} \rightarrow \overline{T}(f)$, collapsing each connected component of $K(f)$ to a point of $J(F)$. In [10], a probability measure μ_F on the Julia set of F is constructed which

coincides with the pushforward of the measure of maximal entropy for a polynomial under the natural projection $K(f) \rightarrow J(F)$.

As in §6.2, let v_0 be the highest branching vertex in $T(f)$. Suppose v is a vertex below v_0 . The level $l(v)$ of v is the least integer $l \geq 0$ so that $h(F^l(v)) \geq h(v_0)$; this implies that $F^{l(v)}(v) = v_j$ is a fundamental vertex for some $j \in \{0, \dots, N-1\}$. There is a unique connected component of the locus $\{h_f \leq h_f(v)\}$ containing v ; it is a subtree of $T(F)$, the *subtree below* v . The ends of this subtree (equivalently, its metric completion) is the *Julia set below* v , denoted $J_v(F)$.

The measure μ_F is constructed by setting

$$(6.2) \quad \mu_F(J_v(F)) = \frac{\deg(v) \deg(F(v)) \cdots \deg(F^{l(v)-1}(v))}{d^{l(v)}}.$$

We refer to this quantity $\mu_F(J_v(F))$ as the *weight* of the vertex v ; it will be used in §7 in the construction of the tree of local models.

The numerator in (6.2) admits the following interpretation which will be used later. For any edge e below v_0 , let A_e be the annulus in $X(f)$ over e . If e is the edge above and adjacent to vertex v , then the ratio of moduli

$$(6.3) \quad \text{mod}(A_e) / \text{mod}(A_{e_j})$$

is the reciprocal of the numerator in (6.2), where e_j is the unique fundamental edge in the orbit of e . This ratio in (6.3) is called the *relative modulus* of the annulus A_e .

6.4. Example: degree 2

Trees in degree 2 are very simple to describe; up to scaling of the height metric, there is only one possibility. Let $f_c(z) = z^2 + c$, and assume that c is not in the Mandelbrot set, so the Julia set $J(f_c)$ is a Cantor set. The level sets of the escape-rate function G_c break the plane into a dyadic tree. That is, for each $h > G_c(0)$, the level curve $\{G_c = h\}$ is a smooth topological circle, mapping by f_c as a degree 2 covering to its image curve $\{G_c = 2h\}$; the level set $\{G_c = G_c(0)\}$ is a “Figure 8”, with the crossing point at 0. Each bounded complementary component of the Figure 8 maps homeomorphically by f_c to its image; there are thus copies of the Figure 8 nested in each bounded component. Consequently, level curves $\{G_c = G_c(0)/2^n\}$ are unions of Figure 8’s for all positive integers n ; all other connected components of level curves in $X(f_c)$ are topological circles. See Figure 6.1.

The tree $T(f_c)$ has a unique highest branch point v_0 ; its height is $h(v_0) = G_c(0)$, and all vertices below v_0 have valence 3. The action of $F : T(f_c) \rightarrow T(f_c)$ is uniquely determined, up to conjugacy, by the condition that $h(F(v)) = 2h(v)$ for every vertex v and that F takes open sets to open sets. Thus, the pair $(F, T(f_c))$ is completely determined by the height of the highest branch point, $G_c(0)$.

6.5. Polynomial type trees

In [10], it is established that these polynomial tree systems $(F, T(f))$ are characterized by a certain collection of axioms, and may be endowed with some additional natural metric structures.

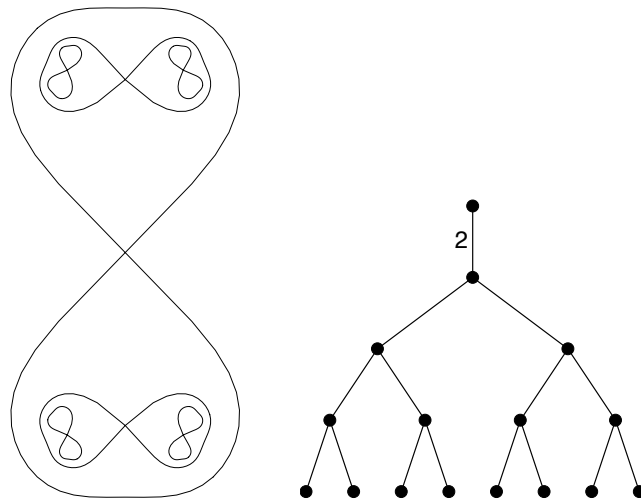


FIGURE 6.1. Critical level sets of the Green’s function G_f and part of the tree $T(f)$ associated to a quadratic polynomial f with disconnected Julia set (from [10, Figure 1]).

Axioms. – By a tree T , we mean a locally finite, connected, 1-dimensional simplicial complex without cycles. Denote the set of edges of T by E and the set of vertices by V . For a given vertex $v \in V$, let E_v denote the set of edges adjacent to v . Given a tree T and a simplicial map $F : T \rightarrow T$, we say (F, T) is of *polynomial type* if the following conditions hold.

1. T has no endpoints (vertices of valence 1),
2. T has a unique isolated end (in the end-point compactification of T),
3. F is proper, open, and continuous,
4. the grand orbit of any vertex includes a vertex of valence ≥ 3 , where $x, y \in T$ lie in the same *grand orbit* if $F^m(x) = F^n(y)$ for some positive integers m, n , and
5. there exists a *local degree function* $\text{deg} : E \cup V \rightarrow \mathbb{N}$ for F , satisfying the following conditions:

(a) for each vertex v ,

$$(6.4) \quad 2 \text{deg}(v) - 2 \geq \sum_{e \in E_v} (\text{deg}(e) - 1),$$

and

(b) for each vertex v and each edge e' adjacent to v ,

$$\text{deg}(v) = \sum_{e \in E_v, F(e)=F(e')} \text{deg}(e).$$

Condition (4) implies that the simplicial structure on T is determined by the dynamics: without this, one could add “artificial” vertices by e.g., subdividing every edge into two pieces. It follows from the axioms that the topological degree of F is well defined and finite, and it satisfies

$$\text{deg } F = \max_{v \in V} \text{deg } v.$$

Further, it is proved in [10] that the degree function for (F, T) is unique.

Stars. – Given a vertex $v \in V$, its *star*, T_v , is the union of half-open edges $[v, w)$ with w incident to v . Thus T_v is the open unit neighborhood of v in T when T is equipped with a length-metric giving each edge length 1. We denote by \overline{T}_v the closed star; it thus consists of the union of closed edges $[v, w]$ with w incident to v .

Critical points and critical ends. – A vertex v is a *critical point* of (F, T) if we have strict inequality in the relation (6.4). An end of T is *critical* if there exists a sequence of vertices of degree > 1 exiting via (and thus converging to) this end. There are at most $d - 1$ critical points and ends, counted with multiplicity, and there is at least one critical point in the grand orbit of every vertex. Note that if $T = T(f)$, a vertex is critical if and only if it is the image under the projection $\pi_f : X(f) \rightarrow T(f)$ of a critical point of f ; an end is critical if and only if there is a critical point of f in the corresponding component of the filled-in Julia set of f .

Realization. – Theorem 7.1 of [10] states that if (F, T) is of polynomial type, then there exists a polynomial f of degree $\deg F$ and a monotone map $X(f) \rightarrow T$ giving a semiconjugacy from $f : X(f) \rightarrow X(f)$ to $F : T \rightarrow T$. Each critical vertex of (F, T) is the image of a critical point of f . We sketch the proof of this realization theorem below in §6.8. A polynomial f lies in the shift locus if and only if (F, T) has no critical ends.

Henceforth, we consider only tree-dynamics (F, T) of polynomial type.

Height metrics. – Any tree of polynomial type (F, T) can be endowed with a *height metric* d_h . This is a length metric, and is determined by the following property. Each edge e is isometric to a Euclidean interval; we denote by $|e|$ its length. We require $|e| = |F(e)|/(\deg F)$. There is a finite-dimensional space of possible height metrics, parameterized by the lengths of fundamental edges. Each height metric induces a *height function*

$$h : T \rightarrow \mathbb{R}_+$$

where $h(x)$ is the distance from x to the set of non-isolated ends (the *Julia set* of F); it satisfies $h(F(x)) = (\deg F)h(x)$. The distance function can be recovered from h by $d_h(v, w) = |h(v) - h(w)|$ on adjacent vertices. When equipped with a height metric, we refer to the triple (F, T, h) as a *metrized polynomial tree*. The realization theorem of [10] states further that every metrized polynomial tree (F, T, h) arises from a polynomial $f : \mathbb{C} \rightarrow \mathbb{C}$ of degree $\deg F$ with h as the height function h_f induced by G_f .

Compatible critical heights. – Set $d = \deg(F)$. A height function is uniquely determined by either one of two pieces of data: (i) assigning positive lengths to the fundamental edges e_1, \dots, e_N , and then propagating to other edges via the functional equation $|e| = |F(e)|/d$, or (ii) by a list of $d - 1$ *compatible critical heights* $h_1 \geq h_2 \geq \dots \geq h_{d-1} \geq 0$. Recall that a critical point c of T is either a critical vertex or a critical end, and that there are $d - 1$ critical points, c_1, \dots, c_{d-1} , counted with multiplicity. The height of a critical end is defined to be zero. The highest branching vertex v_0 is a critical vertex; by definition, h_1 is its height. If c_i, c_j are critical points with heights $h_i, h_j > 0$, and c_i, c_j are in the same grand orbit, so that $F^{l(c_i)} = F^{l(c_j)} = v_k$ for some fundamental vertex $v_k, k \in \{0, \dots, N - 1\}$, then the heights h_i, h_j must satisfy $d^{l(c_i)}h_i = d^{l(c_j)}h_j$ in order to be compatible. This common value will be the height of the fundamental vertex v_k . Thus from compatible critical heights one recovers the heights of fundamental vertices, hence lengths of fundamental edges, and hence the height function $h : T \rightarrow (0, \infty)$. We have shown

PROPOSITION 6.1. – Suppose T has $N \geq 1$ fundamental edges. The set of compatible critical heights $(h_1, \dots, h_{d-1}) \in [0, \infty)^{d-1}$, with $h_1 \geq \dots \geq h_{d-1}$, is homeomorphic to an open N -dimensional simplex.

6.6. The spine of the tree

Suppose (F, T) is of polynomial type. Here, we need only the simplicial structure of T . The *spine* $S(T)$ of a tree (F, T) is the convex hull of its critical points and critical ends (including ∞). In other words, it is the connected subtree consisting of all edges and vertices with degree larger than 1. For example, in degree 2, $S(T)$ includes the highest branching vertex and the ray leading to infinity. In Figure 6.1, this is the upward-pointing ray starting at the segment labeled “2”. We denote by $S_1(T)$ the closed unit simplicial neighborhood of the spine, regarded as a subtree of T . Thus $S_1(T)$ consists of all edges with at least one vertex in the spine.

For a vertex v in the spine $S(T)$, its *first return-time* is $r(v) := \min\{i > 0 : F^i(v) \in S(T)\}$. The *first-return map* of the spine is $R : S(T) \rightarrow S(T)$ is defined by $R(v) := F^{r(v)}(v)$.

PROPOSITION 6.2. – A polynomial tree (F, T) is determined by the triple consisting of: the subtree $S_1(T)$, the return-map $R : S(T) \rightarrow S(T)$, and the spine star return data

$$(6.5) \quad \left\{ R_v := (F^{r(v)} : \bar{T}_v \rightarrow \bar{T}_{R(v)}) \mid v \in S(T) \right\}.$$

In other words, the tree T and the self-map $F : T \rightarrow T$ may be reconstructed from *a priori* a much smaller amount of information.

The proof of Proposition 6.2 is by induction on descending height. The spirit of this argument will be used to establish Propositions 7.2, Proposition 7.3, Lemma 8.4, and Proposition 10.2. Proposition 6.2 in the case of degree 3 polynomial trees is covered by [10, Theorem 11.3].

Proof of Proposition 6.2. – Suppose we are given the spine star return data (6.5). We first observe that we can reconstruct the following invariants.

1. *The end corresponding to ∞ .* To see this: note first that sequences of the form $\lim_{n \rightarrow \infty} R^n(v)$ all converge to a unique end of $S(T)$, which we denote by ∞ .
2. *A partial order, $<$.* We say $v < w$ if w separates v from ∞ .
3. *The fundamental vertices, v_0, v_1, \dots, v_N .* The vertex v_0 is the unique smallest vertex (with respect to the partial order $<$) separating every other vertex of valence at least 3 from ∞ . Let N be the combinatorial distance in $S(T)$ between v_0 and $v_N := R(v_0)$. Then proceeding from v_0 up to v_N we encounter v_0, v_1, \dots, v_N .
4. *A simplicial depth function depth on $S(T)$.* Let d be the combinatorial distance in the simplicial complex $S(T)$. For $v < v_0$, we set $\text{depth}(v) := -d(v, v_0)$; for $v > v_0$, we set $\text{depth}(v) := d(v_0, v)$. Thus $\text{depth}(v_0) = 0$, $\text{depth}(v_i) = i$ for $i = 1, \dots, N$, and $\text{depth}(v) = -1$ for each vertex $v \in S_1(T)$ immediately below v_0 .
5. *The first-return times, $r(v)$, for vertices $v \in S(T)$.* To see this, note that given $v \in S(T)$ we have $r(v) = (\text{depth}(R(v)) - \text{depth}(v))/N$.

It suffices to show that the tree T and map F can be reconstructed from the given data, since the local degree function is uniquely determined by the pair (F, T) [10, Theorem 2.9].

On the infinite vertical ray $[v_0, \infty) \subset S(T)$, we have $F = R$, so the spine star return data determines F on the forward-invariant ray $[0, \infty)$.

We now argue by induction on descending $n := \text{depth}(v)$. We will inductively construct the tree T and the map $F : T \rightarrow T$. At the inductive step, we are in the following setup.

- We have a vertex v of the tree T with $n = \text{depth}(v)$.
- We have determined the image $w = F(v)$ (indeed, we have determined F on the infinite vertical ray above v).
- Since $\text{depth}(v) < \text{depth}(w)$, by the inductive hypothesis, we know the star \overline{T}_w .
- We must construct the portion of the star \overline{T}_v below v , and must extend F over this portion to complete the definition of the restriction $F_v : \overline{T}_v \rightarrow \overline{T}_w$.

There are two cases.

1. If $v \notin S(T)$, we define \overline{T}_v to be a homeomorphic copy of \overline{T}_w , and we extend arbitrarily so that $F_v : \overline{T}_v \rightarrow \overline{T}_w$ is a simplicial homeomorphism.
2. If $v \in S(T)$, put $y := R(v)$. By assumption, we are given the data of the map $R_v : \overline{T}_v \rightarrow \overline{T}_y$. If $r(v) = 1$ then we are done. Otherwise: by the inductive hypothesis, we know the map $F^{r(v)-1} : \overline{T}_w \rightarrow \overline{T}_y$. Since R is a first-return map, we know $F^{r(v)-1} : \overline{T}_w \rightarrow \overline{T}_y$ is a homeomorphism. We define $F : \overline{T}_v \rightarrow \overline{T}_w$ by $(F^{r(v)-1})^{-1} \circ R_v$.

We use the above construction to extend F to all vertices v with $\text{depth}(v) = -n$. We then proceed to vertices v for which $\text{depth}(v) = -(n+1)$. Induction on n completes the proof. \square

6.7. Remark: cubic polynomials and the spine

A polynomial tree dynamical system (F, T) , is *not* determined by the first-return map on the spine $S(T)$ alone. In fact, in the case of cubic polynomial trees, the data of the first return to $S(T)$ is equivalent to the data of the Branner-Hubbard tableau (or the Yoccoz τ -sequence). Examples of distinct cubic trees with the same tableau were presented in [10] and here in Section 3, Figure 3.1.

6.8. Realization of trees, a review

In this subsection, we give an overview of the proof of [10, Theorem 1.2], the realization theorem for trees. This construction motivated the definition of trees of local models, which will be introduced in Section 7.

Suppose (F, T) is of polynomial-type of degree d . We first assume (F, T) has no critical ends; we will produce a corresponding polynomial in the shift locus. As in §6.5, choose a height metric for (T, F) and let h be the corresponding height function. The absence of critical ends implies that the heights of critical vertices are uniformly bounded below away from zero. In particular, on the portion of the tree below some positive height, F is a local homeomorphism. A polynomial in the shift locus with metrized tree (F, T, h) is then constructed as follows. Recall from §6.2 the definition of the fundamental vertices v_0, \dots, v_{N-1} , where v_0 is the highest vertex of valence at least 3.

1. **Inflate the vertices above v_0 .** At each vertex $v_1, v_2, v_3 \dots$ above v_0 , let (X_{v_i}, ω_{v_i}) be a local model surface “modeled on” the vertex v_i in T . As each such vertex has valence 2, the surface X_{v_i} is an annulus, and the moduli of its inner and outer annuli are determined by the height function h .
2. **Local realization.** Inductively on descending height we choose, for each vertex v with $h(v) \leq h(v_0)$, a local model map

$$(X_v, \omega_v) \rightarrow (X_{F(v)}, \omega_{F(v)})$$

“modeled on” F at v . The condition (5) on local degrees in §6.5 guarantees the existence of such a local model. The result of this step is a collection of local model maps, indexed by the vertices of T ; the domain X_v of each is equipped with a natural projection to the open star T_v .

3. **Glue.** Over each edge of T , say joining v to v' above it, glue the outer annulus of X_v with the corresponding inner annulus of v' so that the local model maps extend holomorphically (we do this more formally in §7.5 below). After gluing over all edges, we obtain a proper degree d holomorphic map $f : X \rightarrow X$ from a planar Riemann surface X to itself, $d - 1$ critical points of f in X (counted with multiplicity), and height map $h : X \rightarrow (0, \infty)$ with $h(f(x)) = dh(x)$.

By uniformization, X lies in the Riemann sphere. The assumption that $F : T \rightarrow T$ has no critical ends implies that each end of X is surrounded by a concentric sequence of annuli for which the sum of the moduli diverges. It follows that X is rigid as a Riemann surface ([18, §2.8], [1, §IV.4]). Hence f extends uniquely to a polynomial whose basin dynamics $(f, X(f))$ is isomorphic to (f, X) . By construction, the metric tree dynamics $(F, T(f), h_f)$ of the polynomial f is isomorphic to that of the given metric tree (F, T, h) .

A general metrized polynomial tree is realized by a compactness and continuity argument. There is a dynamical Gromov-Hausdorff topology on the set of metric trees: (F_1, T_1, h_1) is close to (F_2, T_2, h_2) if there is a relation between T_1, T_2 which is close to an isometry and close to a conjugacy on a very large compact subset. With this topology, the map $f \mapsto (F, T(f), h_f)$ is continuous, and the image of the shift locus—namely, trees without critical ends in its Julia set—is dense. The locus of maps f for which the critical heights are less than some given constant is known to be compact. Given an arbitrary (F, T, h) , we approximate it by trees corresponding to the shift locus $(F_n, T_n, h_n) \rightarrow (F, T, h)$, and we construct realizations f_n of (F_n, T_n, h_n) . An accumulation point f of $(f_n)_n$ realizes (F, T, h) .

7. The tree of local models

Suppose f is a polynomial. Recall from §1.1 that the basin dynamics $f : X(f) \rightarrow X(f)$ fits naturally into a sequence of dynamical systems

$$\begin{array}{ccccccc} \begin{array}{c} \mathcal{F} \\ \curvearrowright \\ \mathcal{X}(f) \end{array} & \xrightarrow{g_f} & \begin{array}{c} f \\ \curvearrowright \\ X(f) \end{array} & \xrightarrow{\pi_f} & \begin{array}{c} F \\ \curvearrowright \\ T(f) \end{array} & \xrightarrow{h_f} & \begin{array}{c} \cdot d \\ \curvearrowright \\ (0, \infty) \end{array} \\ & & & \searrow & \text{---} & \nearrow & \\ & & & & G_f & & \end{array}$$

where the *gluing quotient map* g_f depends on f . In this section, we introduce more formally the tree of local models $(\mathcal{F}, \mathcal{X}(f))$. We axiomatize its properties, introduce abstract trees of local models, and show:

THEOREM 7.1. – *Every abstract tree of local models $(\mathcal{F}, \mathcal{X})$ arises from a polynomial basin $(f, X(f))$.*

The proof is similar to the realization of abstract polynomial trees in [10], outlined in §6.8. As with polynomial trees (Proposition 6.2), we define the spine $(\mathcal{R}, \mathcal{S})$ of the tree of local models $(\mathcal{F}, \mathcal{X})$ and prove:

PROPOSITION 7.2. – *A tree of local models $(\mathcal{F}, \mathcal{X})$ is uniquely determined by its first-return map on its spine $(\mathcal{R}, \mathcal{S})$.*

PROPOSITION 7.3. – *A tree of local models $(\mathcal{F}, \mathcal{X})$ and a gluing along its spine $(\mathcal{R}, \mathcal{S})$ determines uniquely a basin dynamical system $(f, X(f))$.*

While the basin dynamical system $(f, X(f))$ in Proposition 7.3 is unique up to conformal conjugacy, the polynomial f is not, due to e.g., renormalizations associated to periodic filled Julia components.

7.1. The tree of local models associated to a polynomial

Let f be a polynomial of degree d with disconnected Julia set, G_f its escape-rate function, and ω its holomorphic 1-form. Recall from §2.1 that each level curve $\{z \in X(f) : G_f(z) = c\}$ has length 2π in the metric $|\omega|$. In particular, the metric $|\omega_f|$, when restricted to connected components of level sets of G_f , coincides with the length function induced by external angles.

Form the metrized polynomial tree $(F, T(f), h_f)$ as in §6.1. Consider the projection $\pi_f : X(f) \rightarrow T(f)$ from the basin of infinity to the tree. For each vertex $v \in T(f)$, let X_v be the preimage in $X(f)$ of the open star T_v , and set

$$\omega_v = \frac{1}{\mu_F(J_v(F))} \omega = \frac{2i d^{l(v)}}{\deg(f^{l(v)}|_{X_v})} \partial G_f,$$

where the weight $\mu_F(J_v(F))$ was defined in equation (6.2). Then the pair (X_v, ω_v) forms a local model surface, where each horizontal leaf of ω_v is the fiber over a point in T_v , and the central leaf is the fiber over v . The scale factor normalization of ω_v is chosen so that the central leaf and boundary of outer annulus of X_v have length 2π in the metric $|\omega_v|$.

The restriction of the polynomial $f|_{X_v}$ defines a local model map

$$f_v : (X_v, \omega_v) \rightarrow (X_{F(v)}, \omega_{F(v)}).$$

Indeed, the level $l(v)$ satisfies $l(F(v)) = l(v) - 1$ whenever $l(v) > 0$, so

$$\begin{aligned} \omega_v &= \frac{d^{l(v)}}{\deg(f^{l(v)}|_{X_v})} \frac{1}{d} f^* \omega = \frac{d^{l(F(v))}}{\deg(f|_{X_v}) \deg(f^{l(F(v))}|_{X_{F(v)}})} f^* \omega \\ &= \frac{1}{\deg(f|_{X_v})} f^* \omega_{F(v)}, \end{aligned}$$

as required for a local model map. For each v , the restriction $\pi_v := \pi_f|_{X_v} : X_v \rightarrow T_v \subset T(f)$ gives a projection to the open star T_v of v in $T(f)$; it collapses the horizontal leaves of the foliation on X_v to points.

Now let

$$\mathcal{X}(f) := \bigsqcup_{v \in V} (X_v, \omega_v)$$

be the disjoint union of the X_v 's equipped with the 1-forms ω_v , and define

$$\mathcal{F}(f) : \mathcal{X}(f) \rightarrow \mathcal{X}(f)$$

by setting $\mathcal{F}|_{X_v} := f_v$. Thus $\mathcal{F} : \mathcal{X}(f) \rightarrow \mathcal{X}(f)$ defines a holomorphic dynamical system on a disconnected complex 1-manifold with countably infinitely many components, equipped with a holomorphic 1-form. Metrically, \mathcal{F} locally expands lengths on X_v by the factor $\deg(v)$. The collection of projections $\{\pi_v : X_v \rightarrow T_v\}_{v \in V}$ then determine a projection $\pi : \mathcal{X}(f) \rightarrow T(f)$ that gives a semiconjugacy from $\mathcal{F} : \mathcal{X}(f) \rightarrow \mathcal{X}(f)$ to $F : T(f) \rightarrow T(f)$. The composition $h_f \circ \pi : \mathcal{X}(f) \rightarrow [0, \infty)$ gives a height function on $\mathcal{X}(f)$. The inclusion $X_v \hookrightarrow \mathcal{X}(f)$ induces a holomorphic, generically two-to-one *gluing quotient map*

$$g_f : \mathcal{X}(f) \rightarrow X(f).$$

In summary: we obtain the following diagram of semiconjugacies:

$$\begin{array}{ccccccc} \begin{array}{c} \mathcal{F} \\ \curvearrowright \\ \mathcal{X}(f) \end{array} & \xrightarrow{g_f} & \begin{array}{c} f \\ \curvearrowright \\ X(f) \end{array} & \xrightarrow{\pi_f} & \begin{array}{c} F \\ \curvearrowright \\ T(f) \end{array} & \xrightarrow{h_f} & \begin{array}{c} \cdot d \\ \curvearrowright \\ (0, \infty) \end{array} \\ & & & \searrow & \xrightarrow{G_f} & & \end{array}$$

The *tree of local models associated to f* is described globally simply by forgetting the gluing quotient map g_f in the above diagram. That is, we record the data

$$\begin{array}{ccc} \begin{array}{c} \mathcal{F} \\ \curvearrowright \\ \mathcal{X}(f) \end{array} & \xrightarrow{\pi} & \begin{array}{c} F \\ \curvearrowright \\ T(f) \end{array} & \xrightarrow{h_f} & \begin{array}{c} \cdot d \\ \curvearrowright \\ (0, \infty) \end{array} \end{array}$$

More formally and locally described: the tree of local models associated to f is the data consisting of (i) the tree $(F, T(f), h_f)$, and (ii) the collection of triples $\{f_v, (X_v, \omega_v), \pi_v\}_{v \in V}$.

7.2. The tree of local models, defined abstractly

We now consider abstract trees of local models. Let (F, T, h) be an abstract metrized polynomial tree. For a vertex v , let T_v denote the open star of v . A *tree of local models over (F, T, h)* is (i) the metrized tree (F, T, h) , and (ii) a collection of triples $\{(f_v, (X_v, \omega_v), \pi_v) : v \in V\}$, indexed by the vertices v of T , such that for each vertex v ,

1. the pair (X_v, ω_v) is a local model surface which is “modeled on” the open star T_v . Specifically, there exists a marking homeomorphism

$$\pi_v : T(X_v, \omega_v) \rightarrow T_v$$

from the quotient tree of (X_v, ω_v) , obtained by collapsing the leaves of the horizontal foliation of ω_v to points, to the open star T_v . We require further that π_v is an isometry

from the induced metric $\mu_F(J_v(F))|\omega_v|$ on $T(X_v, \omega_v)$ to the height metric on T_v , where $\mu_F(J_v(F))$ is the weight of v , defined in equation (6.2);

2. the map

$$f_v : (X_v, \omega_v) \rightarrow (X_{F(v)}, \omega_{F(v)})$$

is a local model map which is “modeled on” F at v . Specifically, via the marking homeomorphisms π_v and $\pi_{F(v)}$, the restriction $F : T_v \rightarrow T_{F(v)}$ is the quotient of f_v , and the local degree function on T_v coincides with the degree of f_v on leaves.

By condition (1), the heights of the inner and outer annuli in X_v are controlled by the metric on (F, T, h) . By condition (2), the widths of these annuli are also controlled, and therefore the moduli are determined. In fact, the moduli coincide with the lengths of edges of (F, T, h) in the *modulus metric* of [10].

Suppose $\{(f_v, (X_v, \omega_v), \pi_v) : v \in V\}$ is a tree of local models over a polynomial tree (F, T, h) . As in §7.1 we let

$$\mathcal{X} := \bigsqcup_{v \in V} (X_v, \omega_v)$$

be the disjoint union of the X_v 's and define

$$\mathcal{F} : \mathcal{X} \rightarrow \mathcal{X}$$

by setting $\mathcal{F}|_{X_v} := f_v$. Thus $\mathcal{F} : \mathcal{X} \rightarrow \mathcal{X}$ defines a holomorphic dynamical system on a disconnected complex 1-manifold with countably infinitely many components. The 1-forms ω_v define a conformal metric $|\omega_v|$ on each X_v (with singularities at the zeros of ω_v). On each local model surface X_v , the holomorphic map \mathcal{F} scales this metric by the factor $\deg(v)$. The collection of projections $\pi_v : X_v \rightarrow T_v \subset T$ then determine a projection $\pi : \mathcal{X} \rightarrow T$. In summary, a tree of local models over a polynomial tree (F, T, h) is defined globally by the data of

$$\begin{array}{ccccc} \mathcal{F} & & F & & \cdot d \\ \curvearrowright & & \curvearrowright & & \curvearrowright \\ \mathcal{X} & \xrightarrow{\pi} & T & \xrightarrow{h} & (0, \infty). \end{array}$$

7.3. Equivalence and automorphisms of trees of local models

A tree of local models $\mathcal{F}_1 : \mathcal{X}_1 \rightarrow \mathcal{X}_1$ is *equivalent* to the tree of local models $\mathcal{F}_2 : \mathcal{X}_2 \rightarrow \mathcal{X}_2$ if there exists a holomorphic isometry

$$i : \mathcal{X}_1 \rightarrow \mathcal{X}_2$$

which induces a conjugacy

$$\mathcal{F}_2 \circ i = i \circ \mathcal{F}_1$$

while respecting the underlying tree structure. That is, the isometry i projects, via the marking homeomorphisms, to an isometry of polynomial trees,

$$i : T_1 \rightarrow T_2$$

which conjugates the tree dynamics of F_1 to that of F_2 .

In particular, an *automorphism* of a tree of local models $\mathcal{F} : \mathcal{X} \rightarrow \mathcal{X}$ is a holomorphic isometry $\mathcal{X} \rightarrow \mathcal{X}$ which induces an isometry of the underlying tree $T \rightarrow T$ and commutes with \mathcal{F} .

7.4. The spine of the tree of local models

Fix a tree of local models $(\mathcal{F}, \mathcal{X})$, and let (F, T) be the underlying polynomial tree. Recall that the spine $S(T)$ of (F, T) is the convex hull of all critical points and critical ends (including ∞) in T . The *spine* \mathcal{S} of \mathcal{X} is the subset of \mathcal{X} lying over the spine $S(T)$ of the tree. We let $\mathcal{R} : \mathcal{S} \rightarrow \mathcal{S}$ denote the first-return map to the spine \mathcal{S} of $(\mathcal{F}, \mathcal{X})$; for each vertex $v \in S(T)$, it is defined by $\mathcal{R}|_{X_v} = \mathcal{F}^{r(v)} : X_v \rightarrow X_{F^r(v)}$ where $r(v) = \min\{i > 0 : F^i(v) \in S(T)\}$ as defined in §6.6. Unlike the first-return map we consider for (F, T) , defined in §6.6, we do not thicken the spine to the unit simplicial-neighborhood $S_1(T)$. Note now that $\mathcal{R} : \mathcal{S} \rightarrow \mathcal{S}$ is a holomorphic dynamical system; in particular, it is continuous and, in the natural Euclidean coordinates from the 1-form, is a homothety with scaling factor $\deg(v)$ away from singular points.

We now prove that $(\mathcal{F}, \mathcal{X})$ is uniquely determined by the first-return map $(\mathcal{R}, \mathcal{S})$. The proof proceeds along exactly the same lines as the proof of Proposition 6.2.

Proof of Proposition 7.2. – The first observation is that the underlying metrized-tree dynamics (F, T, h) can be recovered from the first-return map $(\mathcal{R}, \mathcal{S})$. Indeed, the local model surface over any vertex $v \in S(T)$ collapses to the star of v (and determines the metric, locally). Thus, the spine \mathcal{S} of \mathcal{X} determines the unit simplicial-neighborhood $S_1(T)$, and the first-return map $\mathcal{R} : \mathcal{S} \rightarrow \mathcal{S}$ determines a return map $R_1 : S_1(T) \rightarrow S_1(T)$. Strictly speaking, R_1 is not the *first* return on $S_1(T)$ defined in §6.6, but rather, the first return from the spine to itself, together with the action on stars. Applying the *proof* of Proposition 6.2, we are able to recover the full tree dynamical system (F, T) .

As in the proof of Proposition 6.2, we reconstruct $(\mathcal{F}, \mathcal{X})$ from $(\mathcal{R}, \mathcal{S})$ inductively on descending height. We begin with vertices v in the spine and use \mathcal{R} to reconstruct \mathcal{F} on the local model surface over v . All other vertices have degree 1, so the map \mathcal{F} and surface \mathcal{X} are uniquely determined. □

7.5. The gluing quotient map

Suppose f is a polynomial and $(f, X(f))$ is its basin dynamical system. For each vertex $v \in T(f)$, there is an inclusion $X_v(f) \hookrightarrow X(f)$. The totality of these inclusions define a canonical semiconjugacy $(\mathcal{F}, \mathcal{X}(f)) \rightarrow (f, X(f))$ between the dynamics \mathcal{F} on the tree of local models $\mathcal{X}(f)$ induced by f and that of f on its basin $X(f)$. If v and v' are incident, with v' above v , the inclusions $X_v(f) \hookrightarrow X(f)$ and $X_{v'}(f) \hookrightarrow X(f)$ have the property that the image of the outer annulus of $X_v(f)$ coincides with that of the inner annulus of $X_{v'}(f)$. The composition of the first with the inverse of the second gives a conformal isomorphism between these annuli.

We conclude that a polynomial determines

1. a *gluing*: a collection

$$\iota^f = \{\iota_e^f\}_{e \in E}$$

of conformal isomorphisms ι_e^f from the outer annulus of $X_v(f)$ to the corresponding inner annulus of v' commuting with $\mathcal{F}(f)$, one for each edge e of the tree $T(f)$, and

2. a corresponding *gluing quotient map*

$$g_f : \mathcal{X}(f) \rightarrow X(f).$$

Note that an isomorphism $(f, X(f)) \rightarrow (g, X(g))$ lifts under the gluing quotient maps to an isomorphism $(\mathcal{F}(f), \mathcal{X}(f)) \rightarrow (\mathcal{F}(g), \mathcal{X}(g))$.

Conversely, given an abstract tree of local models $(\mathcal{F}, \mathcal{X})$, one may consider abstract gluings as well. An (abstract) *gluing* is a collection $\iota = \{\iota_e\}_{e \in E}$ of conformal isomorphisms ι_e from the outer annulus of X_v to the corresponding inner annulus of v' commuting with \mathcal{F} , where v and v' are joined by an edge e . An abstract gluing ι defines a gluing quotient map $\mathcal{X} \rightarrow \mathcal{X}/\iota = X^\iota$ to an abstract planar Riemann surface to which the dynamics of \mathcal{F} descends to yield a proper degree d holomorphic self-map $f^\iota : X^\iota \rightarrow X^\iota$. In this way, a gluing ι defines a holomorphic semiconjugacy $(\mathcal{F}, \mathcal{X}) \rightarrow (f^\iota, X^\iota)$.

Recall the definition of the fundamental edges and vertices, from §6.2. The choice of gluings along the N fundamental edges determines the gluings at all vertices above v_0 . As with the tree of local models, a gluing can also be reconstructed from its action on the spine of $(\mathcal{F}, \mathcal{X})$.

Proof of Proposition 7.3. – Fix a tree of local models $(\mathcal{F}, \mathcal{X}) = \{(f_v, (X_v, \omega_v), \pi_v) : v \in V\}$ over a metric polynomial tree (F, T, h) and let $(\mathcal{R}, \mathcal{S})$ be the first-return map to its spine.

Suppose we are given the data consisting of the gluings $\iota_e, e \in S(T)$, along the spine. Note that the gluings at all edges above v_N are determined by those at the fundamental edges e_1, \dots, e_N . We proceed inductively on descending height. Let $n \geq 0$ and suppose ι_e is defined along all edges joining vertices with simplicial distance $\leq n$ from the highest branching vertex v_0 . Let v be a vertex at distance $n + 1$, joined by edge e above it to vertex v' . If v lies in the spine, then ι_e has already been defined. If v is not in the spine, then $\deg(f_v : X_v \rightarrow X_{F(v)}) = 1$ and $f_{v'}$ has degree 1 on the inner annulus corresponding to e . Setting $\iota_e := f_{v'}^{-1} \circ \iota_{F(e)} \circ f_v$ gives the unique extension of the gluing along e so that the needed functional equation is satisfied.

The previous paragraph shows that gluings along the spine determine gluings on the whole tree of local models, yielding a holomorphic degree d branched covering map f of an abstract planar Riemann surface X to itself. The proof of the realization theorem (Theorem 7.1 below) shows that the abstract basin dynamics (f, X) is holomorphically conjugate to that of some polynomial. \square

7.6. Realization theorem

We now prove Theorem 7.1. It may be useful to review the proof sketch of the tree realization theorem, given in §6.8. The final step in the proof is a continuity argument; to make the continuity argument go through in the setting of trees of local models, we rely on some observations from [8], in particular the proof of Lemma 3.2 there.

Proof of Theorem 7.1. – Let $(\mathcal{F}, \mathcal{X}) = \{(f_v, (X_v, \omega_v), \pi_v) : v \in V\}$ be a tree of local models over the metrized tree (F, T, h) . When the tree (F, T, h) lies in the shift locus, so that all critical points have positive height, the realization goes through as for trees. The first two steps of tree realization (as described above in §6.8) are already achieved by the given data. That is, over every vertex we have local model surfaces “modeled on” the vertices of T , and for every pair of vertices v and $F(v)$ we have local model maps “modeled on” the action of F . We glue the local models, first over the fundamental edges (which uniquely determines gluing so that map extends holomorphically above v_0), and choose gluings inductively on

descending height below v_0 so the resulting map on the glued surface is holomorphic. We appeal to the uniformization theorem and extendability of the dynamics on the glued surface to all of \mathbb{C} , and conclude the existence of a polynomial in the shift locus realizing the given tree of local models.

Now suppose the tree (F, T, h) has critical points in its Julia set (i.e., of height 0). By [10, Theorem 5.7], we can approximate (F, T, h) by a sequence of metrized trees (F_k, T_k, h_k) so that (F_k, T_k, h_k) is isometrically conjugate to (F, T, h) at all heights $\geq 1/k$, and further, all critical points of (F_k, T_k, h_k) have height $\geq 1/k$. We may construct trees of local models $(\mathcal{F}_k, \mathcal{X}_k)$ over each (F_k, T_k, h_k) , so that when restricted to heights above $1/k$, the dynamics of \mathcal{F}_k is holomorphically conjugate to that of \mathcal{F} .

Choose arbitrarily a gluing ι for $(\mathcal{F}, \mathcal{X})$. For each k , via the identification from the above conjugacies, we transport the gluing ι to a partially defined gluing for $(\mathcal{F}_k, \mathcal{X}_k)$, and we choose an extension arbitrarily to obtain a gluing ι_k for $(\mathcal{F}_k, \mathcal{X}_k)$. By the first paragraph, these determine polynomials f_k which we may assume are monic and centered. Each of the polynomials f_k has the same maximal critical escape rate, so by passing to a subsequence, we may assume the f_k converge locally uniformly on \mathbb{C} to a polynomial f .

As in the proof of [8, Lemma 3.2], the local uniform convergence $f_k \rightarrow f$ on \mathbb{C} implies that for any $t > 0$ the restrictions to $\{t \leq G_k(z) \leq 1/t\}$ converge uniformly to f on $\{t \leq G_f(z) \leq 1/t\}$ and the 1-forms $\omega_k = \partial G_k$ converge on this subset to $\omega = \partial G_f$; indeed, the escape-rate functions are harmonic where positive, so the uniform convergence implies the derivatives also converge. We therefore conclude that the tree of local models associated to f is isomorphic to $(\mathcal{F}, \mathcal{X})$. \square

8. Symmetries in the tree of local models

A tree of local models may admit many nontrivial automorphisms. The group of such symmetries, unsurprisingly, will play an important role in the problem of counting topological conjugacy classes.

8.1. The automorphism group

Let $\text{Aut}(\mathcal{F}, \mathcal{X})$ be the conformal automorphism group of the tree of local models $(\mathcal{F}, \mathcal{X})$, as defined in §7.3. While any basin of infinity in degree d has only a finite group of automorphisms, which is necessarily a subgroup of the cyclic group of order $d - 1$, the group $\text{Aut}(\mathcal{F}, \mathcal{X})$ can be large and complicated. Consider the following examples.

For any degree 2 tree of local models, we have $\text{Aut}(\mathcal{F}, \mathcal{X}) \simeq \mathbb{Z}/2\mathbb{Z}$. The unique nontrivial automorphism is generated by an order-two rotation of the local model surface containing the critical point. It acts trivially on all local models above the critical point. The action on all vertices below the critical point is uniquely determined by the dynamics, because every such vertex is mapped with degree 1 to its image.

By contrast, consider the tree of local models for the cubic polynomial $f(z) = z^2 + \varepsilon z^3$ for any small ε . This polynomial has one fixed critical point at the origin and one escaping critical point c ; let M be the escape rate of c . While the basin $(f, X(f))$ has no nontrivial automorphisms, the tree of local models has an automorphism of infinite order, acting by a rotation of order 2 at the vertex v of the spine for which the corresponding central leaf L_v

contains a preimage of c . The rotation of order 2 at height $M/3$ induces an order 2^n rotation at the vertex in the spine of height $M/3^n$. The action on the local model surface at each vertex of local degree 1 is uniquely determined; similarly for the vertices at heights greater than M . In fact, for this example, $\text{Aut}(\mathcal{F}, \mathcal{X})$ is isomorphic to the profinite group \mathbb{Z}_2 , the 2-adic integers under addition; this follows from Lemma 8.4 below.

8.2. Local symmetry at a vertex

Denote by \mathbb{S}^1 the quotient group of \mathbb{R} by the subgroup $2\pi\mathbb{Z}$. The group of orientation-preserving isometries of a Euclidean circle of circumference 2π is then canonically isomorphic to \mathbb{S}^1 via the map which measures the displacement between a point and its image.

Let $(\mathcal{F}, \mathcal{X})$ be a tree of local models with underlying tree (F, T) . Let v be any vertex of T . The outer annulus of X_v is metrically the product of an oriented Euclidean circle C of circumference 2π with an interval. Let $\text{Stab}_v(\mathcal{F}, \mathcal{X})$ denote the stabilizer of v in $\text{Aut}(\mathcal{F}, \mathcal{X})$, i.e., all $\varphi \in \text{Aut}(\mathcal{F}, \mathcal{X})$ with $\varphi(X_v) = X_v$. Any element of this stabilizer induces a conformal automorphism of X_v . Because this automorphism must preserve the outer annulus of X_v , it is necessarily a rotation. Consequently, there is a well-defined homomorphism

$$\text{Stab}_v(\mathcal{F}, \mathcal{X}) \rightarrow \text{Aut}(X_v, \omega_v) \hookrightarrow \text{Isom}^+(C) = \mathbb{S}^1.$$

LEMMA 8.1. – *For every vertex v , the image of $\text{Stab}_v(\mathcal{F}, \mathcal{X})$ in \mathbb{S}^1 is a finite cyclic group $\mathbb{Z}/k(v)\mathbb{Z}$.*

Proof. – Because elements of $\text{Aut}(\mathcal{F}, \mathcal{X})$ must commute with the dynamics, the points of the critical grand orbits are permuted, preserving heights; every local model surface (X_v, ω_v) contains at least one and finitely many such points. Therefore the image of $\text{Stab}_v(\mathcal{F}, \mathcal{X})$ in the group of rotations is finite. \square

The order $k(v)$ is called the *local symmetry* of $(\mathcal{F}, \mathcal{X})$ at vertex v .

8.3. Profinite structure

Fix a height $t > 0$. Consider the automorphism group, similarly defined, of the restriction $(\mathcal{F}_t, \mathcal{X}_t)$ of the dynamics of $(\mathcal{F}, \mathcal{X})$ to the local models over vertices with height $> t$. Restriction gives a map $\text{Aut}(\mathcal{F}, \mathcal{X}) \rightarrow \text{Aut}(\mathcal{F}_t, \mathcal{X}_t)$; denote its image by $\text{Aut}_{(\mathcal{F}, \mathcal{X})}(\mathcal{F}_t, \mathcal{X}_t)$. If $0 < s < t$ then restriction gives a compatible natural surjection

$$\text{Aut}_{(\mathcal{F}, \mathcal{X})}(\mathcal{F}_s, \mathcal{X}_s) \rightarrow \text{Aut}_{(\mathcal{F}, \mathcal{X})}(\mathcal{F}_t, \mathcal{X}_t).$$

The structure of $\text{Aut}_{(\mathcal{F}, \mathcal{X})}(\mathcal{F}_t, \mathcal{X}_t)$ for large positive values of t is easy to compute. Recall the definition of the fundamental vertices from §6.2.

LEMMA 8.2. – *Let $(\mathcal{F}, \mathcal{X})$ be a tree of local models over (F, T) with N fundamental vertices v_0, \dots, v_{N-1} . Fix $j \in \{0, \dots, N-1\}$ and let t_j be the height of v_j in $T(F)$. Then*

$$\text{Aut}_{(\mathcal{F}, \mathcal{X})}(\mathcal{F}_{t_j}, \mathcal{X}_{t_j}) \simeq \prod_{i=j}^{j+N-1} \mathbb{Z}/k(v_i)\mathbb{Z}$$

where $k(v_i)$ is the local symmetry of $(\mathcal{F}, \mathcal{X})$ at v_i .

Proof. – The automorphism group $\text{Aut}(\mathcal{F}, \mathcal{X})$ stabilizes all vertices v_j with $j \geq 0$, and the cyclic group $\mathbb{Z}/k(v_i)\mathbb{Z}$ is the stabilizer of v_i . The action of any automorphism at vertex v_i uniquely determines its action at all vertices in its forward orbit, by Lemma 5.3. The fundamental vertices are in distinct grand orbits, so the automorphism group is a direct product. \square

LEMMA 8.3. – *For any tree of local models, $\text{Aut}(\mathcal{F}, \mathcal{X})$ is a profinite group, the limit of the collection of finite groups $\text{Aut}_{(\mathcal{F}, \mathcal{X})}(\mathcal{F}_t, \mathcal{X}_t)$.*

Proof. – It remains to show that the groups $\text{Aut}_{(\mathcal{F}, \mathcal{X})}(\mathcal{F}_t, \mathcal{X}_t)$ are finite for each $t > 0$. The group $\text{Aut}_{(\mathcal{F}, \mathcal{X})}(\mathcal{F}_t, \mathcal{X}_t)$ is finite by Lemma 8.2 for all t large enough. From Lemma 5.3, the action of an automorphism $\varphi \in \text{Aut}(\mathcal{F}, \mathcal{X})$ at any vertex v determines uniquely its action at the image vertex $F(v)$. The vertices of a given height must be permuted by an automorphism, so we may apply Lemma 8.1 to conclude that $\text{Aut}(\mathcal{F}_t, \mathcal{X}_t)$ is finite for any $t > 0$. The restriction maps allow us to view the full automorphism group $\text{Aut}(\mathcal{F}, \mathcal{X})$ as an inverse limit. \square

8.4. The spine and its automorphism group

Now suppose $(\mathcal{F}, \mathcal{X})$ is a tree of local models with first-return map $(\mathcal{R}, \mathcal{S})$ on its spine. Since $(\mathcal{R}, \mathcal{S})$ is again a dynamical system, it too has an automorphism group $\text{Aut}(\mathcal{R}, \mathcal{S})$ which is naturally a profinite group. It follows that $\text{Aut}(\mathcal{R}, \mathcal{S})$ is inductively computable; the base case is covered by Lemma 8.2 at height $t = h(v_0)$. Furthermore, in the shift locus, the subtree of \mathcal{S} below v_0 is finite, and $\text{Aut}(\mathcal{R}, \mathcal{S})$ is a finite group which is inductively computable in finite time.

The restriction of any automorphism $\varphi \in \text{Aut}(\mathcal{F}, \mathcal{X})$ to the spine \mathcal{S} is an automorphism of $(\mathcal{R}, \mathcal{S})$. Indeed, φ preserves local degree, and the spine consists of all vertices with local degree > 1 . The following lemma then implies that $\text{Aut}(\mathcal{F}, \mathcal{X})$ is inductively computable from the data of $(\mathcal{R}, \mathcal{S})$.

LEMMA 8.4. – *The map*

$$\text{Aut}(\mathcal{F}, \mathcal{X}) \rightarrow \text{Aut}(\mathcal{R}, \mathcal{S}),$$

which sends an automorphism to its restriction to the spine, is an isomorphism.

Proof. – Suppose $\psi \in \text{Aut}(\mathcal{R}, \mathcal{S})$ is given. We use the usual inductive argument to show $\psi = \varphi|_{\mathcal{S}}$ for a unique $\varphi \in \text{Aut}(\mathcal{F}, \mathcal{X})$. Define φ by $\varphi = \psi$ on the local model surfaces at and above the vertex v_0 . For the induction step, suppose φ has been constructed at all vertices with simplicial distance at most n from v_0 , and suppose φ commutes with \mathcal{F} . Let v' be a vertex at simplicial distance exactly n from v_0 and suppose v is just below v' . If $v \in \mathcal{S}$ we set $\varphi_v = \psi_v$ on the surface X_v . If $v \notin \mathcal{S}$ then by induction φ has already been defined on v' and on $w = F(v)$. Let $\hat{w} = \varphi(w)$, $\hat{v}' = \varphi(v')$, and denote the image of v under φ , yet to be defined, by \hat{v} .

The restriction $\varphi_{v'}$ to $X_{v'}$ uniquely determines \hat{v} , because an automorphism must preserve the tree structure. In addition, φ commutes with the local model maps at each vertex, so $f_{\hat{v}'} \circ \varphi_{v'} = \varphi_{F(v')} \circ f_{v'}$, and we deduce that $\hat{w} = F(\hat{v})$. Since $v \notin \mathcal{S}$, neither is \hat{v} , and the local model maps $f_v : X_v \rightarrow X_w$ and $f_{\hat{v}} : X_{\hat{v}} \rightarrow X_{\hat{w}}$ are isomorphisms. So the automorphism φ

must send X_v to $X_{\hat{v}}$ via the composition $(f_{\hat{w}})^{-1} \circ \varphi_w \circ f_v$; this composition defines the extension φ_v . In this way, we have extended φ uniquely from simplicial distance n to simplicial distance $n + 1$, completing the proof. \square

8.5. Symmetries in degree 3

We will use the following lemma in our computations for cubic polynomials in Section 11. Recall once more the definition of the fundamental vertices from §6.2.

LEMMA 8.5. – *Suppose f is a cubic polynomial with critical points c_1, c_2 and escape rate G_f , and let $(\mathcal{F}, \mathcal{X})$ be its tree of local models.*

1. *If $c_1 = c_2$, then $k(v_0) = 3, k(v_1) = 1$, and $\text{Aut}(\mathcal{F}, \mathcal{X})$ is cyclic of order 3.*
2. *If $G_f(c_1) = G_f(c_2)$ with $c_1 \neq c_2$, then either*
 - (a). *$k(v_0) = k(v_1) = 1$ and $\text{Aut}(\mathcal{F}, \mathcal{X})$ is trivial, or*
 - (b). *$k(v_0) = k(v_1) = 2$ and $\text{Aut}(\mathcal{F}, \mathcal{X})$ is cyclic of order 2.*
3. *In all other cases, the order of local symmetry of each fundamental vertex is equal to 1.*

Case (1) occurs when f is affine conjugate to $f(z) = z^3 + c$ with c outside the connectedness locus; case 2(b) when f admits an automorphism, i.e., is affine conjugate to an odd map.

Proof. – In case (1), the number of fundamental vertices is $N = 1$, the local model map f_{v_0} has a deck group of order 3, and its range X_{v_1} has a distinguished point, the unique critical value. Case (2) is similar. If f has an automorphism, then there are symmetries of order 2 at v_0 and v_1 commuting with f_{v_0} ; thus $k(v_0) = k(v_1) = 2$. If f fails to have an automorphism but $c_1 \neq c_2$, there are no symmetries at v_0 and consequently no symmetries at v_1 , so $k(v_0) = k(v_1) = 1$. The conclusions about the automorphism groups then follow immediately from Lemma 8.4.

To prove the last statement, suppose that the two critical points have distinct escape rates. Then the local model map from X_{v_0} to its image is a degree 3 branched cover with a unique critical point (of multiplicity 1) in the surface X_{v_0} . Such a branched cover has no symmetries, so $k(v_0) = k(F(v_0)) = 1$. Further, if the two critical points are in distinct foliated equivalence classes, then the local model surface X_{v_1} has a unique marked point on its central leaf (its intersection with the orbit of critical point c_2) that must be preserved by any automorphism; therefore, the local symmetry at v_1 will be 1. \square

9. Topological conjugacy

In this section, we remind the reader of the quasiconformal deformation theory of polynomials, following [19]. We show that the tree of local models is invariant under topological conjugacies that preserve critical escape rates. In other words:

THEOREM 9.1. – *The tree of local models is a twist-conjugacy invariant.*

We recall the topology on \mathcal{B}_d , the moduli space of basins $(f, X(f))$ introduced in [8], and we study the locus $\mathcal{B}_d(\mathcal{F}, \mathcal{X}) \subset \mathcal{B}_d$ of basins with a given tree of local models $(\mathcal{F}, \mathcal{X})$. Since a gluing of $(\mathcal{F}, \mathcal{X})$ determines a basin dynamical system (Proposition 7.3), we refer to elements of $\mathcal{B}_d(\mathcal{F}, \mathcal{X})$ as *gluing configurations*.

Recall the notion of fundamental edges of a tree, from §6.2. If κ is the reciprocal of a positive integer, we denote by $\kappa\mathbb{S}^1$ the quotient group $\mathbb{R}/2\pi\kappa\mathbb{Z}$ of \mathbb{S}^1 by the group generated by a rotation of order κ^{-1} . Carefully accounting for symmetries in $(\mathcal{F}, \mathcal{X})$, we show:

THEOREM 9.2. – *Let $(\mathcal{F}, \mathcal{X})$ be a tree of local models with N fundamental edges. Given a base point $(f, X(f)) \in \mathcal{B}_d(\mathcal{F}, \mathcal{X})$, there is a continuous projection*

$$\mathcal{B}_d(\mathcal{F}, \mathcal{X}) \rightarrow (\kappa\mathbb{S}^1)^N$$

for some positive integer κ^{-1} , giving $\mathcal{B}_d(\mathcal{F}, \mathcal{X})$ the structure of a compact, locally trivial fiber bundle over an N -torus whose fibers are totally disconnected. The twisting action is the lift of the holonomy induced by rotations in each coordinate, and the orbits form the leaves of a foliation of $\mathcal{B}_d(\mathcal{F}, \mathcal{X})$ by N -dimensional manifolds. The leaves are in bijective correspondence with topological conjugacy classes within the space $\mathcal{B}_d(\mathcal{F}, \mathcal{X})$. For $(\mathcal{F}, \mathcal{X})$ in the shift locus, the fibers are finite.

The value of κ depends only on the local symmetries at the fundamental vertices, defined in §8.2; a formula for κ is given in equation (9.1) below.

From Theorem 9.2, the problem of classifying basin dynamics up to topological conjugacy amounts to computing the monodromy action of twisting in the bundle $\mathcal{B}_d(\mathcal{F}, \mathcal{X})$. Leading to the proof of Theorem 1.2, we observe:

COROLLARY 9.3. – *Under the hypotheses of Theorem 9.2, let $\theta \in (\kappa\mathbb{S}^1)^N$ be any point in the base torus. Then the set of topological conjugacy classes in $\mathcal{B}_d(\mathcal{F}, \mathcal{X})$ is in bijective correspondence with the orbits of the monodromy action of $\mathbb{Z}^N = \pi_1((\kappa\mathbb{S}^1)^N, \theta)$ on the fiber above the base point θ .*

9.1. Fundamental subannuli

Fix a polynomial representative $f : \mathbb{C} \rightarrow \mathbb{C}$ of its conjugacy class, and let G_f be its escape-rate function. The *foliated equivalence class* of a point z in the basin $X(f)$ is the closure of its grand orbit

$$\{w \in X(f) : \exists n, m \in \mathbb{Z}, f^n(w) = f^m(z)\}$$

in $X(f)$. Let N be the number of distinct foliated equivalence classes containing critical points of f . Note that $N = 0$ if and only if the Julia set of f is connected, if and only if the maximal critical escape rate $M(f) = 0$. is zero. For $N > 0$, these critical foliated equivalence classes subdivide the fundamental annulus

$$A(f) = \{z \in X(f) : M(f) < G_f(z) < d M(f)\}$$

into N *fundamental subannuli* A_1, \dots, A_N linearly ordered by increasing escape rate.

The number N coincides with the number of fundamental edges of the tree $(F, T(f))$, as defined in §6.2, and the number of independent critical escape rates, defined in §2.1. For each $i = 1, \dots, N$, the annulus A_i lies over the fundamental edge e_i .

9.2. Quasiconformal deformations of the basin

For each conformal conjugacy class of polynomial $f \in \mathcal{M}_d$, there is a canonical space of marked quasiconformal deformations of f supported on the basin of infinity. The general theory, developed in [19], shows that this space admits the following description; see also [7]. The wring motion of [4] is a special case.

One can define quasiconformal stretching and twisting deformations on each of the subannuli A_j independently so that the resulting deformation of the basin $X(f)$ is continuous and well-defined and an isometry on each horizontal leaf. We will parametrize the deformations of each subannulus by a parameter $t + is$ in the upper half-plane $\mathbb{H} = \{t + is : s > 0\}$, acting by the linear transformation

$$\begin{pmatrix} 1 & t \\ 0 & s \end{pmatrix}$$

on a rectangular representative of the annulus in \mathbb{R}^2 , of width 1 and height equal to the modulus mod A_j , with vertical edges identified. Extending the deformation to the full basin of infinity by the dynamics of f , the deformation thus defines an analytic map

$$\mathbb{H}^N \rightarrow \mathcal{M}_d,$$

sending point (i, i, \dots, i) to f . By construction, the twisting deformations (where $s = 1$ in each factor) preserve escape rates, while stretching (with $t = 0$ in each factor) preserves external angles. Both stretching and twisting send horizontal leaves isometrically to horizontal leaves.

An important idea of [19] in this context is that any two polynomial basins $(f, X(f))$ and $(g, X(g))$ which are topologically conjugate are in fact quasiconformally conjugate by a homeomorphism of the above type: it has a decomposition into N stretching and twisting factors, each factor determined by its effect on the N fundamental subannuli. Moreover, if the forward orbits of two critical points meet a common level set in the closure $\{M(f) \leq G_f \leq d \cdot M(f)\}$ of the fundamental annulus, the arc length (angular difference) between these points is preserved under any topological conjugacy. (See §5 of [19].)

9.3. Normalization of twisting

For the proofs of Theorems 12.1, 4.1, and 4.2, it will be convenient to work with the following normalization for the twisting action. Fix $f \in \mathcal{M}_d$ and consider the real analytic map

$$\text{Twist}_f : \mathbb{R}^N \rightarrow \mathcal{M}_d$$

which parametrizes the twisting deformations in the N fundamental subannuli of f , sending the origin to f . We normalize the parameterization Twist_f so that the basis vector

$$\mathbf{e}_j = (0, \dots, 0, 1, 0, \dots, 0) \in \mathbb{R}^N$$

induces a full twist in the j -th fundamental subannulus. That is, if mod A_j is the modulus of the j -th subannulus of f , then $\text{Twist}_f(t \mathbf{e}_j)$ corresponds to the action of $1 + i t / \text{mod } A_j \in \mathbb{H}$ in the coordinates described in §9.2.

9.4. Twisting and the tree of local models

We now prove that the tree of local models is invariant under the twisting deformation. More precisely, a twisting deformation induces, via restriction to central leaves and extension by isometries, an isomorphism between trees of local models.

Proof of Theorem 9.1. – Fix a tree of local models associated to a polynomial $f \in \mathcal{M}_d$ and suppose a twisting deformation conjugates $(f, X(f))$ to $(g, X(g))$ by a quasiconformal map h . Then h induces an isomorphism $H : (F, T(f)) \rightarrow (G, T(g))$, and so for each $v \in T(f)$ the restriction of h gives an affine map of local model surfaces $h_v : (X_v(f), \omega_v) \rightarrow (X_{H(v)}(g), \omega_{H(v)})$. Since h_v is an isometry on the corresponding central leaves, it extends to an isometry $\varphi_v : X_v(f) \rightarrow X_{H(v)}(g)$. The dynamics of f and of g is locally a constant scaling, so $\varphi = \{\varphi_v\}$ yields an isomorphism $(\mathcal{F}(f), \mathcal{X}(f)) \rightarrow (\mathcal{F}(g), \mathcal{X}(g))$. \square

9.5. The space of basins \mathcal{B}_d

We begin by recalling results from [8]. The set \mathcal{B}_d of conformal conjugacy classes of basins $(f, X(f))$ inherits a natural Gromov-Hausdorff topology: two basins $(f, X(f)), (g, X(g))$ are ε -close if there is a relation Γ on the product $\{\varepsilon < G_f < 1/\varepsilon\} \times \{\varepsilon < G_g < 1/\varepsilon\}$ which is ε -close to the graph of an isometric conjugacy. The natural projection $\pi : \mathcal{M}_d \rightarrow \mathcal{B}_d$ is continuous, proper, and monotone (i.e., has connected fibers). Both spaces are naturally stratified by the number N of fundamental subannuli and the projection respects this stratification. While discontinuous on \mathcal{M}_d , twisting is continuous on each stratum \mathcal{B}_d^N , by [7, Lemma 5.2].

9.6. The bundle of gluing configurations

Fix a tree of local models $(\mathcal{F}, \mathcal{X})$. Recall from §7.5 that an abstract gluing ι defines a quotient map $\mathcal{X} \rightarrow \mathcal{X}/\iota = X^\iota$ to an abstract planar Riemann surface to which the dynamics of \mathcal{F} descends to yield a proper degree d holomorphic self-map $f^\iota : X^\iota \rightarrow X^\iota$. In this way, a gluing ι defines a holomorphic semiconjugacy $(\mathcal{F}, \mathcal{X}) \rightarrow (f^\iota, X^\iota)$. The holomorphic conjugacy class of (f^ι, X^ι) we call the associated *gluing configuration*. Given an abstract tree of local models $(\mathcal{F}, \mathcal{X})$, we let $\mathcal{B}_d(\mathcal{F}, \mathcal{X}) \subset \mathcal{B}_d$ be the collection of all gluing configurations. Theorem 7.1 implies this is nonempty.

We begin with an identification of $\mathcal{B}_d(\mathcal{F}, \mathcal{X})$ as a set.

The automorphism group $\text{Aut}(\mathcal{F}, \mathcal{X})$ acts naturally on the set of gluings as follows. Given an automorphism $\varphi \in \text{Aut}(\mathcal{F}, \mathcal{X})$ and a gluing $\iota = \{\iota_e\}_{e \in E}$, the gluing $\varphi.\iota$ is the collection of isomorphisms $\{(\varphi.\iota)_e\}_{e \in E}$ defined as follows. Suppose edge $e \in E$ joins v to the vertex v' above it; set $\hat{v} = \varphi^{-1}(v)$ and $\hat{e} = \varphi^{-1}(e)$ and define

$$(\varphi.\iota)_e := \varphi_{\hat{v}'} \circ \iota_{\hat{e}} \circ \varphi_v^{-1}.$$

Put another way: a gluing ι defines an equivalence relation \sim_ι , which is a subset of $\mathcal{X} \times \mathcal{X}$; the gluing $\varphi.\iota$ corresponds to the equivalence relation given by $(\varphi \times \varphi)(\sim_\iota) \subset \mathcal{X} \times \mathcal{X}$.

PROPOSITION 9.4. – *The natural map $\iota \mapsto (f^\iota, X^\iota)$ descends to a bijection between $\text{Aut}(\mathcal{F}, \mathcal{X})$ -orbits of gluings and gluing configurations.*

Proof. – In one direction, an automorphism sending one gluing to another, by definition, descends to holomorphic map conjugating the two gluing configurations. In the other, a conjugacy between two gluing configurations lifts to an automorphism sending the first corresponding gluing to the second. \square

With respect to the topology on the space of basins \mathcal{B}_d , we now prove that the set of all gluing configurations forms a compact fiber bundle over a torus.

The main idea in the proof of Theorem 9.2 is the following. Suppose $(\mathcal{F}, \mathcal{X})$ is a tree of local models. Gluing over the N fundamental edges gives a continuous set of choices; there should be one circle's worth for each such edge. The product of these N circles should give the torus that is the base of our bundle. However, the possible presence of symmetries of $(\mathcal{F}, \mathcal{X})$ that act nontrivially at the local model surfaces corresponding to fundamental vertices means that we need to pass to a finite quotient of this torus. This is again a torus, and now this is the base of our bundle. Gluing at the fundamental edges determines the gluing at all higher edges. Now suppose gluings over the fundamental edges have been chosen, and consider the possibilities for gluing over the remaining, lower edges. Fix a distance n below v_0 as in §6.6, and consider the gluings of edges at this distance. For fixed choice of fundamental gluings, this is a finite set. Again, the possible presence of symmetries of $(\mathcal{F}, \mathcal{X})$ among local model surfaces X_v at vertices of distance n means that two distinct such gluing choices might yield the same result. Considering inductively distances $n = 1, 2, 3, \dots$, we see that the totality of all such gluing choices is naturally either finite, or a Cantor set. Twisting deformations—that is, altering continuously the gluing choices along the fundamental edges—gives an action of \mathbb{R}^N on the set of gluings at distance n , and the orbits are the leaves of our bundle.

Proof of Theorem 9.2. – Let v_0, \dots, v_{N-1} denote the fundamental vertices of the underlying polynomial tree and $v_N = F(v_0)$. Recall the definition of the local symmetry $k(v)$ of $(\mathcal{F}, \mathcal{X})$ at a vertex v , given in §8.2. We set

$$(9.1) \quad \kappa = \frac{1}{\text{lcm}\{k(v_0), k(v_1), \dots, k(v_N)\}}.$$

We first define the continuous projection

$$\mathcal{B}_d(\mathcal{F}, \mathcal{X}) \rightarrow (\kappa\mathbb{S}^1)^N$$

which will define the fiber bundle structure. Fix any base point $(f, X(f))$ in $\mathcal{B}_d(\mathcal{F}, \mathcal{X})$. Let θ be an angular coordinate in \mathbb{R}/\mathbb{Z} on the fundamental annulus $A_f := \{M_f < G_f(z) < dM_f\}$; it is defined up to an additive constant. Now suppose $g \in \mathcal{B}_d(\mathcal{F}, \mathcal{X})$. By assumption there exists a (not necessarily unique) isomorphism $\varphi(g) : (\mathcal{F}(f), \mathcal{X}(f)) \rightarrow (\mathcal{F}(g), \mathcal{X}(g))$ which restricts to isomorphisms

$$\varphi_i(g) : X_i(f) \rightarrow X_i(g), i = 0, \dots, N$$

between the local model surfaces over vertices v_0, v_1, \dots, v_N for f and g . Note that the $\varphi_i(g)$'s must respect the markings by the orbits of critical points, as in §8. There are choices for the $\varphi_i(g)$'s: they are unique only up to pre-composition by the restriction to $X_i(f)$ of an element of $\text{Aut}(\mathcal{F}(f), \mathcal{X}(f))$. For each $i = 0, \dots, N - 1$, the outer annulus of $X_i(f)$ coincides with the inner annulus of $X_{i+1}(f)$, and so $\varphi_{i+1}(g)^{-1} \circ \varphi_i(g)$ is well-defined on

the outer annulus of $X_i(f)$. Suppose x is an arbitrary point in the outer annulus of $X_i(f)$. Define

$$\Delta_i(g) := \theta(\varphi_{i+1}(g)^{-1} \circ \varphi_i(g)(x)) - \theta(x) \in \kappa\mathbb{S}^1.$$

This depends only on g : changing the angular coordinate or the base point x changes each term in the difference by the same additive constant, and the ambiguity in the choice of isomorphisms $\varphi_i(g)$ is annihilated by recording the difference in $\kappa\mathbb{S}^1$ instead of in just \mathbb{S}^1 . The projection $\mathcal{B}_d(\mathcal{F}, \mathcal{X}) \rightarrow (\kappa\mathbb{S}^1)^N$ is then well-defined by the formula

$$g \mapsto (\Delta_i(g))_{i=0}^{N-1}.$$

Local triviality and continuity of the projection can be seen from the twisting action. We proved in [8, Lemma 5.2] that the twisting action of \mathbb{R}^N is well-defined on the stratum \mathcal{B}_d^N of polynomial basins with N fundamental subannuli. It is continuous and locally injective. The space $\mathcal{B}_d(\mathcal{F}, \mathcal{X})$ is invariant under twisting by Theorem 9.1. The definitions of the twisting action and of the projection imply that twisting by t in the i th fundamental subannulus translates the i th coordinate of the image under projection to the base by $t \bmod 2\pi\kappa$. It follows that twisting defines a local holonomy map between fibers in the bundle of gluing configurations and the space of gluing configurations is foliated by N -manifolds whose leaves are the orbits under the twisting action.

Recall from §9.2 that two polynomial basins are topologically conjugate and have the same critical escape rates if and only if they are equivalent by a twisting deformation. Thus, the topological conjugacy classes within the space of gluing configurations are easily seen to be in one-to-one correspondence with the twisting orbits, i.e., leaves.

We now show that the fibers are totally disconnected. Recall the gluing construction used in the proof of Theorem 7.1. First, fix a point b in the base torus of the projection. This corresponds to choosing one from among finitely many choices of gluings over the fundamental edges joining v_0, \dots, v_N ; this determines all gluings at vertices above v_0 . The collection of gluing choices is now made sequentially by descending height. At the inductive stage, we have a vertex v joined up to a vertex v' along an edge e of degree k ; there are k choices for the gluing isomorphism over e . After a choice is made at every vertex in the tree, we obtain a holomorphic self-map $f : X \rightarrow X$ which is conformally conjugate to $f : X(f) \rightarrow X(f)$ for some polynomial f , by Theorem 7.1. All basins in $\mathcal{B}_d(\mathcal{F}, \mathcal{X})$ over the base point b are obtained in this way. By the discreteness of gluing choices at each vertex and the definition of the Gromov-Hausdorff topology on \mathcal{B}_d , for any fixed simplicial distance n from v_0 , the set of gluing configurations which can be produced using the continuous choices corresponding to the base point b and to a fixed set of choices at the finite set of vertices v below and at distance at most n from v_0 is an open set in $\mathcal{B}_d(\mathcal{F}, \mathcal{X})$. In this way, we see that each gluing configuration over the base point b is in its own connected component and the fibers are finite if $(\mathcal{F}, \mathcal{X})$ lies in the shift locus.

It remains to show that the bundle of gluing configurations is compact. By properness of the critical escape rate map $f \mapsto \{G_f(c) : f'(c) = 0\}$ on the space of basins \mathcal{B}_d [7], the bundle must lie in a compact subset of \mathcal{B}_d . Let $(f_n, X(f_n))$ be any sequence in the bundle converging to a basin $(f, X(f))$. Exactly as in the proof of Theorem 7.1, we may deduce that $(f, X(f))$ has the same tree of local models, and is therefore in the bundle of gluing configurations; see also [8, Lemma 3.2]. \square

LEMMA 9.5. – *Let $(\mathcal{F}, \mathcal{X})$ be a tree of local models. If the fibers in the bundle of gluing configurations have infinite cardinality, then they are homeomorphic to Cantor sets.*

Proof. – The fibers are compact and totally disconnected by the previous lemma. By Brouwer’s topological characterization of the Cantor set [13, Thm. 2-97], we need only show the fiber is perfect. From the inductive construction of basins from the tree of local models, we see that the fiber of the bundle of gluing configurations has infinite cardinality if and only if there are conformally inequivalent gluing choices at an infinite collection of heights tending to 0. By the definition of the Gromov-Hausdorff topology on the space of basins \mathcal{B}_d , basins are close if they are “almost” conformally conjugate above some small height $t > 0$. Consequently, any basin in the bundle of gluing configurations can be approximated by a sequence where a different gluing choice has been made at heights $\rightarrow 0$. \square

9.7. The bundle of gluing configurations, in degree 2

We can give a complete picture of the bundle of gluing configurations in degree two. Let $(\mathcal{F}, \mathcal{X})$ be a tree of local models in degree 2. In the notation of the proof of Theorem 9.2, we have $N = 1$, $k(v_0) = 2$, and $k(v_1) = 1$, so $\kappa = 1/2$. Since every edge below v_0 has degree one, once the base point $b \in (1/2)\mathbb{S}^1$ corresponding to the gluing along the fundamental edge e joining v_0 and v_1 has been chosen, the remaining gluings are uniquely determined. Hence the projection map $\mathcal{B}_d(\mathcal{F}, \mathcal{X}) \rightarrow (1/2)\mathbb{S}^1$ is 1-to-1 and the bundle of gluing configurations $\mathcal{B}_2(\mathcal{F}, \mathcal{X}) \subset \mathcal{B}_2$ is homeomorphic to a circle. In more familiar language: it is the image of an equipotential curve around the Mandelbrot set in the moduli space \mathcal{M}_2 via the homeomorphism from the shift locus in \mathcal{M}_2 to that of \mathcal{B}_2 . A full loop around the Mandelbrot set corresponds to an external angle displacement running from 0 to $2\pi/2$. In fact, this is the same as the loop in Blanchard-Devaney-Keen inducing the generating automorphism of the shift [2]; the two lobes of the central leaf at v_0 are interchanged under the monodromy generator.

9.8. The bundle of gluing configurations in degree 3

In degree three, we can give a complete succinct picture of the bundle of gluing configurations in a few special cases. The remaining ones are handled by Theorems 4.1 and 4.2.

Suppose f is a cubic polynomial with an automorphism and disconnected Julia set. Then both critical points escape at the same rate, the automorphism has order 2, and it interchanges the two critical points and their distinct critical values. It is easy to see that there is a unique branched cover of laminations of degree 3 with this symmetry. It follows that, for a given critical escape rate, there is a unique tree of local models $(\mathcal{F}, \mathcal{X})$ with this configuration. By Lemma 8.5, $k(v_0) = k(v_1) = 2$, so $\kappa = 1/2$. Like in the quadratic case, a basin of infinity is uniquely determined by the gluing of the local models along the fundamental edge, because all edges below v_0 have local degree 1. But it now takes *two* turns around the base (= one full twist in the fundamental annulus) to return to a given basin, because the angle displacement between a critical point and its critical value is an invariant of conformal conjugacy. Thus the projection $\mathcal{B}_3(\mathcal{F}, \mathcal{X}) \rightarrow (1/2)\mathbb{S}^1$ is 2-to-1 and the bundle of gluing configurations $\mathcal{B}_3(\mathcal{F}, \mathcal{X})$ is homeomorphic to a circle.

Suppose f is a cubic polynomial where the two critical points coincide and escape to infinity, so it has a monic and centered representation as $f(z) = z^3 + c$, with c not in the connectedness locus. Let $(\mathcal{F}, \mathcal{X})$ be its tree of local models. By Lemma 8.5, $k(v_0) = 3$, $k(v_1) = 1$, and $\text{Aut}(\mathcal{F}, \mathcal{X})$ is cyclic of order 3. The bundle $\mathcal{B}_3(\mathcal{F}, \mathcal{X})$ therefore projects to the circle $(1/3)\mathbb{S}^1$. Again, since all edges below v_0 map by degree 1, the gluing at the fundamental edge determines the basin. Going around this base circle of length $1/3$ forms a closed loop in $\mathcal{B}_3(\mathcal{F}, \mathcal{X})$, because a basin of infinity is uniquely determined by the gluing along the fundamental edge; the bundle is homeomorphic to a circle. Note that lifting this path to the family $\{z^3 + c : c \in \mathbb{C}\}$ induces only a half-loop around the connectedness locus, since $z \mapsto -z$ conjugates $z^3 + c$ to $z^3 - c$.

Suppose $(\mathcal{F}, \mathcal{X})$ is a tree of local models for a cubic polynomial in the shift locus with $N = 2$ fundamental edges. (Recall the definition of fundamental edges from §6.2.) By Lemma 8.5, there are no symmetries over v_0, v_1, v_2 , so $\kappa = 1$. The base of the fiber bundle is $\mathbb{S}^1 \times \mathbb{S}^1$. For polynomials in the shift locus, there exists a height $t > 0$ such that all vertices below height t have local degree 1, so all fibers of the fiber bundle must be finite. In fact, the bundle of gluing configurations $\mathcal{B}_3(\mathcal{F}, \mathcal{X})$ is homeomorphic to a finite union of smooth 2-tori; compare [7, Theorem 1.2]. The question of how many tori comprise this finite union is answered by Theorem 4.1; each torus corresponds to a distinct topological conjugacy class of polynomials.

Finally, let $(f, X(f))$ be any other basin in the space \mathcal{B}_3 , so it has $N = 1$ fundamental edge and there are no symmetries at the fundamental vertices by Lemma 8.5. Therefore, $\kappa = 1$ and the base of the fiber bundle is the circle \mathbb{S}^1 . The fibers are necessarily finite if f lies in the shift locus, but the fibers can be finite or infinite in the case where one critical point lies in the filled Julia set. The number of connected components in the bundle $\mathcal{B}_3(\mathcal{F}, \mathcal{X})$ (and their topological structure) is given in Theorems 4.1 and 4.2.

10. The pictograph

Suppose f is a polynomial of degree $d \geq 2$, with disconnected Julia set, and with N independent critical escape rates; equivalently, N fundamental subannuli. In this section, we define the pictograph $\mathcal{D}(f)$. Using Theorem 9.1, we will first show

THEOREM 10.1. – *The pictograph is a topological-conjugacy invariant.*

The pictograph is defined in terms of the tree of local models $(\mathcal{F}, \mathcal{X}(f))$ of the polynomial f . Formally speaking, the pictograph is a static object; there is no map. We show nevertheless that

THEOREM 10.2. – *A tree of local models $(\mathcal{F}, \mathcal{X})$ is determined up to holomorphic conjugacy by its pictograph \mathcal{D} and either*

- (i) *the heights of the critical points, or*
- (ii) *the lengths of the fundamental edges e_1, \dots, e_N in the height metric on the tree.*

It follows from Theorem 10.2 that the pictograph encodes the symmetry group $\text{Aut}(\mathcal{F}, \mathcal{X})$ of the tree of local models. It also determines the number of fundamental vertices of the underlying tree. Theorems 10.2 and 9.2 immediately imply Theorem 1.3.

An *abstract pictograph* \mathcal{D} is defined as the pictograph associated to an abstract tree of local models, as defined in §7.2. Recall that the notion of compatible critical heights was defined in §6.5. Proposition 6.1 implies:

PROPOSITION 10.3. – *For each abstract pictograph of degree d with N fundamental vertices, the set of compatible critical heights $(h_1, \dots, h_{d-1}) \in [0, \infty)^{d-1}$, with $h_1 \geq \dots \geq h_{d-1}$, is homeomorphic to an open N -dimensional simplex.*

10.1. Pictographs

Fix a polynomial f of degree d with disconnected Julia set and N fundamental subannuli (defined in §9.1). Let $(\mathcal{F}, \mathcal{X})$ be the tree of local models associated to f , and let $(F, T) = (F, T(f))$ be its simplicial polynomial tree. Recall that the spine $S(T)$ of the tree is the convex hull of its critical points and critical ends; equivalently, it is the set of edges and vertices mapping by degree > 1 . The fundamental edges e_1, \dots, e_{N-1} and vertices v_0, \dots, v_{N-1} of T were defined in §6.2. The *pictograph* is a collection of labeled lamination diagrams, one for each vertex in $S(T)$ at and below vertex $v_N = F(v_0)$, where each diagram is labeled by its intersection with the critical orbits. It is defined as follows.

Recall that v_0 denotes the highest branching vertex of $T(f)$ and $v_N = F(v_0)$. We consider the vertices $v \in S(T)$ which are at and below the height of v_N . This gives us a simplicial subtree of the spine that we denote by $S_{\leq N}(T)$. For each vertex $v \in S_{\leq N}(T)$, record the lamination diagram for the central leaf of the local model surface $X_v(f)$. To record simultaneously the tree structure of $S_{\leq N}(T)$, we join these lamination diagrams by an edge if the corresponding vertices are joined by an edge in $S(T)$. This forms a *spine of lamination diagrams*.

To define the labels, we first choose an indexing of the critical points of f so that $G_f(c_1) \geq \dots \geq G_f(c_{d-1})$. Given a vertex v , we label the corresponding lamination diagram as follows. Given an index $i \in \{1, \dots, d-1\}$ and an integer $k \geq 0$, consider the point $f^k(c_i)$ and how this point is located relative to $X_v(f)$.

- If $f^k(c_i)$ lies in one of the bounded complementary components of $X_v(f)$, we label the corresponding gap in the lamination diagram for $X_v(f)$ with the symbol k_i .
- If $f^k(c_i)$ lands on the central leaf of $X_v(f)$, we label the corresponding equivalence class in the lamination diagram for $X_v(f)$ by the symbol k_i . When indicated by a drawing, we label only one representative point in the equivalence class.
- Otherwise, the label k_i does not appear in the lamination diagram for $X_v(f)$; note that the point $f^k(c_i)$ lies neither in the outer annulus nor in an inner annulus of $X_f(f)$.

Thus, the data in the pictograph is the same as the static data of the collection, for the above vertices v in the spine, of the local model surfaces $X_v(f)$ labeled in the above fashion, with the map forgotten.

Suppose now f and g are two polynomials. We say f and g have *equivalent* pictographs if, after applying some permutation of the set of indices $i = 1, \dots, d-1$ for the critical points, there exists

- a simplicial isomorphism $\varphi : S_{\leq N}(T(f)) \rightarrow S_{\leq N}(T(g))$ between their spines of lamination diagrams, such that:
- for each vertex $v \in S_{\leq N}(T(f))$, there is a rotation of the closed unit disk sending the lamination diagram for f at v to the lamination diagram for g at $\varphi(v)$ and preserving the labels. In other words: a rotation makes the two labeled lamination diagrams coincide.

An abstract tree of local models $(\mathcal{F}, \mathcal{X})$ determines a pictograph as well. Counting both critical points in \mathcal{X} and those critical ends in $J(F)$ with multiplicity, there are again $d - 1$ critical points. Given a vertex v with local model surface (X_v, ω_v) , we regard a critical point c_i below v (in the tree) as “lying in” the gap of X_v corresponding to the edge leading to c_i .

10.2. Examples of pictographs

The degree 2 pictographs are the easiest to describe: in fact, there is only one possibility. For quadratic polynomials $z^2 + c$ with disconnected Julia set, the spine of the tree is the ray from the unique critical vertex v_0 heading to ∞ . The lamination diagram over the vertex v_0 is a circle cut by a diameter, representing the Figure 8 level set $\{z \in \mathbb{C} : G_c(z) = G_c(0)\}$, with arc length measured by external angle. The pictograph includes the data of this single diagram together with the image lamination (the trivial equivalence relation corresponding to level set $\{G_c = G_c(c)\}$), labeled by the symbol 0 to mark the critical point and 1 to mark the critical value. See Figure 10.1. Because there is a unique critical point, we have dropped the subscript indexing. Because angles are *not* marked on lamination diagrams, the pictographs are equivalent for all c outside the Mandelbrot set. (Recall that the tree of local models, and therefore the pictograph, is not defined for polynomials with connected Julia set.)

For degree 3, Figure 10.2 shows a pictograph for a cubic polynomial with critical escape rates $G_f(c_1) = M$ and $G_f(c_2) = M/3^3$ for some $M > 0$. The spine of its tree is the linear subtree containing the four edges between critical point c_2 and critical value $f(c_1)$. For the pictograph, we include five lamination diagrams at heights $M/3^i$, $i = -1, 0, 1, 2, 3$. The two critical points are labeled by 0_1 and 0_2 . Note that every spine in degree 3 will be a linear subtree of $T(f)$, because there are only two critical points.

In degree 4, Figure 1.2 of the Introduction shows a pictograph for a quartic polynomial with critical escape rates $G(c_1) = M$, $G(c_2) = M/4^2$, and $G(c_3) = M/4^3$; the tree structure of the spine is now non-linear.

In each of these examples, there is only one fundamental edge: $N = 1$. Figure 12.1 shows a cubic example with two fundamental edges.

Figure 12.3 shows a pictograph that admits a self-equivalence, i.e., an automorphism; the involution of indices $3 \leftrightarrow 4$ and swapping the left- and right-hand branches realizes the equivalence.

Proof of Theorem 10.1. – Suppose f and g are topologically conjugate. Then there exists a quasiconformal conjugacy between basins $(f, X(f))$ and $(g, X(g))$. By applying the stretching deformations from §9.2, we may assume the heights of the fundamental subannuli are the same, and that $(f, X(f))$ and $(g, X(g))$ are conjugate via a twisting deformation. By Theorem 9.1, the trees of local models $(\mathcal{F}_f, \mathcal{X}(f))$ and $(\mathcal{F}_g, \mathcal{X}(g))$ are isomorphic

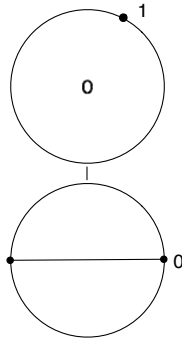


FIGURE 10.1. The pictograph for every quadratic polynomial with disconnected Julia set.

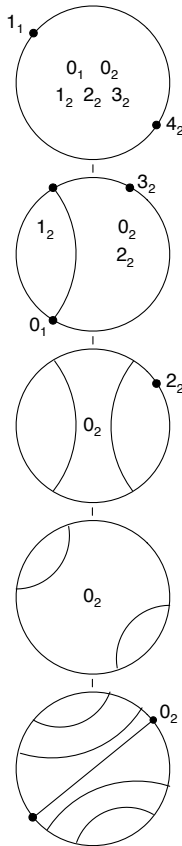


FIGURE 10.2. A cubic pictograph, with critical escape rates $(M, M/3^3)$ for some $M > 0$.

via a holomorphic conjugacy φ . Choose arbitrarily an indexing of the critical orbits for f . This indexing can be transported via φ to an indexing of those for g , so f and g will have equivalent pictographs. \square

10.3. Reconstructing the tree of local models

We can now prove that a pictograph plus the list of critical escape rates determines the full tree of local models over a metrized polynomial tree. The strategy is the following. The critical orbit labels allow us to first reconstruct the first-return map $(R, S(T))$ on the spine of the underlying tree (F, T) . Then we use the lamination diagrams (and Theorem 5.1) to reconstruct the local model maps and thus the first-return map $(\mathcal{R}, \mathcal{S})$ on the tree of local models. The heights of the local model surfaces and the metric on the underlying tree are determined by the given compatible critical heights.

Proof of Theorem 10.2. – Suppose we are given the pictograph \mathcal{D} for a polynomial f of degree d and the list of compatible critical heights $h_1 \geq h_2 \geq \dots \geq h_{d-1} \geq 0$. By Theorem 7.2, it suffices to reconstruct the spine \mathcal{S} of the tree of local models and its first-return map. We begin with the reconstruction of the first-return map $(R, S(T))$ on the spine of the underlying tree.

Let N be the number of independent critical heights. Denote by v_0 the vertex associated to the highest non-trivial lamination in \mathcal{D} . There are exactly N trivial laminations above v_0 in the pictograph, each marked by points of the critical orbits. Denote these vertices by v_1, v_2, \dots, v_N , in ascending order. The spine $S(T)$ is part of the data of the pictograph, after adjoining the ray from v_0 to ∞ . As usual, to reconstruct the action of R we proceed inductively on descending height. Above v_0 , we have $R = F$, acting as translation by simplicial distance N . Each vertex of $S(T)$ below v_0 at simplicial distance j from v_0 , with $0 < j \leq N$, is sent by F to the vertex v_{N-j} .

Now suppose we have computed the action of R on $S(T)$ for all vertices at simplicial distance $\leq n$ from v_0 , and assume $n \geq N$. Let v be a vertex in $S(T)$ at simplicial distance $n+1$ from v_0 , and let v' be the adjacent vertex above it. Suppose $w' = R(v')$. From the simplicial distance between w' and v_0 , we can determine the iterate k for which $w' = F^k(v')$. Namely, if there are n' edges on the path from w' to v_0 , then necessarily we have $n - n' = kN$ for some positive integer k . Then $w' = F^k(v')$.

Choose any index j so that the symbol 0_j appears in the lamination diagram of v ; since v belongs to the spine, such j exists. Then the symbol 0_j must also appear in the lamination diagram of v' , and the symbol k_j must appear in the lamination diagram $L_{w'}$ of w' . If k_j lies in a gap of $L_{w'}$ together with a symbol 0_ℓ for some index ℓ , then necessarily k_j must appear in the lamination diagram below w' also containing 0_ℓ . This vertex $v(\ell)$ is uniquely determined by ℓ , and we may conclude that $R(v) = v(\ell)$.

If k_j lies in a gap of $L_{w'}$ containing no symbols of the form 0_ℓ , then $F^k(v)$ is not in the spine. We must pass to a further iterate. For each iterate R^m , define $k(m)$ by $R^m(v') = F^{k(m)}(v')$. Choose the smallest positive integer m so that the symbol $k(m)_j$ lies in a gap together with a symbol of the form 0_ℓ for some index ℓ in the lamination over $R^m(v')$. Such an integer always exists because some iterate of R must send v' to one of the vertices $\{v_1, \dots, v_N\}$. For this integer m , we choose the vertex $v(\ell)$ below $R^m(v')$ containing 0_ℓ , and we set $R(v) = v(\ell)$. In this way, we reconstruct $(R, S(T))$ to all vertices at simplicial distance $n+1$ from v_0 , completing the induction argument.

Our next step is to reconstruct the height function h on the spine $S(T)$. It suffices to determine the height of the fundamental vertices v_i , for $i = 0, 1, \dots, N-1$, because of

the relation $h(F(v)) = d h(v)$ on vertices. We are given that $h(v_0) = h_1$, the height of the highest critical point. For each $i > 0$, the lamination diagram over v_i must contain at least one marked point, labeled by the symbol k_j for some positive integer k and index $j \in \{2, \dots, d-1\}$. It follows that $h(v_i) = d^k h_j$.

At this point, we observe that we could have taken our initial data to be the lengths of the N fundamental edges, rather than the heights of the critical points. Indeed, if l_i is the length of fundamental edge e_i , then the height function h is determined as follows. Set $l = l_1 + \dots + l_N$. Then $h(v_0) = \sum_{k=1}^{\infty} l/d^k$, the distance from v_0 to the Julia set $J(F)$. Then $h(v_i) = h(v_0) + l_1 + \dots + l_i$ for each $i = 1, \dots, N$. The height of all other vertices is determined by the relation $h(F(v)) = d h(v)$.

We now apply Theorem 5.1(1) to reconstruct the local model surfaces X_v over each vertex v in $S(T)$. Setting the length of the central leaf to 2π , the heights of the inner and outer annuli coincide with the length of the underlying edges of the trees, scaled by a certain factor $c_v > 0$. The factor c_v is the reciprocal of the weight $\mu_F(J(F, v))$ defined in (6.2); the weight of v is computable from the first-return map $(R, S(T))$ because all vertices with degree > 1 are contained in the spine.

By Theorem 5.1(2), the local model maps over the vertices in $S(T)$ can be reconstructed from the lamination diagrams. Indeed, the degree is obtained by counting the number of symbols of the form 0_j and adding 1. Recall, however, that we are able to so reconstruct a local model map only up to pre- and post-composition with rotational symmetries.

Since such symmetries consist entirely of rotations and must preserve all labels, the only configurations of labeled lamination diagrams which are symmetric are those for which all labels lie in a central gap which is fixed by this rotational symmetry. So suppose $R(v) = w = F^m(w)$, and consider the labeled lamination diagrams for X_v and X_w . We now consider several cases.

1. Suppose neither X_v nor X_w admit label-preserving symmetries. Then there is a unique map $X_v \rightarrow X_w$ sending a label k_i in X_v to the corresponding label $(k+m)_i$ in X_w .
2. Suppose X_v admits label-preserving symmetries but X_w does not. Then all labels for X_v lie in a common central gap and the covering $X_v \rightarrow X_w$ is cyclic. Up to isomorphism there is a unique such covering; we choose a representative arbitrarily. Note that any two such choices differ by precomposition by an isometry which is a symmetry of the labeled diagram for X_v , yielding a holomorphic conjugacy between the two different extensions of the dynamics to X_v which is the identity on X_w .
3. Suppose both X_v and X_w admit label-preserving symmetries. Again, all labels for X_v and for X_w must lie in central gaps fixed by the rotational symmetries, and the covering $X_v \rightarrow X_w$ is cyclic. By elementary covering space theory, given any fixed covering $\mathcal{R}_v : X_v \rightarrow X_w$ and any rotation $\beta : X_w \rightarrow X_w$, there exists a lift $\alpha : X_v \rightarrow X_v$ of β under \mathcal{R}_v . This lift α again yields a holomorphic conjugacy between the two different extensions \mathcal{R}_v and $\beta \circ \mathcal{R}_v$ of the dynamics to X_v which is the identity on X_w .

Given any fixed covering $\mathcal{R}_v : X_v \rightarrow X_w$ and any label-preserving symmetry $\alpha : X_v \rightarrow X_v$, rotation by $\alpha^{-1} : X_v \rightarrow X_v$ yields a holomorphic conjugacy between the two different extensions \mathcal{R}_v and $\mathcal{R}_v \circ \alpha$ of the dynamics to X_v which is the identity on X_w .

The previous two paragraphs cover all sources of ambiguity in the extension of the dynamics.

Thus as the induction proceeds, we see that at the inductive stage, we make choices for the extension of the dynamics, but that different choices are holomorphically conjugate by a map which affects only the surface over which the extension is made.

It follows that any two different collections of choices will yield holomorphically conjugate dynamics $\mathcal{R} : \mathcal{S} \rightarrow \mathcal{S}$ on the spine of the tree of local models.

The dynamical system $(\mathcal{R}, \mathcal{S})$ determines the full tree of local models by Theorem 7.2. \square

10.4. Abstract pictographs and Theorem 1.1.

We defined the abstract tree of local models in §7.2, and we proved in Theorem 7.1 that every abstract tree of local models arises for a polynomial. An abstract pictograph is defined to be the pictograph associated to an abstract tree of local models. Therefore, Theorem 1.1 is an immediate corollary of Theorem 7.1.

Proof of Proposition 10.3. – Let $(\mathcal{F}, \mathcal{X})$ be an abstract tree of local models, and let \mathcal{D} be its pictograph. Fix any $M > 0$ to be the height of the highest critical vertex v_0 in \mathcal{D} , and set $h(c_1) = M$. Denote the vertices above v_0 in ascending order by v_1, v_2, \dots, v_N so the lamination of v_N contains the symbol 1_1 on its central leaf. We may choose any sequence of heights $M < h(v_1) < h(v_2) < \dots < h(v_N) = dM$ for these vertices. For each $i = 2, \dots, d-1$, there is at most one $j \in \{1, \dots, N\}$ for which a symbol k_i lies on the central leaf over v_j . If such a j exists, then we set

$$h(c_i) = h(v_j)/d^k.$$

If no such j exists, then we set $h(c_i) = 0$.

From Theorem 10.2, the pictograph with the data of critical escape rates uniquely determines the full tree of local models. \square

11. Counting topological conjugacy classes in degree 3

In this section, we provide the proofs of Theorems 4.1 and 4.2. These proofs are inspired by the arguments of Branner in [3, Theorem 9.1] and Harris in [12]. We conclude the section by comparing our constructions in the case of degree 3 to those appearing in [4], [5], and [3].

11.1. The space of cubic polynomials

Let $\mathcal{P}_3 \simeq \mathbb{C}^2$ denote the space of monic and centered cubic polynomials. It is a degree 2 branched cover of \mathcal{M}_3 . Explicitly, a polynomial $f(z) = z^3 + az + b$ is conformally conjugate to $g(z) = z^3 + a'z + b'$ if and only if they are conjugate by $z \mapsto -z$; consequently $a = a'$ and $b = -b'$. Therefore, \mathcal{M}_3 has the structure of a complex orbifold with underlying manifold \mathbb{C}^2 ; the projection $\mathcal{P}_3 \rightarrow \mathcal{M}_3$ is given by $(a, b) \mapsto (a, b^2)$, and its branch locus $\{b = 0\}$ is precisely the set of polynomials with a nontrivial automorphism (necessarily of the form $z \mapsto -z$). Observe that the critical points for cubic polynomials with a nontrivial automorphism are interchanged by the automorphism; they therefore escape at the same rate.

11.2. The length of a cubic polynomial

Fix a cubic polynomial f with disconnected Julia set. Denote its critical points by c_1 and c_2 , so that $G_f(c_1) \geq G_f(c_2)$. Recall from §2.1 that the length of f is the least integer $L = L(f)$ such that $G_f(c_2) \geq G_f(c_1)/3^L$. If no such integer exists, we set $L(f) = \infty$. Thus, $L(f) = \infty$ if and only if c_2 lies in the filled Julia set of f ; and $L(f) = 0$ if and only if $G_f(c_1) = G_f(c_2) > 0$.

LEMMA 11.1. – *Let \mathcal{D} be a pictograph for a cubic polynomial of length $L(f) = 0$. There is a unique topological conjugacy class of polynomials in \mathcal{M}_3 with pictograph \mathcal{D} .*

Proof. – Any length 0 cubic polynomial f has $G_f(c_1) = G_f(c_2) = M$ for some $M > 0$. Fix $M > 0$ and let $(\mathcal{F}, \mathcal{X})$ be the unique tree of local models with pictograph \mathcal{D} and critical height M . The underlying tree (F, T) has a unique fundamental edge. Let v_0 denote the vertex at height M , and set $v_1 = F(v_0)$. To construct any polynomial f with tree of local models $(\mathcal{F}, \mathcal{X})$, we first glue the outer annulus of the local model surface (X_{v_0}, ω_{v_0}) to the unique inner annulus of the local model surface (X_{v_1}, ω_{v_1}) . The choice of gluing along the fundamental edge uniquely determines the gluing choices of all local models above v_0 , because the local model maps must extend holomorphically. Because $L(f) = 0$, the local degree at all vertices below v_0 is 1, and therefore the choice of gluing along the fundamental edge also determines the gluing along every edge below v_0 . In other words, the gluing at the fundamental edge determines the conformal conjugacy class of an entire basin. By uniformization, we may conclude that this gluing choice determines a unique point in \mathcal{M}_3 ; see e.g., [8, Lemma 3.4, Proposition 5.1].

Finally, it is easy to see from the definition of the twisting deformation that all choices of gluing X_{v_0} to X_{v_1} can be obtained by twisting. Therefore, all polynomials in \mathcal{M}_3 with tree of local models $(\mathcal{F}, \mathcal{X})$ are twist-conjugate. Combined with Theorem 10.3, it follows that all polynomials in \mathcal{M}_3 with pictograph \mathcal{D} are topologically conjugate. \square

11.3. Reducing to the case of 1 fundamental edge

The main idea of the proofs of Theorems 4.1 and 4.2 is the following. We begin with a tree of local models $(\mathcal{F}, \mathcal{X})$ with the given pictograph, and we fix a point in the base torus of the bundle of gluing configurations $\mathcal{B}_3(\mathcal{F}, \mathcal{X})$. In the absence of symmetry, the basepoint corresponds to a unique choice of gluing along the fundamental edges of $(\mathcal{F}, \mathcal{X})$. That is, the conformal structure of the basin at and above the highest critical point is fixed.

As usual, we let v_0 denote the highest branching vertex of the tree, so the local model surface at v_0 contains a critical point. Inductively on descending height, we glue the local models along the spine of $(\mathcal{F}, \mathcal{X})$ below the vertex v_0 . Each local model map below v_0 has degree 2, and there are exactly two ways to glue the local model surface so that the map extends holomorphically. At each stage we determine which gluing choices are conformally conjugate and which gluing choices are topologically (twist) conjugate.

It turns out that the only choices that contribute to our count of topological conjugacy classes are those made at the vertices of the spine that map to v_0 . Suppose the given tree has two fundamental edges, and let v be a vertex in the spine that does not lie in the grand orbit of v_0 . Let e be the edge above v . If the forward orbit of the lower critical point does not contain v , then the two gluing choices along e are easily seen to be conformally conjugate.

If the orbit of the lower critical point does contain v , then the distinct gluing choices for the local model at v will always be topologically conjugate, as the following lemma shows.

LEMMA 11.2. – *Fix a tree of local models for a cubic polynomial with two fundamental edges. Let v be a vertex in the spine, below v_0 and in the forward orbit of the lower critical point. Suppose we have glued all local models in the spine above vertex v . Then the two gluing choices of (X_v, ω_v) are topologically conjugate, via a conjugacy that preserves the orbit of the lower critical point and leaves the conformal structure above v unchanged.*

Proof. – Let f be any cubic polynomial with the given tree of local models $(\mathcal{F}, \mathcal{X})$. As $(\mathcal{F}, \mathcal{X})$ has two fundamental edges, f lies in the shift locus and the two critical points have distinct escape rates; let c_1, c_2 denote the critical points so that $G_f(c_1) > G_f(c_2)$. Let $L = L(f)$ be the length of f . The fundamental annulus is decomposed into two subannuli,

$$A_0^2 = \{G_f(f^L(c_2)) < |z| < 3G_f(c_1)\}$$

and

$$A_0^1 = \{G_f(c_1) < |z| < G_f(f^L(c_2))\},$$

which can be twisted independently.

For each $0 < n < L(f)$, denote by A_n the annular component of $\{G_f(c_1)/3^n < |z| < G_f(c_1)/3^{n-1}\}$ separating the two critical points. Let $0 < n_1 < \dots < n_m < L(f)$ index the values of n for which the orbit of c_2 intersects A_n . The vertex v corresponds to a level curve of G_f in the annulus A_{n_i} for some $i \in \{1, \dots, m\}$. We proceed inductively on i .

For $i = 1$, a full twist in A_0^1 followed by a full twist in the opposite direction in A_0^2 induces the opposite gluing choice for the local model surface (X_v, ω_v) without affecting the conformal class of the basin above v . This is because the annulus A_{n_1} maps with degree 2 by f^{n_1} to the annulus A_0 ; a full twist in A_0 induces a half-twist in A_{n_1} .

Similarly for each i : the annulus A_{n_i} is mapped with degree 2^i by f^{n_i} to A_0 . Therefore, 2^{i-1} full twists in A_0^1 followed by -2^{i-1} full twists in A_0^2 will induce a half twist at the level of v while preserving the conformal structure of the basin above v . □

11.4. Simplified pictographs

The simplified pictograph of a cubic polynomial, defined in §2.2, is a subset of its pictograph: it consists of the laminations at vertices of height $G_f(c_1)/3^n$ for all $0 \leq n < L(f)$, where $L(f)$ is the length of f , or of only the lamination at height $G_f(c_1)$ for $L(f) = 0$. The lamination at level n (height $G(c_1)/3^n$) is labeled by integer $0 \leq k \leq L(f) - n$, if $f^k(c_2)$ lies in one of its gaps or on the level curve. Figure 2.3 shows the simplified pictograph for the example of Figure 10.2. Figure 11.1 contains pictographs for two cubic polynomials with length $L(f) = 1$ and the simplified pictographs for each of them.

For drawing diagrams, it is more convenient to use the simplified pictograph rather than the full pictograph. The next lemma shows that we do not lose any information by doing so.

LEMMA 11.3. – *The pictograph can be recovered from the simplified pictograph.*

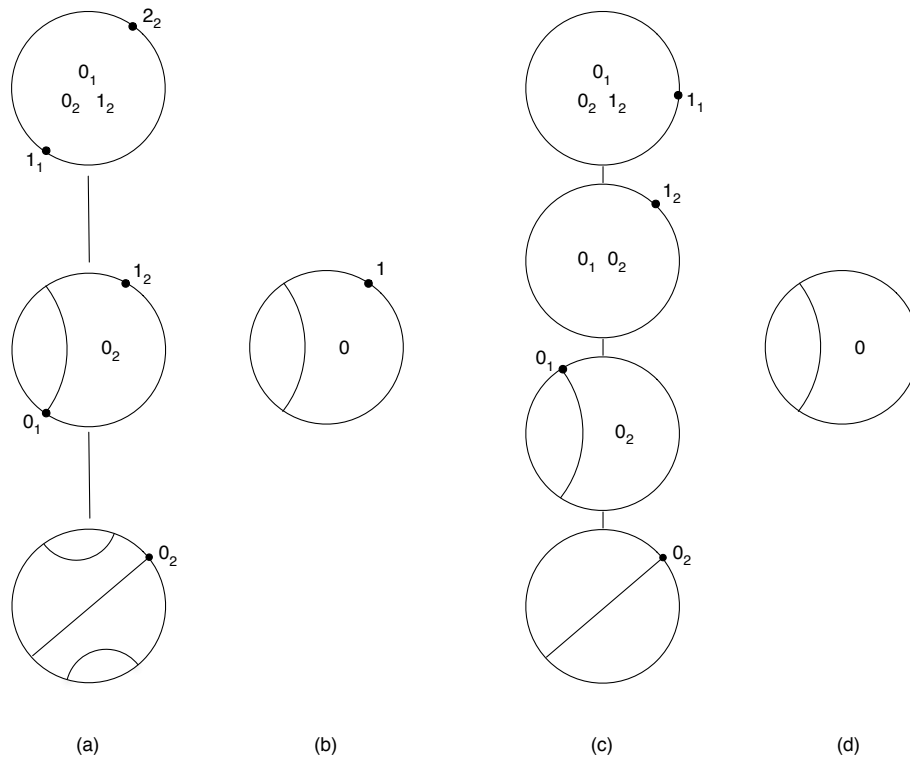


FIGURE 11.1. Length 1 cubics: (a) a pictograph, with critical heights $(M, M/3)$; (b) the simplified pictograph for the pictograph of (a); (c) the generic pictograph at level 1, with critical heights (M, M') where $M/3 < M' < M$; (d) the simplified pictograph for the pictograph of (c).

Proof. – For any polynomial f , the lamination at height $3G_f(c_1)$ with its marked points is uniquely determined by the marked lamination at height $G_f(c_1)$ (see Lemma 5.3). For length $L(f) = 0$, this shows that the simplified pictograph determines the pictograph. Similarly for length $L(f) = \infty$.

Assume f is a cubic polynomial with finite length $L(f) > 0$. Observe that there are marked points on the lamination at height $G_f(c_1)$ (not just in the gaps) if and only if f has one fundamental edge, meaning that $G_f(c_2) = G_f(c_1)/3^{L(f)}$. In this case, the simplified pictograph is almost the complete pictograph. The lamination diagram containing the critical point c_2 is also uniquely determined: it is a degree 2 branched cover of the lamination at level n , where n is the greatest integer such that the symbol $L(f) - n$ marks the lamination at height $G_f(c_1)/3^n$, branched over the marked point.

In the case of two fundamental edges, it is easy to see how to fill in the pictograph. We first add the subscript “2” to each of the labels in the simplified pictograph, and we mark the unique non-trivial equivalence class at the height of c_1 with the symbol 0_1 . We next include the trivial lamination (a circle) to the column of lamination diagrams above each lamination of the simplified pictograph. These laminations correspond to vertices in the spine intersecting the grand orbit of the second critical point c_2 , except at the height of c_2

itself. The lamination at the height $G_f(c_2)$ will be the “Figure 8”: it is a circle cut by a diameter; the diameter is marked with the symbol 0_2 . Finally, at each height $G_f(c_1)/3^n$ where the symbol $(L(f) - n - 1)_2$ appears in the same component as the symbol 0_2 , we mark the trivial lamination below it with the symbol $(L(f) - n - 1)_2$, in one of two ways: (1) if $(L(f) - n - 1)_2$ also appears at height $G_f(c_1)/3^{n+1}$ then we place $(L(f) - n - 1)_2$ in the gap, and (2) otherwise, we place the symbol on the lamination circle.

From the definition of the pictograph, we see that this is the complete diagram. □

11.5. Marked levels and the τ sequence

Fix a cubic polynomial f with a disconnected Julia set; let $L(f)$ be its length, so $G_f(c_2) = G_f(c_1)/3^{L(f)}$. For each $0 \leq n \leq L(f)$, the *level n puzzle piece* P_n is the connected component of $\{G < G(c_1)/3^{n-1}\}$ containing c_2 . Note that P_0 contains both critical points and $f^n(P_n) = P_0$ for all n . The Yoccoz τ -function associated to f ,

$$\tau_f : \{1, 2, 3, \dots, L(f)\} \rightarrow \mathbb{N},$$

is defined by the following: let $k(n) = \min\{k > 0 : c_2 \in f^k(P_n)\}$; then $f^{k(n)}(P_n) = P_{\tau_f(n)}$. In particular, $\tau_f(1) = 0$ and $\tau_f(i + 1) \leq \tau_f(i) + 1$ for all i and every f with $L(f) > 0$. The data of τ_f is equivalent to the information in the tableau (or marked grid) of f defined in [5]. In §3.1, we showed how to read the τ -sequence off from the simplified pictograph of f .

We defined the notion of marked levels in §4.1, but we recall the definition here. For each $n \geq 0$, let B_n be the closed subset of the level n puzzle piece P_n where $G_f(z) \leq G_f(c_1)/3^n$. A marked level is an integer $n > 0$ where the orbit of c_2 intersects $B_n \setminus P_{n+1}$.

LEMMA 11.4. – *A level $n > 0$ is marked if and only if at least one of the following holds:*

1. *there exists $i < L(f)$ so that $\tau(i) = n$ and $\tau(i + 1) \leq n$;*
2. *$G_f(c_2) = G_f(c_1)/3^{L(f)}$ and $n = \tau^k(L(f))$ for some $k > 0$.*

The proof is immediate from the definitions. From this lemma, we see that a marked level coincides with the “semi-critical” levels of [20] and with the “off-center” levels n_0, n_1, \dots, n_j of f of [3, Theorem 9.1] when $L(f) = \infty$.

In terms of the simplified pictograph and symmetries, we may characterize the marked levels as follows.

LEMMA 11.5. – *The marked levels coincide with the degree 2 vertices of the simplified pictograph where the order of rotational symmetry is 1.*

Again the proof is immediate from the definitions. The marking of a level n means that the symmetry is broken at that level.

11.6. Counting topological conjugacy classes

We begin by defining relative moduli and twist periods, quantities involved in the computations of Theorems 4.1 and 4.2. Relative moduli were first defined in §4.1.

Let $(\mathcal{F}, \mathcal{X})$ be a tree of local models with a given pictograph \mathcal{D} . Let \mathcal{S} be the spine of $(\mathcal{F}, \mathcal{X})$ and suppose we have chosen a gluing of all the local models along \mathcal{S} . From Proposition 7.3, the gluing choices along \mathcal{S} , together with its first-return map, uniquely determine a complete basin of infinity $(f, X(f))$. Let c_1 and c_2 denote the critical points of f so that $G_f(c_1) \geq G_f(c_2)$. Let $L(f)$ be the length. Let

$$A_0 = \{z : G_f(c_1) < |z| < 3 G_f(c_1)\}$$

denote the fundamental annulus. For each $0 < n < L(f)$, denote by A_n the annular component of $\{G_f(c_1)/3^n < |z| < G_f(c_1)/3^{n-1}\}$ separating the two critical points.

For each $0 \leq n < L(f)$, the relative modulus at level n is the ratio

$$m(n) = \text{mod}(A_n) / \text{mod}(A_0).$$

Note that $m(n)$ is completely determined by the τ -sequence τ_f . In fact, $m(n) = 2^{-k(n)}$, where $k(n)$ is the least integer such that $\tau^{k(n)}(n) = 0$. That is, $k(n)$ counts the number of times the orbit of A_n intersects the set $\{A_0, \dots, A_{n-1}\}$.

Note also that a full twist in A_0 induces a $m(n)$ -twist in the annulus A_n . For each $n < L(f)$, the *twist period* of the basin $(f, X(f))$ at level n is the minimum number of twists $T_n > 0$ in the fundamental annulus A_0 that returns all marked levels $\leq n$ to their original gluing configuration. This means that the induced twist, summing along the annuli from A_0 down to each marked level $j \leq n$, must be integral.

We shall see in the proof of Theorem 4.1 that these twist periods can be computed from the τ -sequence and are independent of the choice of gluing configuration.

Proof of Theorem 4.1. – Let \mathcal{D} be a pictograph with finitely many marked levels. Fix $M > 0$, and let $(\mathcal{F}, \mathcal{X})$ be any tree of local models with pictograph \mathcal{D} and maximal critical height M . Let $L(f)$ denote the length of any cubic polynomial basin with tree of local models $(\mathcal{F}, \mathcal{X})$. If both critical points have the same height, the length is $L(f) = 0$, there are no marked levels, and we are done by Lemma 11.1. We may assume that the critical points have distinct heights.

Fix a point in the base torus for the bundle $\mathcal{B}_3(\mathcal{F}, \mathcal{X})$. By Lemma 8.5, there are no symmetries at the fundamental vertices; it follows that the base torus parametrizes the gluing choices in the fundamental edges. From the structure of the bundle of gluing configurations, it follows that each point in the fiber corresponds to a unique conformal conjugacy class of basins (with the chosen gluing configuration above height M); the topological conjugacy classes are in one-to-one correspondence with their orbits under twisting. As described in §11.3, we will proceed inductively, on descending height, to glue the local models along the spine. By Lemma 11.2, we may disregard the gluing choices at the “intermediate levels,” corresponding to vertices in the grand orbit of the lower critical point, when there are two fundamental edges. At each vertex of height $M/3^n$, for integers $0 < n < L(f)$, we will compute the number of distinct topological conjugacy classes arising from the two gluing choices.

First assume that $(\mathcal{F}, \mathcal{X})$ has no marked levels. Then for every n , the two gluing choices of the local model at height $M/3^n$ are conformally equivalent. If there are two fundamental edges, we conclude from Lemma 11.2 that there is a unique topological conjugacy class. If there is only one fundamental edge, then in fact there is a unique point in any fiber of the bundle $\mathcal{B}_3(\mathcal{F}, \mathcal{X})$, so clearly $\text{Top}(\mathcal{D}) = 1$. Note that the absence of marked levels can be discerned from the τ -sequence of \mathcal{D} , by Lemma 11.4.

Suppose now that $(\mathcal{F}, \mathcal{X})$ has $k > 0$ marked levels, and let

$$0 < l_1 < l_2 < \dots < l_k < L(f)$$

denote the marked levels. Let m_j be the sum of relative moduli to level l_j :

$$m_j = \sum_{n=1}^{l_j} m(n).$$

Let t_j be the smallest positive integer so that $t_j m_j$ is integral; it is always a power of 2, because the vertices of the spine (below v_0) are mapped with degree 2 to their images. Then the twist period at level l_j is easily seen to be the maximum

$$T_{l_j} = \max\{t_i : i \leq j\}.$$

LEMMA 11.6. – We have $T_{l_j} \in \{T_{l_{j-1}}, 2T_{l_{j-1}}\}$ for all j .

Proof. – Suppose it takes t full twists to return to a given configuration at marked level l , and suppose the next marked level is $l' > l$. The level $\tau(l')$ must also be a marked, so $\tau(l') \leq l$. Thus, after t twists, the gluing at level $\tau(l')$ is in its original configuration; therefore l' must be either in its original configuration or twisted halfway around. Therefore, at most $2t$ twists are needed to return to the original configuration at level l' . \square

Lemma 11.6 says that the twist period between marked levels can increase at most by a factor of two. It follows that twisting reaches all possible gluing configurations if and only if $T_{l_k} = 2^k$. Or, more precisely, the number of distinct topological conjugacy classes associated to the given tree of local models is the ratio $2^k / T_{l_k}$. This completes the proof of the theorem. \square

Proof of Theorem 4.2. – Suppose \mathcal{D} is a pictograph with infinitely many marked levels. For any fixed value $M > 0$, there is a unique tree of local models $(\mathcal{F}, \mathcal{X})$ with the given pictograph \mathcal{D} and critical point at height M . Note that the infinitely many marked levels implies, in particular, that one critical point lies in the filled Julia set.

As in the proof of Theorem 4.1, we begin by fixing a point in the base torus of $\mathcal{B}_3(\mathcal{F}, \mathcal{X})$. Note that the base torus is a circle in this case. At each marked level of the pictograph, the two gluing choices produce conformally inequivalent basins in $\mathcal{B}_3(\mathcal{F}, \mathcal{X})$; it follows that there are infinitely many points in any fiber of $\mathcal{B}_3(\mathcal{F}, \mathcal{X})$. From Lemma 9.5, the fiber is then homeomorphic to a Cantor set; in particular, there are uncountably many points in the fiber. On the other hand, two basins in a fiber are topologically conjugate if and only if they lie in the same twist orbit; thus, there can only be countably many topologically conjugate points in a fiber. Therefore, there are infinitely many topological conjugacy classes within $\mathcal{B}_3(\mathcal{F}, \mathcal{X})$.

As proved in [5] and discussed further in [3] and [12], the topological conjugacy classes in the cubic moduli space \mathcal{M}_3 organize themselves into solenoids or a union of circles,

depending on the twist periods. In the notation of the proof of Theorem 4.1, the twist period of a complete basin with tree $(\mathcal{F}, \mathcal{X})$ is the value

$$T = \lim_{j \rightarrow \infty} T_{l_j}.$$

If T is infinite, then necessarily the bundle of gluing configurations is a union of

$$\text{Sol}(\mathcal{D}) := \lim_{j \rightarrow \infty} \frac{2^j}{T_{l_j}}$$

solenoids. Note that the limit $\text{Sol}(\mathcal{D})$ exists and lies in the set $\{1, 2, 2^2, 2^3, \dots, \infty\}$, because $2^j/T_{l_j}$ defines a non-decreasing sequence of powers of 2. For $T < \infty$, the bundle of gluing configurations forms an infinite union of closed loops. \square

11.7. The Branner-Hubbard description

Branner and Hubbard showed that there are two important dynamically-defined fibrations in the space of monic and centered cubic polynomials \mathcal{P}_3 . Let \mathcal{C}_3 denote the connectedness locus, the set of polynomials in \mathcal{P}_3 with connected Julia set. First, the maximal critical escape rate

$$M : \mathcal{P}_3 \setminus \mathcal{C}_3 \rightarrow (0, \infty)$$

defined by

$$M(f) = \max\{G_f(c) : f'(c) = 0\}$$

is a trivial fibration with fibers homeomorphic to the 3-sphere [3, Theorem 6.1] (which follows from [4, Theorem 11.1, Corollary 14.6]). Branner and Hubbard analyzed the quotient of a fiber of M in \mathcal{M}_3 ; it follows from [4, Cor 14.9] that the induced map

$$M : \mathcal{M}_3 \setminus \mathcal{C}_3 \rightarrow (0, \infty)$$

is also trivial fibration with fibers homeomorphic to the 3-sphere. The trivialization is given by the stretching deformation; see §9.2.

For each $r > 0$, let $H_r \subset M^{-1}(r) \subset \mathcal{P}_3$ be the locus of polynomials with $G(c_2) < G(c_1) = r$. Let c'_1 denote the *cocritical point* of c_1 , so that $f^{-1}(f(c_1)) = \{c_1, c'_1\}$, and let $\theta(c'_1) \in \mathbb{R}/2\pi\mathbb{Z}$ be its external angle. Then

$$\Phi_r : H_r \rightarrow S^1$$

defined by $\Phi_r(f) = \theta(c'_1)$ is a trivial fibration with fibers homeomorphic to the unit disk \mathbb{D} [3, Theorem 6.2]. The fiber of Φ_r over θ will be denoted $F_r(\theta)$. Note that every polynomial in $F_r(\theta)$ is conjugate by $z \mapsto -z$ to a unique polynomial in $F_r(\theta + \pi)$. (It is worth observing that the polynomials with nontrivial automorphism cannot be in H_r ; the automorphism interchanges the two critical points, so they must escape at the same rate.)

The turning deformation of [4] induces a monodromy action on a fiber $F_r(\theta)$; its first entry into $F_r(\theta + \pi)$ determines the *hemidromy action*. Alternatively, the hemidromy action is the monodromy of the induced fibration on the quotient of H_r in \mathcal{M}_3 :

$$\Phi_r : [H_r] \rightarrow S^1$$

given by $\Phi_r(f) = 2\theta(c'_1) \bmod 2\pi$ which is well-defined on the conjugacy class of f . The fibers of Φ_r in \mathcal{M}_3 are again topological disks.

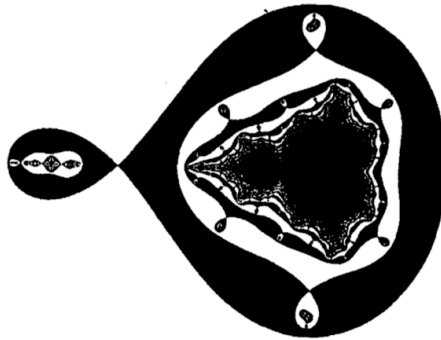


FIGURE 11.2. A fiber of Φ_r showing critical level sets of $f \mapsto G_f(c_2)$, from [5, Figure 9.3].

Let us fix $\theta = 0$ and consider the fiber $[F_r(0)]$ in \mathcal{M}_3 . The hemidromy action on this fiber will be denoted

$$T_r : [F_r(0)] \rightarrow [F_r(0)].$$

It corresponds to a full twist in the fundamental annulus; compare §9.2. The escape rate of the second critical point further decomposes $[F_r(0)]$. The critical level sets of $G(c_2)$ are precisely the levels $r/3^n$ for integers $n > 0$. The connected components of $\{G(c_2) < r/3^n\}$ are called the *level n disks*. The hemidromy action permutes these disks. The *period* of a level n disk D is the least number of iterates $p > 0$ such that $T_r^p(D) = D$. Branner-Hubbard showed that these periods are always powers of 2. The period of the level n disk coincides with the twist period T_n (defined in §11.6) for any cubic polynomial in that disk.

Suppose $(\mathcal{F}, \mathcal{X})$ is a cubic tree of local models with both critical heights positive. If there is only one fundamental edge, then the Branner-Hubbard turning curves through any polynomial f with tree $(\mathcal{F}, \mathcal{X})$ constitute the connected components of the bundle $\mathcal{B}_3(\mathcal{F}, \mathcal{X})$. In fact, twisting coincides with the turning deformation, up to the normalization of the parametrization. For a cubic tree $(\mathcal{F}, \mathcal{X})$ with two fundamental edges, the base torus of $\mathcal{B}_3(\mathcal{F}, \mathcal{X})$ is two-dimensional. Intersecting with a fiber of the Branner-Hubbard bundle Φ_r , the bundle $\mathcal{B}_3(\mathcal{F}, \mathcal{X})$ consists of finitely many connected components of a level set of $f \mapsto G_f(c_2)$. In this case, a full turn around the base of $\Phi_r : [H_r] \rightarrow S^1$ corresponds to a twist by

$$\frac{m_1}{m_1 + m_2} \mathbf{e}_1 + \frac{m_2}{m_1 + m_2} \mathbf{e}_2$$

where m_i is the modulus of the fundamental annulus A_i , so that $m_1 + m_2 = 2r$.

Among the polynomials f with length $L(f) = \infty$, there are two types of connected components in the Branner-Hubbard slice $F_r(0)$. They showed that the Mandelbrot sets in their picture correspond to cubic polynomials where the connected component of the filled Julia set containing the critical point is periodic. Equivalently, the tableau is periodic. The twist periods of these Mandelbrot sets are always finite; there are only finitely many marked levels in the corresponding pictograph. In this case, the bundle $\mathcal{B}_3(\mathcal{F}, \mathcal{X})$ is a finite union of circles. Branner and Hubbard proved that all other cubic polynomials with infinite length correspond to points in their slice. For these polynomials, the bundle $\mathcal{B}_3(\mathcal{F}, \mathcal{X})$ may be a union of circles or a union of solenoids.

12. Counting argument, all degrees

In this final section, we give the proof of Theorem 1.2. We apply the algorithm to two examples in degree 5 (§12.7 and §12.8) to illustrate the role of the symmetry calculations. We provide an example of a pictograph associated to multiple topological conjugacy classes in any degree $d > 2$ (§12.9).

Towards Theorem 1.2, we have already established the topological-conjugacy invariance of the pictograph (Theorem 10.1). Here, we show:

THEOREM 12.1. – *Let \mathcal{D} be a pictograph. The number $\text{Top}(\mathcal{D})$ of topological conjugacy classes of basins $(f, X(f))$ with pictograph \mathcal{D} is inductively computable from the discrete data of \mathcal{D} . Specifically, the computation depends only on the first-return map along the spine $(R, S(T))$ of the underlying tree and the automorphism group of the full tree of local models.*

It is useful to compare this statement to those of Theorems 4.1 and 4.2 containing the degree 3 computation. In degree 3, the data of $(R, S(T))$ is equivalent to the Branner-Hubbard tableau and Yoccoz τ -sequence; see §6.7. Also in degree 3, the symmetries of the tree of local models are easy to describe. Recall that the automorphism group is itself inductively computable from a pictograph in all degrees; see Section 8.

For the general degree case, we introduce the *restricted basin* of infinity for a polynomial, with a notion of equivalence that carries information from the full tree of local models. This allows us to define an analog of the “marked levels” in degree 3 (see §11.5). We introduce the *lattice of twist periods* to generalize the sequence of twist periods used to compute the number of conjugacy classes in degree 3. In higher degrees, the markings and symmetries are significantly more complicated, so computing the number of twists needed to return to a given gluing configuration involves more ingredients.

12.1. Restricted basins, conformal equivalence

Let $(f, X(f))$ be a basin of infinity. Fix any real number $t > 0$. Let G_f denote the escape-rate function on $X(f)$, and set

$$X_t(f) = \{z \in X(f) : G_f(z) > t\}.$$

We refer to the pair $(f, X_t(f))$ as a *restricted basin*. We define in the obvious way *restricted trees* and *restricted trees of local models*. However, here we introduce a special, and unobvious, notion of equivalence of restricted basins that will be useful in the proof of Theorem 12.1.

Let $(\mathcal{F}_1, \mathcal{X}(f_1))$ and $(\mathcal{F}_2, \mathcal{X}(f_2))$ denote the trees of local models for the basins $(f_1, X(f_1))$ and $(f_2, X(f_2))$, respectively. By construction, there are gluing quotient maps

$$g_i : (\mathcal{F}_i, \mathcal{X}(f_i)) \rightarrow (f_i, X(f_i))$$

that are conformal isomorphisms from each local model surface to its image, inducing conjugacies between the restrictions of \mathcal{F}_i and f_i .

We say the restricted basins $(f_1, X_t(f_1))$ and $(f_2, X_t(f_2))$ are *conformally equivalent over* $(\mathcal{F}, \mathcal{X})$ if their *unrestricted* trees of local models are both isomorphic to $(\mathcal{F}, \mathcal{X})$, and there exists a conformal isomorphism

$$\psi : X_t(f_1) \rightarrow X_t(f_2)$$

inducing a conjugacy between the restrictions $f_1|_{X_t(f_1)}$ and $f_2|_{X_t(f_2)}$ that extends to the full tree of local models. Specifically, there is an isomorphism between trees of local models

$$\varphi : (\mathcal{F}_1, \mathcal{X}(f_1)) \rightarrow (\mathcal{F}_2, \mathcal{X}(f_2))$$

which restricts to the induced isomorphism $\tilde{\psi}$ on the restricted trees, at heights $> t$, defined by lifting ψ via the gluing quotient maps g_i :

$$\begin{array}{ccc} (\mathcal{F}_1, \mathcal{X}_t(f_1)) & \xrightarrow{\tilde{\psi}} & (\mathcal{F}_2, \mathcal{X}_t(f_2)) \\ g_1 \downarrow & & \downarrow g_2 \\ (f_1, X_t(f_1)) & \xrightarrow{\psi} & (f_1, X_t(f_2)). \end{array}$$

Similarly, we define $\text{Aut}_{(\mathcal{F}, \mathcal{X})}(f, X_t(f))$ to be the group of conformal automorphisms of the restricted basin $(f, X_t(f))$ that extend to automorphisms of the tree $(\mathcal{F}, \mathcal{X})$. Denoting by $\text{Aut}(f, X(f))$ and $\text{Aut}(f, X_t(f))$ the groups of conformal isomorphisms (of $X(f)$ and $X_t(f)$, respectively) commuting with f , we find:

LEMMA 12.2. – *For any basin of infinity $(f, X(f))$ of degree $d \geq 2$, and any $t > 0$, we have a chain of subgroups*

$$\text{Aut}(f, X(f)) \subset \text{Aut}_{(\mathcal{F}, \mathcal{X})}(f, X_t(f)) \subset \text{Aut}(f, X_t(f)) \subset C_{d-1},$$

where C_{d-1} is the cyclic group of order $d - 1$, acting by rotation in the uniformizing coordinates near ∞ .

Proof. – The first two inclusions follow easily from the definitions. Indeed, any automorphism of a basin $(f, X(f))$ induces an automorphism of the tree of local models and of any restricted basin. The last inclusion follows because an automorphism of $(f, X_t(f))$ must commute with f near infinity, where it is conformally conjugate to z^d . \square

12.2. Restricted basins, topological equivalence

As for conformal equivalence of restricted basins, defined in §12.1, we say restricted basins $(f_1, X_t(f_1))$ and $(f_2, X_t(f_2))$ are *topologically equivalent over* $(\mathcal{F}, \mathcal{X})$ if there exists a topological conjugacy

$$\psi : X_t(f_1) \rightarrow X_t(f_2)$$

that extends to an isomorphism of the full tree of local models.

It is important to observe that topologically conjugate restricted basins are also quasi-conformally conjugate; the proof is identical to the one for full basins of infinity. Further, if the restricted basins come from basins with the same critical escape rates, the quasiconformal conjugacy can be taken to be a twist deformation. On each level set of G_f , the twist deformation acts by isometries (in the $|\partial G_f|$ metric), and therefore it preserves the conformal

structure of the local models in the tree of local models (compare the proof of Theorem 9.1). This proves:

LEMMA 12.3. – *A topological conjugacy between restricted basins $(f_1, X_t(f_1))$ and $(f_2, X_t(f_2))$ with the same critical escape rates induces, via the gluing quotient maps, an isomorphism of restricted trees of local models $(\mathcal{F}_1, \mathcal{X}_t(f_1))$ and $(\mathcal{F}_2, \mathcal{X}_t(f_2))$.*

In the definition of topological equivalence of restricted basins, then, we are requiring that this induced isomorphism of restricted trees of local models can be extended to an isomorphism on the full tree of local models.

12.3. Twist periods

As described in §9.2, a quasiconformal deformation of a basin of infinity has a canonical decomposition into its twisting and stretching factors. Fix $f \in \mathcal{M}_d$ and consider the analytic map of §9.3,

$$\text{Twist}_f : \mathbb{R}^N \rightarrow \mathcal{M}_d,$$

which parametrizes the twisting deformations in the N fundamental subannuli of f , sending the origin to f . Recall that the basis vector

$$\mathbf{e}_j = (0, \dots, 0, 1, 0, \dots, 0) \in \mathbb{R}^N$$

induces a full twist in the j -th fundamental subannulus.

A *twist period* of f is any vector $\tau \in \mathbb{R}^N$ which preserves the conformal conjugacy class of $(f, X(f))$; that is, $\text{Twist}_f(\tau) = \text{Twist}_f(0)$. When f is in the shift locus, the set of twist periods forms a lattice in \mathbb{R}^N [7, Lemma 5.2]. In general, the set of twist periods forms a discrete subgroup (though possibly not a lattice),

$$\text{TP}(f) \subset \mathbb{R}^N,$$

that we will refer to as the *lattice of twist periods*. As we shall see in the proof of Theorem 12.1, polynomials with equivalent pictographs can have different lattices of twist periods; this can happen when one gluing configuration has automorphisms while another does not. Nevertheless, we will see that the possibilities for $\text{TP}(f)$ can still be computed from the data of the pictograph.

For each $t > 0$, we define $\text{TP}_t(f) \supset \text{TP}(f)$ to be the set of vectors $\tau \in \mathbb{R}^N$ that preserve the conformal equivalence class of the restricted basin $(f, X_t(f))$ over $(\mathcal{F}, \mathcal{X}(f))$; the equivalence of restricted basins was defined in §12.1.

LEMMA 12.4. – *For any $t_1 > t_2 > 0$ and any f with N fundamental subannuli, each group $\text{TP}_{t_i}(f)$ forms a lattice in \mathbb{R}^N , with index $[\text{TP}_{t_1}(f) : \text{TP}_{t_2}(f)] < \infty$ and*

$$\text{TP}(f) = \bigcap_{t>0} \text{TP}_t(f).$$

Proof. – The argument is similar to the proof of [7, Lemma 5.2]. Let $X_t(f) = \{G_f > t\} \subset X(f)$. For each fundamental subannulus A_j , there are only finitely many connected components B_j of preimages of A_j inside $X_t(f)$ under any iterate of f . A full twist in the

annulus A_j induces a $1/k$ -twist in a preimage B_j , where k is the degree of the iterate f^n sending B_j to A_j . Let

$$d_j = \text{lcm}\{k : k = \deg(f^n|_{B_j \rightarrow A_j})\}$$

over all such components $B_j \subset X_t(f)$. Then the subgroup $\text{TP}_t(f)$ of \mathbb{R}^N must contain the vector

$$d_j \mathbf{e}_j = (0, \dots, 0, d_j, 0, \dots, 0)$$

for each j ; indeed, this vector induces an automorphism of $(f, X_t(f))$ that extends to the identity automorphism on the full tree of local models. Because $\text{TP}_t(f)$ is a discrete subgroup of \mathbb{R}^N , we see that it must be a lattice. The same argument also shows that $[\text{TP}_{t_1}(f) : \text{TP}_{t_2}(f)] < \infty$.

Finally, if $\tau \in \text{TP}(f)$, then τ must induce an equivalence of the restricted basin $(f, X_t(f))$ over $(\mathcal{F}, \mathcal{X}(f))$ for every $t > 0$, because a conjugacy between basins induces an equivalence on trees of local models. Therefore,

$$\text{TP}(f) \subset \bigcap_{t>0} \text{TP}_t(f).$$

Conversely, we observe that if $\tau \cdot (f, X_t(f))$ is conformally equivalent to $(f, X_t(f))$ for all $t > 0$, then there is a conformal conjugacy between the basins $\tau \cdot (f, X(f))$ and $(f, X(f))$, so $\tau \in \text{TP}(f)$. We conclude that $\text{TP}(f) = \bigcap_{t>0} \text{TP}_t(f)$. □

12.4. Twist periods in degree 3

We remark that the definition of twist period given here differs from that given in §11.6 for degree 3 maps. They coincide in the case of one fundamental annulus, in the sense that the twist periods $\{T_n\}$ form a sequence of generators for the one-dimensional twist lattices $\text{TP}_{t_n}(f) \subset \mathbb{R}$ for heights t_n just below level n .

A cubic polynomial f with two fundamental subannuli is necessarily in the shift locus (and structurally stable) with finite length $L(f) > 0$. We describe here how to recover the sequence of twist periods T_n at levels $0 \leq n < L(f)$ from the lattices of twist periods $\text{TP}_t(f)$.

For a cubic polynomial f with two fundamental subannuli, let $(F, T(f))$ denote its tree, let v_0 be the highest branching vertex of $T(f)$, and let $h : T(f) \rightarrow \mathbb{R}$ be the height function. Choose a sequence of descending heights

$$(12.1) \quad t_0 > t_1 > t_2 > \dots$$

so that t_n is a height “just below” a vertex of simplicial distance n from v_0 . That is, $t_0 = h(v_0) - \varepsilon$ for any sufficiently small $\varepsilon > 0$, and there is a unique vertex in each connected component of $h^{-1}(t_{n+1}, t_n)$.

From the definitions, and the absence of symmetries at v_0 , we have $T_0 = 1$ and

$$\text{TP}_{t_0} = \langle \mathbf{e}_1, \mathbf{e}_2 \rangle = \mathbb{Z}^2 \subset \mathbb{R}^2$$

for every such polynomial.

Let $S(T)$ be the spine of the tree $(F, T(f))$. Denote by w the lowest vertex in the spine (the lower critical point). For each positive integer $n < L(f)$, set

$$J(n) = \#\{L(f) - n \leq j < L(f) : F^j(w) \in S(T)\},$$

the number of times the critical orbit intersects the spine, above level n and below v_0 . From the proof of Theorem 12.1 given below, an inductive argument shows that

$$(12.2) \quad T_n = \frac{[\text{TP}_{t_0} : \text{TP}_{t_{2n}}]}{2^{J(n)}}.$$

12.5. A cubic example

Because the computation of the twist period lattices is crucial in the proof of Theorem 12.1, we illustrate with an example in degree 3.

Consider the cubic pictograph shown in Figure 12.1. It is the unique pictograph associated to the τ -sequence $(0, 1, 2, 3)$ with two fundamental edges. Any associated polynomial has length $L(f) = 4$. There are no marked levels, in the sense defined in §11.5. Consequently, $T_0 = T_1 = T_2 = T_3 = 1$. From Theorem 4.1, there is a unique topological conjugacy class of cubic polynomials with this pictograph.

Now let $\{t_n\}$ be a descending sequence of escape rates, as defined in (12.1). Every polynomial f with this pictograph has the following lattices of twist periods:

$$\begin{aligned} \text{TP}_{t_0} &= \langle \mathbf{e}_1, \mathbf{e}_2 \rangle \\ \text{TP}_{t_1} &= \text{TP}_{t_2} = \langle \mathbf{e}_1, 2\mathbf{e}_2 \rangle \\ \text{TP}_{t_3} &= \text{TP}_{t_4} = \langle 2\mathbf{e}_1, \mathbf{e}_1 + 2\mathbf{e}_2 \rangle \\ \text{TP}_{t_n} &= \langle 4\mathbf{e}_1, 3\mathbf{e}_1 + 2\mathbf{e}_2 \rangle \text{ for all } n \geq 5. \end{aligned}$$

These lattices are computed inductively with n , with the base case $\text{TP}_{t_0} = \langle \mathbf{e}_1, \mathbf{e}_2 \rangle$. To determine TP_{t_n} from $\text{TP}_{t_{n-1}}$, we compute the induced twisting at each vertex of the spine, down to height t_n , for elements of $\text{TP}_{t_{n-1}}$. Specifically, let v be the lowest vertex in the spine above height t_n , and fix $\tau = \tau_1 \mathbf{e}_1 + \tau_2 \mathbf{e}_2 \in \text{TP}_{t_{n-1}}$. We compute (1) the relative modulus of $\text{mod}(e)$ of each edge e in the spine (as the reciprocal of the degree by which e maps to a fundamental edge) down to the vertex v , and (2) the sum

$$R_\tau(v) = \sum_e \tau_{j(e)} \text{mod}(e)$$

where $j(e)$ is the index of the fundamental edge in the orbit of e . If the lamination diagram at vertex v is invariant under rotation by the amount $R_\tau(v)$ (leaving also all labels invariant), then $\tau \in \text{TP}_{t_n}$. If not, we consider integer multiples of τ .

Finally, $\text{TP}(f) = \langle 4\mathbf{e}_1, 3\mathbf{e}_1 + 2\mathbf{e}_2 \rangle$ by Lemma 12.4. Observing that $J(n) = n$ for each $n = 1, 2, 3$, we also see that equation (12.2) holds.

12.6. Proof of Theorem 12.1

Fix a pictograph \mathcal{D} . We aim to show that the number $\text{Top}(\mathcal{D})$ of topological conjugacy classes of basins $(f, X(f))$ with pictograph \mathcal{D} can be inductively computed from the discrete data of \mathcal{D} .

For any $M > 0$, there exists a vector of compatible critical heights with maximal critical height M . Let $(\mathcal{F}, \mathcal{X})$ be the tree of local models with pictograph \mathcal{D} and the chosen vector of critical heights given by Proposition 10.2. Let (F, T) be the underlying polynomial tree

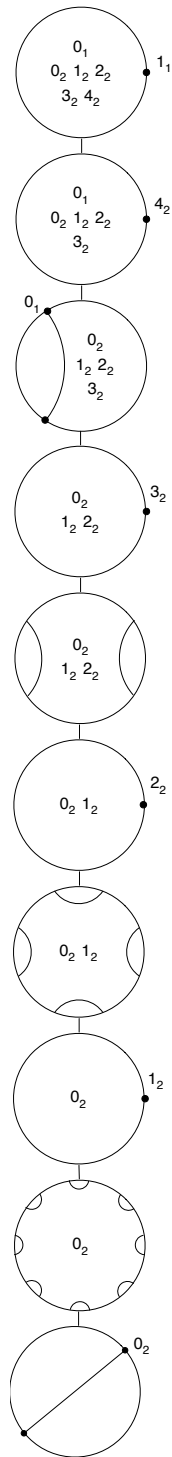


FIGURE 12.1. A cubic pictograph with τ sequence $(0, 1, 2, 3)$. Its twist periods are computed in §12.5.

with height function $h : T \rightarrow (0, \infty)$, so that $h(v_0) = M$ for the highest branching vertex v_0 and $h(F(x)) = d \cdot h(x)$ for all $x \in T$. Choose a descending sequence of real numbers

$$t_{-1} > M > t_0 > t_1 > t_2 > \cdots > 0$$

so that

- the points of $h^{-1}(t_i)$ are not vertices of T for any $i \geq 0$, and
- there is a unique vertex of T in each connected component of $h^{-1}[t_i, t_{i-1}]$ for all $i \geq 0$.

For each $i \geq 0$, we will inductively compute the number $\text{Top}(\mathcal{D}, i)$ of topological conjugacy classes of restricted basins

$$f : X_{t_i}(f) \rightarrow X_{t_i}(f)$$

over $(\mathcal{F}, \mathcal{X})$; the equivalence was defined in §12.2.

The number $\text{Top}(\mathcal{D})$ is not simply the limit of these numbers $\text{Top}(\mathcal{D}, i)$ as $i \rightarrow \infty$, as we shall see, but it can be determined from the sequence $\{\text{Top}(\mathcal{D}, i)\}_i$ and the data used to compute it.

Let $i = 0$. The conformal equivalence class of the restricted basin $(f, X_{t_0}(f))$ over $(\mathcal{F}, \mathcal{X})$ depends only on the gluing along each of the fundamental subannuli. It is easy to see, from the definition of twisting, that all gluing choices within the fundamental annulus are equivalent under twisting. We conclude that

$$\text{Top}(\mathcal{D}, 0) = 1$$

for any pictograph \mathcal{D} .

For the induction argument, we need to compute the lattice of twist periods $\text{TP}_{t_0}(f)$ and the automorphism group $\text{Aut}_{(\mathcal{F}, \mathcal{X})}(f, X_{t_0}(f))$ for any choice of restricted basin $(f, X_{t_0}(f))$ from the discrete data of \mathcal{D} at and above the vertex v_0 and automorphism group $\text{Aut}(\mathcal{F}, \mathcal{X})$. Recall that the automorphism group of the full tree of local models is isomorphic to the automorphism group of the first-return map $(\mathcal{R}, \mathcal{S})$ on the spine (Lemma 8.4), so any information we need about $\text{Aut}(\mathcal{F}, \mathcal{X})$ is determined by \mathcal{D} .

Suppose \mathcal{D} has N fundamental edges (so any basin with pictograph \mathcal{D} has N fundamental subannuli). As usual, we label the ascending consecutive vertices $v_0, v_1, \dots, v_N = F(v_0), v_{N+1}, \dots$ in the tree (F, T) , where v_0 is the highest branching vertex. In §8.2, we defined the order of local symmetry of the tree $(\mathcal{F}, \mathcal{X})$ at the vertex v_j ; we denote this order by k_j .

LEMMA 12.5. – For each $j \geq 0$, the orders of symmetry at v_j and v_{j+N} satisfy

$$k_{j+N} = k_j / \gcd(k_j, d).$$

Proof. – The local degree of F at each vertex v_j is d . From Lemma 5.4, we know that $k_j / \gcd(k_j, d)$ must divide k_{j+N} . On the other hand, by the definition of the local symmetry order (coming from an automorphism of $(\mathcal{F}, \mathcal{X})$), any symmetry at v_{j+N} must lift to the domain v_j . Therefore, we have equality. \square

LEMMA 12.6. – The automorphism group $\text{Aut}_{(\mathcal{F}, \mathcal{X})}(f, X_{t_0}(f))$ is cyclic of order equal to

$$\alpha = \gcd\{k_0, k_1, \dots, k_{N-1}, d - 1\}.$$

Proof. – From Lemma 12.5, the value α will divide the orders of local symmetry at every vertex v_j , $j \geq 0$. Further, a rotation by $2\pi/\alpha$ at any vertex v_j in the tree $(\mathcal{F}, \mathcal{X})$ will induce a rotation by $2\pi d/\alpha \equiv 2\pi/\alpha \pmod{2\pi}$ at its image, because $\alpha|(d-1)$. Therefore, rotation by $2\pi/\alpha$ can act on any gluing of $(\mathcal{F}, \mathcal{X})$ to form a restricted basin $(f, X_{t_0}(f))$. The automorphism must extend to the full tree of local models, by the definition of the orders k_j . It follows that the order of $\text{Aut}_{(\mathcal{F}, \mathcal{X})}(f, X_{t_0}(f))$ is at least α . On the other hand, the order of any element in $\text{Aut}_{(\mathcal{F}, \mathcal{X})}(f, X_{t_0}(f))$ must divide α , combining the definitions with Lemma 5.4. \square

Fix a conformal equivalence class of restricted basin $(f, X_{t_0}(f))$ over $(\mathcal{F}, \mathcal{X})$. To compute $\text{TP}_{t_0}(f)$, note first that each of the basis vectors

$$\mathbf{e}_j = (0, \dots, 0, 1, 0, \dots, 0)$$

for $j = 1, \dots, N$, are contained in $\text{TP}_{t_0}(f)$, by construction. Indeed, a full twist in any subannulus induces the identity automorphism on the tree of local models $(\mathcal{F}, \mathcal{X})$.

We claim that for each $0 < j < N$, the twist vector

$$\tau_j = \frac{1}{k_j} (\mathbf{e}_{j+1} - \mathbf{e}_j)$$

is also contained in $\text{TP}_{t_0}(f)$. This vector τ_j twists by $1/k_j$ in the fundamental subannulus A_{j+1} and by $-1/k_j$ in A_j . It therefore twists by the order of symmetry at the vertex v_j , and it induces a twist by d/k_j in the image of A_{j+1} and by $-d/k_j$ in the image of A_j . By Lemma 12.5, these twists commute with the action of f . The restricted basins $(f, X_{t_0}(f))$ and $\tau_j \cdot (f, X_{t_0}(f))$ are conformally conjugate; for $k_j > 1$, the isomorphism extends to a non-trivial isomorphism of the underlying tree of local models where the action on $(\mathcal{F}, \mathcal{X})$ rotates vertices in the grand orbit of v_j .

Finally, we treat the symmetry at v_0 . Set

$$\tau_0 = \frac{1}{k_0} (\mathbf{e}_1 - d \mathbf{e}_N).$$

As for τ_j , $j > 0$, the twist vector τ_0 induces the symmetry at v_0 . The term $(d/k_0)\mathbf{e}_N$ is subtracted off so that the correct order of symmetry is induced at the image v_N , as in Lemma 12.5. Putting the pieces together, we find that $\text{TP}_{t_0}(f)$ is generated by all twist vectors of the form

$$\tau = (a_1, \dots, a_N),$$

where $0 \leq a_j \leq 1$, $\sum_{j=j_0}^N a_j$ is an integer multiple of $1/k_{j_0-1}$ for each $j_0 > 1$, and $\sum_{j=1}^N a_j$ is an integer multiple of $(1-d)/k_0 \pmod{1}$. Observe that this computation is independent of the initial choice of restricted basin $(f, X_{t_0}(f))$.

Now fix $i \geq 0$ and a restricted basin $(f, X_{t_0}(f))$. Let $\mathcal{B}_i(\mathcal{D})$ denote the set of conformal equivalence classes of restricted basins $(f, X_{t_i}(f))$ over $(\mathcal{F}, \mathcal{X})$ that extend the restricted basin $(f, X_{t_0}(f))$. Suppose we have computed

1. the number of conformal equivalence classes $|\mathcal{B}_i(\mathcal{D})|$;
2. the order of the automorphism group $\text{Aut}_{(\mathcal{F}, \mathcal{X})}(f, X_{t_i}(f))$ for each element of $\mathcal{B}_i(\mathcal{D})$;
- and
3. the lattice of twist periods $\text{TP}_{t_i}(f)$ for each element of $\mathcal{B}_i(\mathcal{D})$.

As explained above, the conformal classes in $\mathcal{B}_i(\mathcal{D})$ are topologically equivalent if and only if they are equivalent by twisting, via a conjugacy that extends to an isomorphism of the full tree of local models, so we need only compute the number of classes in each twist orbit to obtain $\text{Top}(\mathcal{D}, i)$ from this data. That is,

$$(12.3) \quad \text{Top}(\mathcal{D}, i) = \sum_{(f, X_{t_i}(f)) \in \mathcal{B}_i(\mathcal{D})} \frac{1}{[\text{TP}_{t_0}(f) : \text{TP}_{t_i}(f)]}.$$

Now we pass to $i + 1$. Let $\{(X_v, \omega_v)\}$ be the set of local models in the spine of $(\mathcal{F}, \mathcal{X})$ with vertex v in the height interval (t_{i+1}, t_i) . Let d_v be the degree of the local model map with domain (X_v, ω_v) . Let k_v be the order of local symmetry of $(\mathcal{F}, \mathcal{X})$ at v .

Fix a conformal class $(f, X_{t_i}(f)) \in \mathcal{B}_i(\mathcal{D})$, and assume that $\text{Aut}_{(\mathcal{F}, \mathcal{X})}(f, X_{t_i}(f))$ is the trivial group. Then the number of classes in $\mathcal{B}_{i+1}(\mathcal{D})$ that extend $(f, X_{t_i}(f))$ is given by

$$\prod_v \frac{d_v}{\text{gcd}(k_v, d_v)},$$

where the product is taken over all vertices v of the spine in the height interval (t_{i+1}, t_i) . Indeed, the extension to height t_{i+1} along any edge of degree 1 is uniquely determined. We need only compute how many distinct ways we may glue each local model (X_v, ω_v) of degree $d_v > 1$ along the edge above v so that f extends holomorphically. The absence of automorphisms shows that the local symmetry (fixing v) and local degree are the only contributing factors. It is easy to see that each extension will also have a trivial automorphism group.

Now suppose $(f, X_{t_i}(f)) \in \mathcal{B}_i(\mathcal{D})$ has automorphism group $\text{Aut}_{(\mathcal{F}, \mathcal{X})}(f, X_{t_i}(f))$ of order $m > 1$. By Lemma 12.2, the automorphism group is cyclic, acting by rotation in the uniformizing coordinates near infinity. By construction, every such automorphism extends to the full tree of local models, so there is a certain amount of symmetry among the vertices in the height interval (t_{i+1}, t_i) . First, there is at most one vertex v' in the spine at this height fixed by the automorphism of order m , and m must divide the local symmetry $k_{v'}$. All other vertices v of the spine have orbit of length m , and the order of local symmetry k_v is constant along an orbit. Choose a representative vertex \hat{v} for each orbit. The number of conformal classes in $\mathcal{B}_{i+1}(\mathcal{D})$ extending $(f, X_{t_i}(f))$ are organized as follows. There are

$$N(m) = \frac{d_{v'}}{\text{gcd}(k_{v'}, d_{v'})} \cdot \prod_{\text{orbits of length } m} \frac{d_{\hat{v}}}{\text{gcd}(k_{\hat{v}}, d_{\hat{v}})}$$

conformal conjugacy classes of extensions with an automorphism of order m ; indeed, a choice of gluing at vertex \hat{v} determines the choice (up to local symmetry) at each vertex in its orbit. For each factor $l|m$, we can also compute the number of extensions of $(f, X_{t_i}(f))$ with automorphism of order l . A simple inclusion-exclusion argument shows that there are

$$N(l) = \frac{d_{v'}}{\text{gcd}(k_{v'}, d_{v'})} \cdot \prod_{\text{orbits of length } l} \frac{d_{\hat{v}}}{\text{gcd}(k_{\hat{v}}, d_{\hat{v}})} - \sum_{\{l' : l|l'|m, l' \neq l\}} N(l')$$

conformal equivalence classes of extensions with an automorphism of order l , under the extra restriction that we require the equivalence to act by the identity on the restriction $(f, X_{t_i}(f))$. Consequently, there are

$$\frac{l}{m} \cdot N(l)$$

distinct conformal equivalence classes of extensions with automorphism of order l (without the extra assumption): for each new basin in the initial count of $N(l)$, there is an isomorphism that acts as rotation by l/m near infinity, producing another gluing configuration in the count of $N(l)$. We observe that the computation depends only on the data $\{d_v, k_v\}$ at each of the vertices in the spine.

Now we compute the lattice of twist periods $\text{TP}_{t_{i+1}}(f)$ for each class $(f, X_{t_{i+1}}(f)) \in \mathcal{B}_{i+1}(\mathcal{D})$. Note that any element $\tau \in \text{TP}_{t_{i+1}}(f)$ also induces a conformal equivalence of the restricted basin $(f, X_{t_i}(f))$ over $(\mathcal{F}, \mathcal{X})$, so $\text{TP}_{t_{i+1}}(f)$ forms a subgroup of $\text{TP}_{t_i}(f)$. We will examine linear combinations of basis elements of $\text{TP}_{t_i}(f)$ to determine which elements lie in $\text{TP}_{t_{i+1}}(f)$. We need to use the order of the automorphism group of the chosen basin $(f, X_{t_{i+1}})$ and the order of the automorphism group of the restriction $(f, X_{t_i}(f))$.

First assume that both $(f, X_{t_{i+1}}(f))$ and the restriction $(f, X_{t_i}(f))$ have trivial automorphism group. Fix any element $\tau \in \text{TP}_{t_i}(f)$, so that $\tau \cdot (f, X_{t_i}(f))$ is conformally equivalent to $(f, X_{t_i}(f))$ over $(\mathcal{F}, \mathcal{X})$. One can check algorithmically whether a multiple $a\tau$ lies in $\text{TP}_{t_{i+1}}(f)$, for each $a = 1, 2, 3, \dots$, via the following steps:

1. Compute all relative moduli, down to the vertex v , for each v in the spine in the height interval (t_{i+1}, t_i) : each edge e between v and v_0 is mapped by a degree $d(e) > 1$ to one of the fundamental edges, and its relative modulus is $1/d(e)$.
2. Compute the rotation induced by $a\tau$ at each vertex v : if $a\tau = (t_1, \dots, t_N)$, then v is rotated by

$$R_{a\tau}(v) = \sum_e \frac{t_{j(e)}}{d(e)},$$

where the sum is over all edges e between v and v_0 , and $j(e)$ is the index of the unique fundamental edge in the orbit of e .

3. If the rotation $R_{a\tau}(v)$ is an integer multiple of $1/k_v$ at each vertex v , then $a\tau \in \text{TP}_{t_{i+1}}(f)$.

Note that this process terminates at some finite value of a : by Lemma 12.4, we know that $\text{TP}_{t_{i+1}}$ is a lattice of finite index within TP_{t_i} . With trivial automorphism group, the computation of $\text{TP}_{t_{i+1}}(f)$ is independent of the choice of extension $(f, X_{t_{i+1}}(f))$.

We remark that, even in the absence of global automorphisms, there can be local symmetries of $(\mathcal{F}, \mathcal{X})$ that act nontrivially on the spine of the underlying tree. A given twist vector τ may induce one of these nontrivial automorphisms of the spine; so the computation of steps (2) and (3) above requires that we compare the action on v to a symmetry at a different vertex, say v' . In that case, the local symmetries k_v and $k_{v'}$ will coincide, so the computation is the same.

Suppose now that our chosen $(f, X_{t_{i+1}}(f))$ has automorphism group of order

$$|\text{Aut}_{(\mathcal{F}, \mathcal{X})}(f, X_{t_{i+1}}(f))| = l$$

and the restriction $(f, X_{t_i}(f))$ has

$$|\text{Aut}_{(\mathcal{F}, \mathcal{D})}(f, X_{t_i}(f))| = m \geq l.$$

Note that $l \mid m$. Fix any element $\tau \in \text{TP}_{t_i}(f)$. For $l = m$, we may proceed as above: we check integer multiples of τ and compute the rotation induced at each of the lowest vertices v . For $l < m$, we have an additional possibility. It can happen that the twisted basin $a\tau \cdot (f, X_{t_{i+1}})$ is conformally equivalent to the basin $(f, X_{t_{i+1}})$ via an isomorphism that acts as rotation by k/m near infinity, for some integer $1 \leq k < m/l$. Thus our algorithmic procedure involves an extra computation. The three steps above become:

1. Compute all relative moduli, down to the vertex v , for each v in the spine in the height interval (t_{i+1}, t_i) , as before.
2. Compute the rotation induced by $\psi^k \circ (a\tau)$ at each vertex v , where ψ^k acts as rotation by k/m near infinity, for each $k = 1, \dots, m/l$: it is given by the simple relation $R_{\psi^k \circ (a\tau)}(v) = R_{a\tau}(v) + (k/m)$.
3. If for any k , the rotation $R_{\psi^k \circ (a\tau)}(v)$ is an integer multiple of $1/k_v$ at each vertex v , then $a\tau \in \text{TP}_{t_{i+1}}(f)$.

We illustrate with one example in degree 5 the delicacy of computing twist periods in the presence of automorphisms; see §12.8 and Figure 12.3.

To make the above algorithmic process implementable, it is useful to compute an explicit basis for $\text{TP}_{t_{i+1}}(f)$. For example, let τ_1, \dots, τ_N be a set of basis vectors for the lattice $\text{TP}_{t_i}(f)$. We can apply the above steps to each basis vector. Let a_j be the smallest positive integer so that $a_j \tau_j \in \text{TP}_{t_{i+1}}(f)$. We next compute the rotation effect of each vector of the form

$$n_1 \tau_1 + \dots + n_N \tau_N$$

for all N -tuples of non-negative integers $\{n_i\}$ with $n_i \leq a_i$. This is a finite process and will produce a basis for $\text{TP}_{t_{i+1}}(f)$.

Once we have computed the twist periods for each class $(f, X_{t_{i+1}}(f)) \in \mathcal{B}_{i+1}(\mathcal{D})$, the number $\text{Top}(\mathcal{D}, i+1)$ is computed by equation (12.3).

Finally, we need to compute $\text{Top}(\mathcal{D})$. Note that the number of conformal classes extending a given $(f, X_{t_0}(f))$ is non-decreasing with i ; that is,

$$|\mathcal{B}_i(\mathcal{D})| \leq |\mathcal{B}_{i+1}(\mathcal{D})|.$$

We claim

1. $\text{Top}(\mathcal{D}) = \infty$ if and only if $\lim_{i \rightarrow \infty} |\mathcal{B}_i(\mathcal{D})| = \infty$; and
2. if $\lim_{i \rightarrow \infty} |\mathcal{B}_i(\mathcal{D})| = |\mathcal{B}_n(\mathcal{D})|$ for some n , then $\text{Top}(\mathcal{D}) = \text{Top}(\mathcal{D}, n)$.

From Theorem 9.2, the number $\text{Top}(\mathcal{D})$ is bounded above by the number of points in the fiber of the bundle of gluing configurations. By the construction of the bundle (from the proof of Theorem 9.2) the number of points in a fiber is equal to an integer multiple of $\lim_{i \rightarrow \infty} |\mathcal{B}_i(\mathcal{D})|$. Therefore, if $\text{Top}(\mathcal{D}) = \infty$, then it must be that $\lim_{i \rightarrow \infty} |\mathcal{B}_i(\mathcal{D})| = \infty$. On the other hand, when the fiber of the bundle of gluing configurations has infinite cardinality, Lemma 9.5 states that the fibers are Cantor sets. In particular, the fibers are uncountable. A topological conjugacy class within the fiber contains at most countably many elements, as the image of a lattice in \mathbb{R}^N . Therefore, there are infinitely many topological conjugacy classes. This proves statement (1). The second statement is immediate from

the arguments and definitions above; once the number of classes $|\mathcal{B}_i(\mathcal{D})|$ has stabilized, the lattice of twist periods $\text{TP}_{t_i}(f)$ also stabilizes. \square

12.7. An example in degree 5 without symmetry

Following the steps in the proof of Theorem 12.1, we compute the number of topological conjugacy classes associated to the degree-5 pictograph in Figure 12.2, with two fundamental subannuli. Fix any restricted basin $(f, X_{t_0}(f))$ with the given pictograph. It is easy to see from the diagram that the automorphism group is trivial, as are the local symmetries at the two fundamental vertices. The lattice of twist periods TP_{t_0} is generated by the standard basis vectors,

$$\text{TP}_{t_0} = \langle \mathbf{e}_1, \mathbf{e}_2 \rangle \subset \mathbb{R}^2.$$

There are two vertices v_1 and w_1 in the height interval (t_1, t_0) , with local degrees $d_{v_1} = 2$ and $d_{w_1} = 3$. Each has trivial local symmetry, so we compute that

$$|\mathcal{B}_1(\mathcal{D})| = 2 \cdot 3 = 6,$$

and each class has trivial automorphism group. A full twist in fundamental subannulus A_1 leaves v_1 and w_1 invariant, but a full twist in subannulus A_2 induces a $1/2$ twist at v_1 and a $1/3$ twist at w_1 . It requires 6 twists in A_2 to return to the given gluing configuration at level 1. We compute,

$$\text{TP}_{t_1} = \langle \mathbf{e}_1, 6\mathbf{e}_2 \rangle.$$

The computation is independent of the conformal class in $\mathcal{B}_1(\mathcal{D})$. We find that

$$\text{Top}(\mathcal{D}, 1) = 6 \cdot \frac{1}{6} = 1.$$

In the height interval (t_2, t_1) , there are again two vertices, say v_2 below v_1 and w_2 below w_1 . We have local degrees $d_{v_2} = 2, d_{w_2} = 2$ and local symmetries $k_{v_2} = 2, k_{w_2} = 1$. Therefore,

$$|\mathcal{B}_2(\mathcal{D})| = |\mathcal{B}_1(\mathcal{D})| \cdot 1 \cdot 2 = 12,$$

and each class has trivial automorphism group. A full twist in fundamental subannulus A_1 induces a $1/2$ twist at v_2 , and $1/2$ is an integer multiple of $1/k_{v_2}$. On the other hand, a $1/2$ twist is also induced at w_2 with $k_{w_2} = 1$, so we find that $\mathbf{e}_1 \notin \text{TP}_{t_2}$ but $2\mathbf{e}_1 \in \text{TP}_{t_2}$. For the subannulus A_2 , the action of $6\mathbf{e}_2$ induces full rotations of both v_2 and w_2 , so $6\mathbf{e}_2 \in \text{TP}_{t_2}$. We find that

$$\text{TP}_{t_2} = \langle 2\mathbf{e}_1, 6\mathbf{e}_2 \rangle$$

and

$$\text{Top}(\mathcal{D}, 2) = 12 \cdot \frac{1}{12} = 1.$$

For all vertices in the spine below v_2 and w_2 , the local symmetry at a vertex coincides with the local degree. Therefore

$$|\mathcal{B}_i(\mathcal{D})| = |\mathcal{B}_2(\mathcal{D})| = 12$$

for all $i \geq 2$. As explained at the end of the proof of Theorem 12.1, the number of topological conjugacy classes also stabilizes, so we may conclude that the pictograph determines

$$\text{Top}(\mathcal{D}) = \text{Top}(\mathcal{D}, 2) = 1$$

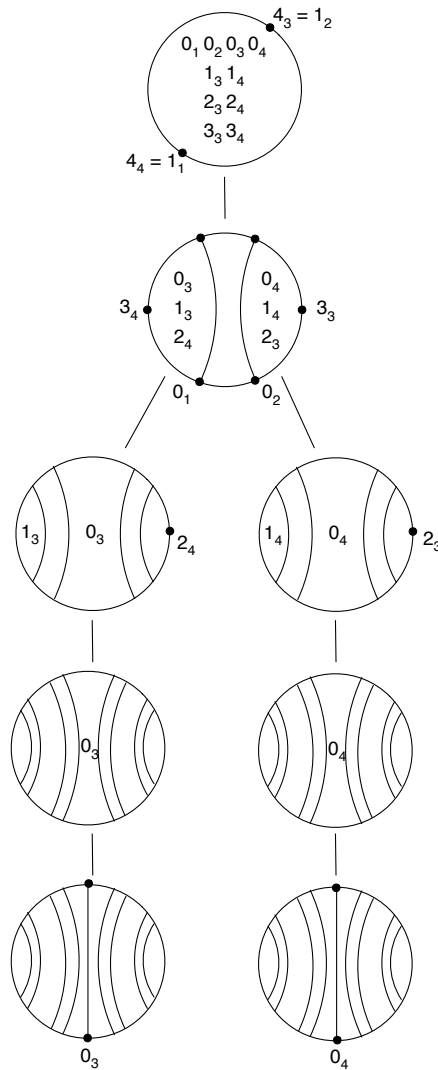


FIGURE 12.3. A degree 5 pictograph with symmetry. See §12.8.

topological conjugacy class of basins $(f, X(f)) \in \mathcal{B}_5$. In fact, because these polynomials are in the shift locus, this pictograph determines a unique topological conjugacy class of polynomials in \mathcal{M}_5 .

12.8. A degree 5 example with symmetry

Consider the pictograph of Figure 12.3. It has one fundamental edge. Fix the critical escape rate $M > 0$ of the highest critical points c_1 and c_2 , and choose heights

$$M > t_0 > M/5 > t_1 > M/25$$

as in the proof of Theorem 12.1.

Any choice of restricted basin $(f, X_{t_0}(f))$ has $\text{Aut}_{(\mathcal{F}, \mathcal{X})}(f, X_{t_0}(f))$ of order 2, interchanging the critical points labeled by 0_1 and 0_2 . The extension to the full tree $(\mathcal{F}, \mathcal{X})$ also interchanges the critical points labeled by 0_3 and 0_4 . We have

$$\text{TP}_{t_0} = \mathbb{Z}.$$

Fixing $(f, X_{t_0}(f))$, there are three conformal equivalence classes of extensions over $(\mathcal{F}, \mathcal{X})$ to level t_1 . Two of these extensions, say (f_1, X_{t_1}) and (f_2, X_{t_1}) , will have an automorphism of order 2. The third (f_3, X_{t_1}) has trivial automorphism group. The restricted basins (f_1, X_{t_1}) and (f_2, X_{t_1}) are in the same topological conjugacy class over $(\mathcal{F}, \mathcal{X})$, as one full twist in the fundamental annulus interchanges them; we have

$$\text{TP}_{t_1}(f_1) = \text{TP}_{t_1}(f_2) = 2\mathbb{Z}.$$

In the conformal class without automorphisms, one full twist arrives at a basin that is conformally equivalent via an isomorphism that rotates the basin by 180 degrees, and

$$\text{TP}_{t_1}(f_3) = \mathbb{Z}.$$

These restricted basins have unique conformal extensions to basins $(f_i, X(f_i))$, $i = 1, 2, 3$. This pictograph determines exactly two topological conjugacy classes of polynomials, one with automorphisms and one without.

12.9. Multiple topological conjugacy classes in arbitrary degree > 2

Figure 12.4 shows a pictograph \mathcal{D} in degree 4 that determines two topological conjugacy classes. This example can easily be generalized to any degree $d \geq 3$ by replacing the critical point at the highest branching vertex v_0 with one of multiplicity $d-2$. It has one fundamental subannulus.

Let $v_0, v_{-1}, v_{-2}, \dots$ denote the consecutive vertices in descending order. To compute the number of topological conjugacy classes, we evaluate the twist periods at each level. First, choose any restricted basin $(f, X_{t_0}(f))$. The automorphism group $\text{Aut}_{(\mathcal{F}, \mathcal{X})}(f, X_{t_0}(f))$ is trivial. As with every pictograph, $\text{Top}(\mathcal{D}, 0) = 1$. Because of the local symmetry at v_{-1} , there is only one conformal equivalence class of extension to $(f, X_{t_1}(f))$, so we also have $\text{Top}(\mathcal{D}, 1) = 1$. At v_{-2} , however, the symmetry is broken by the location of the second iterate of the lower critical point, so the two gluing choices determine distinct conformal equivalence classes. The sum of relative moduli at v_{-2} is $1/2 + 1/2 = 1$, so a full twist in the fundamental annulus induces a full twist at v_{-2} . Consequently, the two conformal classes lie in two distinct topological conjugacy classes and $\text{Top}(\mathcal{D}, 2) = 2$.

For each vertex below v_{-2} , there is a local symmetry of order at least 2, so the two gluing choices are conformally equivalent. We conclude that there are exactly two conformal equivalence classes of basins extending the given $(f, X_{t_0}(f))$, and these lie in exactly two topological conjugacy classes. Because this is the pictograph for polynomials in the shift locus, there are exactly two topological conjugacy classes of polynomials in \mathcal{M}_d with the given pictograph.

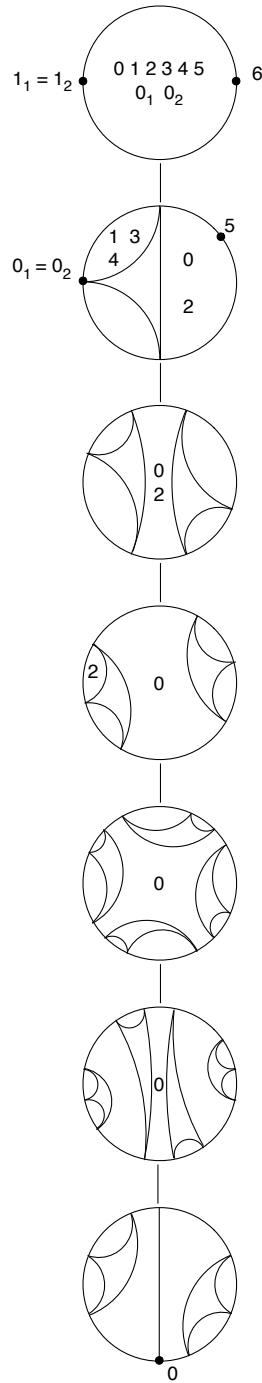


FIGURE 12.4. A degree 4 pictograph determining two topological conjugacy classes; see §12.9. The labels without subscript mark the orbit of the lowest critical point.

BIBLIOGRAPHY

- [1] L. V. AHLFORS, L. SARIO, *Riemann surfaces*, Princeton Mathematical Series, No. 26, Princeton Univ. Press, Princeton, N.J., 1960.
- [2] P. BLANCHARD, R. L. DEVANEY, L. KEEN, The dynamics of complex polynomials and automorphisms of the shift, *Invent. math.* **104** (1991), 545–580.
- [3] B. BRANNER, Cubic polynomials: turning around the connectedness locus, in *Topological methods in modern mathematics (Stony Brook, NY, 1991)*, Publish or Perish, Houston, TX, 1993, 391–427.
- [4] B. BRANNER, J. H. HUBBARD, The iteration of cubic polynomials. I. The global topology of parameter space, *Acta Math.* **160** (1988), 143–206.
- [5] B. BRANNER, J. H. HUBBARD, The iteration of cubic polynomials. II. Patterns and parapatterns, *Acta Math.* **169** (1992), 229–325.
- [6] L. DE MARCO, A. SCHIFF, The geometry of the critically periodic curves in the space of cubic polynomials, *Exp. Math.* **22** (2013), 99–111.
- [7] L. DEMARCO, K. PILGRIM, Critical heights on the moduli space of polynomials, *Adv. Math.* **226** (2011), 350–372.
- [8] L. DEMARCO, K. M. PILGRIM, Polynomial basins of infinity, *Geom. Funct. Anal.* **21** (2011), 920–950.
- [9] L. DEMARCO, A. SCHIFF, Enumerating the basins of infinity of cubic polynomials, *J. Difference Equ. Appl.* **16** (2010), 451–461.
- [10] L. G. DEMARCO, C. T. MCMULLEN, Trees and the dynamics of polynomials, *Ann. Sci. Éc. Norm. Supér.* **41** (2008), 337–382.
- [11] A. DOUADY, J. H. HUBBARD, On the dynamics of polynomial-like mappings, *Ann. Sci. École Norm. Sup.* **18** (1985), 287–343.
- [12] D. M. HARRIS, Turning curves for critically recurrent cubic polynomials, *Nonlinearity* **12** (1999), 411–418.
- [13] J. G. HOCKING, G. S. YOUNG, *Topology*, second ed., Dover Publications, Inc., New York, 1988.
- [14] H. INOU, Combinatorics and topology of straightening maps II: Discontinuity, preprint arXiv:0903.4289.
- [15] J. KIWI, Real laminations and the topological dynamics of complex polynomials, *Adv. Math.* **184** (2004), 207–267.
- [16] J. KIWI, Combinatorial continuity in complex polynomial dynamics, *Proc. London Math. Soc.* **91** (2005), 215–248.
- [17] O. KOZLOVSKI, S. VAN STRIEN, Local connectivity and quasi-conformal rigidity of non-renormalizable polynomials, *Proc. Lond. Math. Soc.* **99** (2009), 275–296.
- [18] C. T. MCMULLEN, *Complex dynamics and renormalization*, Annals of Math. Studies **135**, Princeton Univ. Press, Princeton, NJ, 1994.
- [19] C. T. MCMULLEN, D. P. SULLIVAN, Quasiconformal homeomorphisms and dynamics. III. The Teichmüller space of a holomorphic dynamical system, *Adv. Math.* **135** (1998), 351–395.

- [20] J. MILNOR, Local connectivity of Julia sets: expository lectures, in *The Mandelbrot set, theme and variations*, London Math. Soc. Lecture Note Ser. **274**, Cambridge Univ. Press, Cambridge, 2000, 67–116.
- [21] J. MILNOR, *Dynamics in one complex variable*, third ed., Annals of Math. Studies **160**, Princeton Univ. Press, Princeton, NJ, 2006.
- [22] J. MILNOR, Cubic polynomial maps with periodic critical orbit. I, in *Complex dynamics*, A K Peters, Wellesley, MA, 2009, 333–411.
- [23] R. A. PÉREZ, Quadratic polynomials and combinatorics of the principal nest, *Indiana Univ. Math. J.* **54** (2005), 1661–1695.
- [24] W. QIU, Y. YIN, Proof of the Branner-Hubbard conjecture on Cantor Julia sets, *Sci. China Ser. A* **52** (2009), 45–65.
- [25] W. P. THURSTON, On the geometry and dynamics of iterated rational maps, in *Complex dynamics*, A K Peters, Wellesley, MA, 2009, 3–137.
- [26] Y. YIN, Y. ZHAI, No invariant line fields on Cantor Julia sets, *Forum Math.* **22** (2010), 75–94.

(Manuscrit reçu le 11 janvier 2012 ;
accepté, après révision, le 3 octobre 2016.)

Laura DEMARCO
Northwestern University
Department of Mathematics
2033 Sheridan Road
Evanston, IL 60208, USA
E-mail: demarco@math.northwestern.edu

Kevin PILGRIM
Indiana University
Department of Mathematics
Rawles Hall
831 E 3rd street
Bloomington, IN 47405, USA
E-mail: pilgrim@indiana.edu

